②

AD-A194 750

THE DYNAMIC BEHAVIOR OF NYLON AND POLYESTER ROPE
UNDER SIMULATED TOWING CONDITIONS

Captain Christopher J. Toomey

Final Report, 6 May 1988

Approved for Public Release

Master of Science in Mechanical Engineering and
Master of Science in Materials Science and Engineering

REPORT DOCUMENTATION PAGE

Form Approved
OMB No 0704-0188
Exp. Date Jun 30, 1986

1a. REPORT SECURITY CLASSIFICATION	1b. RESTRICTIVE MARKINGS
2a. SECURITY CLASSIFICATION AUTHORITY	3. DISTRIBUTION / AVAILABILITY OF REPORT
2b. DECLASSIFICATION / DOWNGRADING SCHEDULE	

4. PERFORMING ORGANIZATION REPORT NUMBER(S) The Dynamic Behavior of Nylon and Poly- ester Rope Under Simulated Towing Conditions.	5. MONITORING ORGANIZATION REPORT NUMBER(S) Final Report, 6 May 1988

6a. NAME OF PERFORMING ORGANIZATION	6b. OFFICE SYMBOL (If applicable)	7a. NAME OF MONITORING ORGANIZATION
6c. ADDRESS (City, State, and ZIP Code)		7b. ADDRESS (City, State, and ZIP Code)

8a. NAME OF FUNDING / SPONSORING ORGANIZATION	8b. OFFICE SYMBOL (If applicable)	9. PROCUREMENT INSTRUMENT IDENTIFICATION NUMBER Student, HQDA, Milpercen(DAPC-OPA-E 200 Storall St., Alexandria,VA.22352

8c. ADDRESS (City, State, and ZIP Code)	10. SOURCE OF FUNDING NUMBERS			
	PROGRAM ELEMENT NO.	PROJECT NO.	TASK NO.	WORK UNIT ACCESSION NO

11. TITLE (Include Security Classification)
HQDA, Milpercen,Attn.: DAPC-OPA-E, 200 Stovall St., Alexandria, VA. 22337

12. PERSONAL AUTHOR(S)
6 May 1988 Christopher J. Toomey

13a. TYPE OF REPORT Final	13b. TIME COVERED FROM 86/Aug TO 88/May	14. DATE OF REPORT (Year, Month, Day) 88 May 6	15. PAGE COUNT 102

16. SUPPLEMENTARY NOTATION
Approved for Public Release

17. COSATI CODES			18. SUBJECT TERMS (Continue on reverse if necessary and identify by block number)
FIELD	GROUP	SUB-GROUP	Thesis, M.I.T., Dynamic Behavior of Rope

19. ABSTRACT (Continue on reverse if necessary and identify by block number) The increasing use of man-made synthetic fiber ropes in the marine environment has generated a need to understand their dynamic mechanical behavior during actual operations. Towing is an operation of primary concern.

A method was developed to simulate actual tow conditions with emphasis on constant strain amplitude dynamic loading rather than the more commonly used constant load amplitude dynamic loading. Emphasis was directed towards investigating the change in the dynamic modulus, or stiffness, of the rope when subjected to varying loading conditions, and the change in the hysteresis per cycle of the rope when subjected to varying loading conditions. Finally, measurements were made of the temperature generated during cyclic tensioning and correlations determined between temperature and power input, per cycle. The ropes used were 1/2 inch polyester and nylon rope produced by Samson Ocean Products. Theses

20. DISTRIBUTION / AVAILABILITY OF ABSTRACT ☐ UNCLASSIFIED/UNLIMITED ☒ SAME AS RPT ☐ DTIC USERS	21 ABSTRACT SECURITY CLASSIFICATION
22a NAME OF RESPONSIBLE INDIVIDUAL	22b TELEPHONE (Include Area Code) 22c OFFICE SYMBOL

DD FORM 1473, 84 MAR

83 APR edition may be used until exhausted
All other editions are obsolete

THE DYNAMIC BEHAVIOR OF NYLON AND POLYESTER ROPE
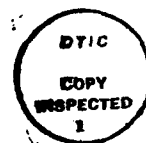## UNDER SIMULATED TOWING CONDITIONS

by

Captain Christopher James Toomey, U.S.A.
BS, United States Military Academy
(1981)

Submitted in partial fulfillment of the
requirements for the degrees of
Master of Science in
Mechanical Engineering
and
Master of Science in
Materials Science and Engineering

at the

Massachusetts Institute of Technology
May, 1988

© Christopher James Toomey
The author hereby grants to M.I.T. and the
United States Government permission
to reproduce and to distribute copies of this thesis
document in whole or in part.

Signature of Author

Department of Mechanical Engineering
May, 1988

Certified By

Professor Stanley Backer, Department of Mechanical Engineering
Thesis Supervisor

Certified By

Dr. John Mandell, Department of Materials Science and Engineering
Thesis Supervisor

Certified By

Professor Frederick J. McGarry, Department of Materials Science and Engineering
Thesis Supervisor

Accepted By

Professor Ain A. Sonin, Chairman
Departmental Graduate Committee, Department of Mechanical Engineering

Accepted By

Professor John B. Vander Sande, Chairman
Department Graduate Committee
Department of Materials Science and Engineering

THE DYNAMIC BEHAVIOR OF NYLON AND POLYESTER ROPE UNDER SIMULATED TOWING CONDITIONS

by

Captain Christopher James Toomey,U.S.A.

Submitted to the Department of Mechanical Engineering
on May, 1988, in partial fulfillment of the requirements
for the Degrees of Master of Science in Mechanical Engineering and
Master of Science in Materials Science and Engineering

ABSTRACT

The increasing use of man-made synthetic fiber ropes in the marine environment has generated a need to understand their dynamic mechanical behavior during actual operations. Towing is an operation of primary concern.

A method was developed to simulate actual tow conditions with emphasis on constant strain amplitude dynamic loading rather than the more commonly used constant load amplitude dynamic loading. Emphasis was directed towards investigating the change in the dynamic modulus, or stiffness, of the rope when subjected to varying loading conditions, and the change in the hysteresis per cycle of the rope when subjected to varying loading conditions. Finally, measurements were made of the temperature generated during cyclic tensioning and correlations determined between temperature and power input, per cycle. The ropes used were 1/2 inch polyester and nylon rope produced by Samson Ocean Products.

Thesis Supervisor: Professor Stanley Backer
              Department of Mechanical Engineering

Thesis Supervisor: Dr. John Mandell
              Department of Materials Science and Engineering

Thesis Supervisor: Professor Frederick J. McGarry
              Department of Materials Science and Engineering

ACKNOWLEDGEMENTS

TABLE OF CONTENTS

LIST OF FIGURES

Chapter 1

Introduction

1.1 General

Since World War II, man made synthetic fiber ropes have been increasingly used in support of both military and commercial operations in the marine environment. Due to their high strength, extensibility, relative low cost and resistance to degrading environmental effects in comparison to comparably sized natural fiber ropes, synthetic fiber ropes have become very popular in a myriad of uses including moorings and towings.

One drawback with the use of man made synthetic fiber ropes is the lack of data and understanding of the behavior and mechanical properties of these ropes during actual operations. Only recently have comprehensive, scientific investigations been made into their behavior. Understanding the mechanical behavior of ropes subjected to dynamic loads such as encountered in actual conditions of deployment is a prerequisite to the ability to predict their failure and to recommend the type of rope most applicable to a given situation.

In many marine applications, such as towing, the rope is subjected to a dynamic, cyclic load which is a function of the vessels, the rope employed and the dynamic marine environment. This is in contrast to the case of static or quasi-static conditions which involve the imposition of a constant load or a slowly applied monotonic load.

When examining the effects of dynamic loads, two primary mechanical properties are of interest. The first of these is the stiffness or modulus of the rope. Knowledge of the dynamic modulus allows for a prediction of tension build-up under certain use conditions. The second property is the hysteresis which serves as a measure of the net energy absorbed or dissipated by the rope during any particular cycle. Hysteresis is a measure of mechanical damping manifested in the rope in the form of heat build-up and viscoelastic deformation [1].

1.2 Background and past studies

Previous studies have attempted to examine the dynamic behavior of rope. However, because of the many different types of construction (such as 3-str

and, double-braid and 8-strand) and materials (polyester, Nylon 6, Nylon 6.6, polyethylene, Kevlar) and multiple diameters, the data derived from such studies are often not comparable. Further, a variety of methods and experimental conditions have been employed which adds to the inconsistency of results. However, despite these drawbacks, several conclusions relevant to this study can be inferred from published results.

Parsey [2] cycled nylon and polyester 8-strand ropes and double braided nylon at a period of 6 seconds. The ropes, which were initially wet and had been soaked in fresh water for 24 hours, were cycled between various constant load levels ranging from 10-28% of the manufacturer's Guaranteed Minimum Breaking Load (GMBL) to 10-75% of the GMBL. Parsey found that the dynamic stiffness, or dynamic modulus (defined as the local secant modulus over a given load or displacement range) was up to 4 times greater than the quasi-static modulus, (the local tangent modulus derived at a given point on the monotonic load elongation curve). He also reported that the ropes absorbed from 20-30% of the energy input i.e., the relative hysteresis was 20-30%. Figure 1 shows his results for the moduli of the ropes.

Bitting[3] did an extensive study in the dynamic behavior of nylon and polyester line which included cycling the continuously wet ropes between fixed load levels and at various mean loads and frequencies. As with Parsey, he found that the dynamic stiffness, (the local secant modulus or the apparent spring constant) exceeded the quasi-static stiffness by a factor of 3 or 4, depending upon the material and construction of the ropes. Figure 2 shows his results for nylon 8-strand plaited line.

In these two studies, as with most studies investigated, the ropes were cycled between fixed load levels. Because ropes behave as viscoelastic structures which stiffen and experience creep as they are cycled in tension, they will manifest decreasing extension amplitudes when cycled between constant load limits. In terms of energy for loading to a fixed limit of tension, stiffer ropes may require less energy than softer ropes as seen in Figure 3.

An alternate form of testing is to cycle the rope between fixed extension limits. As seen in Figure 4, this requires less energy in loading for the rope with the lower modulus. When evaluating the results of any testing, it is critical to know whether the rope was cycled under constant load or constant extension. Indeed, in cycling to failure, Parsey [2] , who cycled between fixed load limits, found that polyester ropes had a much greater cyclic lifetime than similarly constructed nylon ropes. In contrast, Prevorsek and Kwon [4], in cycling fibers
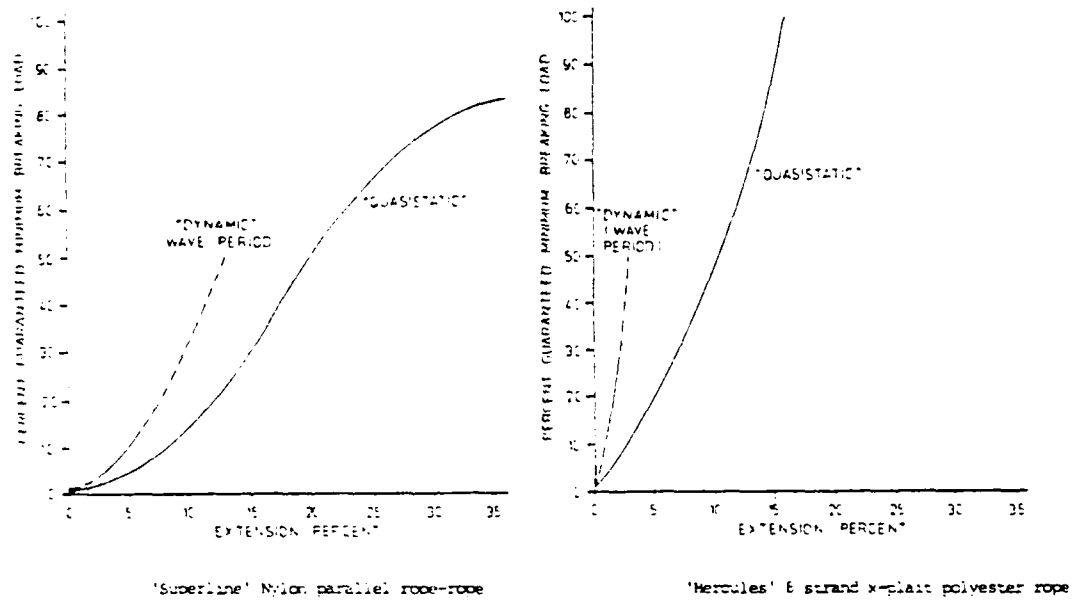
Figure 1
The difference between the dynamic and quasi-static moduli of
several ropes as found by Parsey . [Parsey,Ref 2]
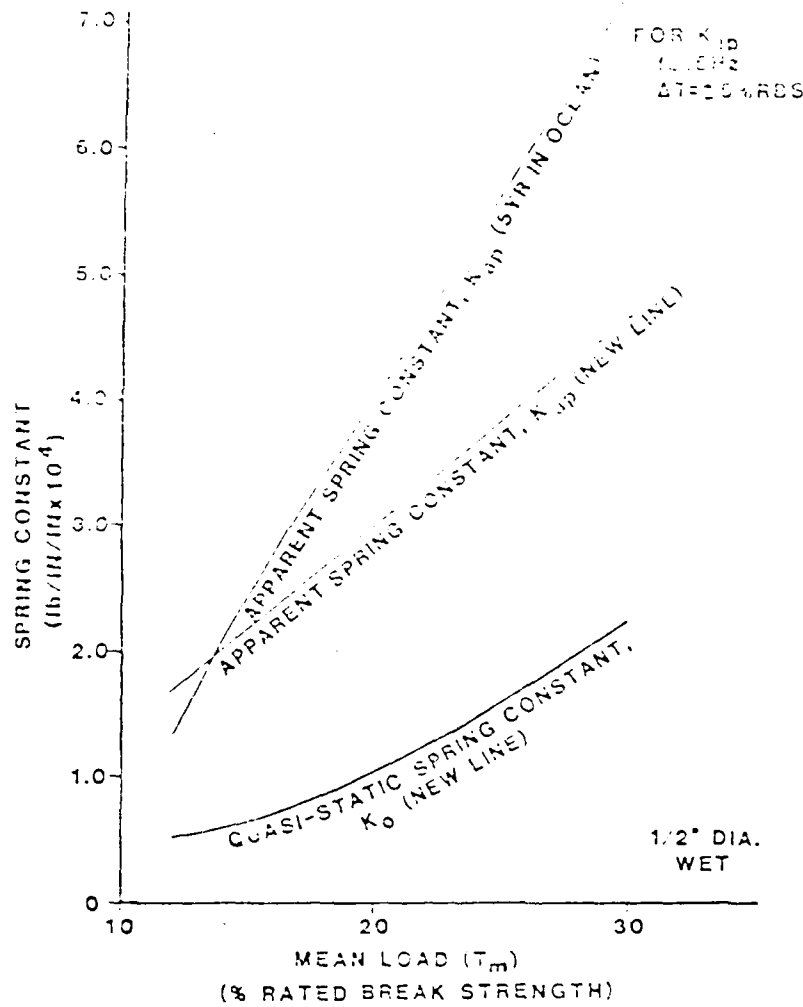
Figure 2
The difference between the dynamic and quasi-static moduli of
polyester 8-strand plaited ropes as found by Bitting . [Bitting, Ref 3]
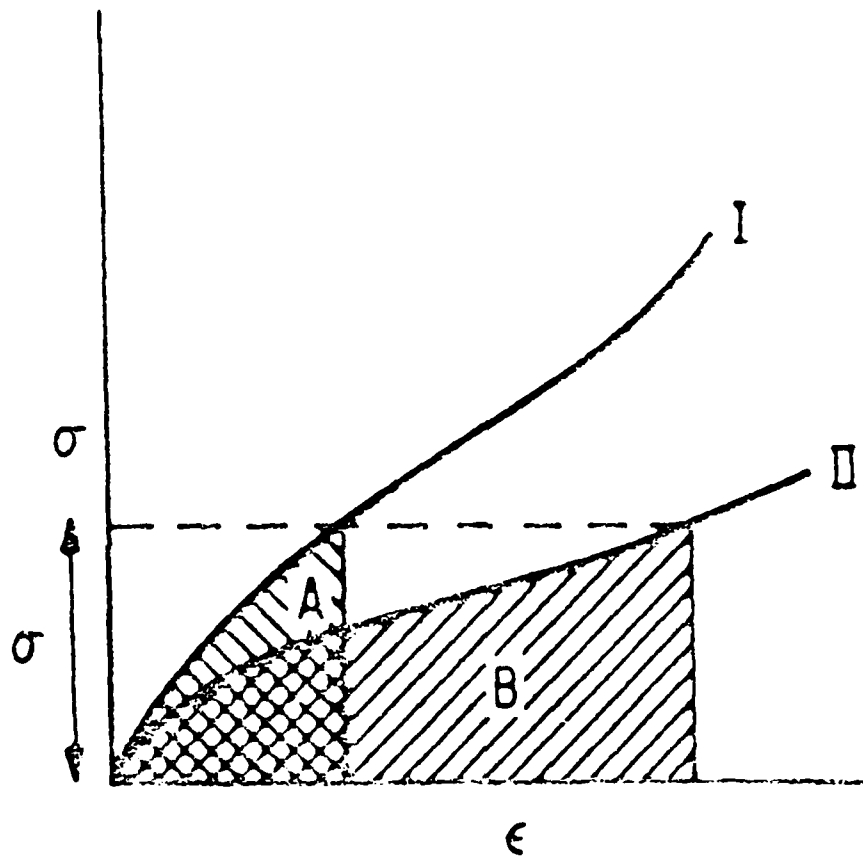
Figure 3
The difference in strain energy under constant load between stiffer
(I) and softer (II) material. [Prevorsek and Kwon, Ref 4]
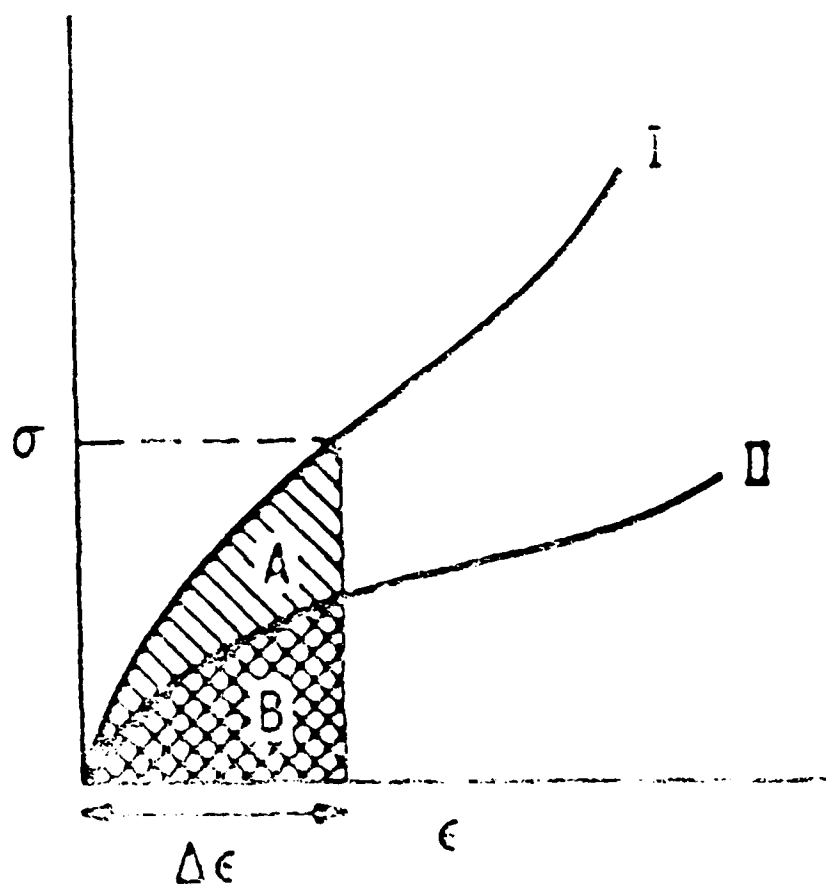
Figure 4
The difference in strain energy under constant elongation between
a stiffer (I) and softer (II) material. [Prevorsek and Kwon, Ref 4]

between fixed extension limits, found that nylon outperformed polyester in terms of cyclic lifetime. Figure 5 displays their results. Of course, a direct comparison between these two results is difficult because they dealt with different structures. Yet, it does raise the important question as to the effect of tension cycling ropes between fixed extension limits, as has been indicated by Dunn[5].

Cycling between fixed extension limits causes a dynamic load to be induced in the rope while cycling between fixed load limits induces an extension. In a purely linearly elastic structure, these would yield essentially the same results. However, because ropes are structures which behave in essentially a viscoeslastic manner and experience primary and secondary creep, these two cycling methods can be expected to yield different results.

1.3 Purpose

The purpose of this study is to establish the dynamic behavior of polyester and nylon ropes, specifically 1/2 in Samson ropes, under simulated towing conditions. The approach taken here is that the cyclic relative displacement which takes place between the tow and the tug, in a towing operation, are independent of tow hawser material or structure, which corresponds in a laboratory test to the imposition of cyclic displacement.
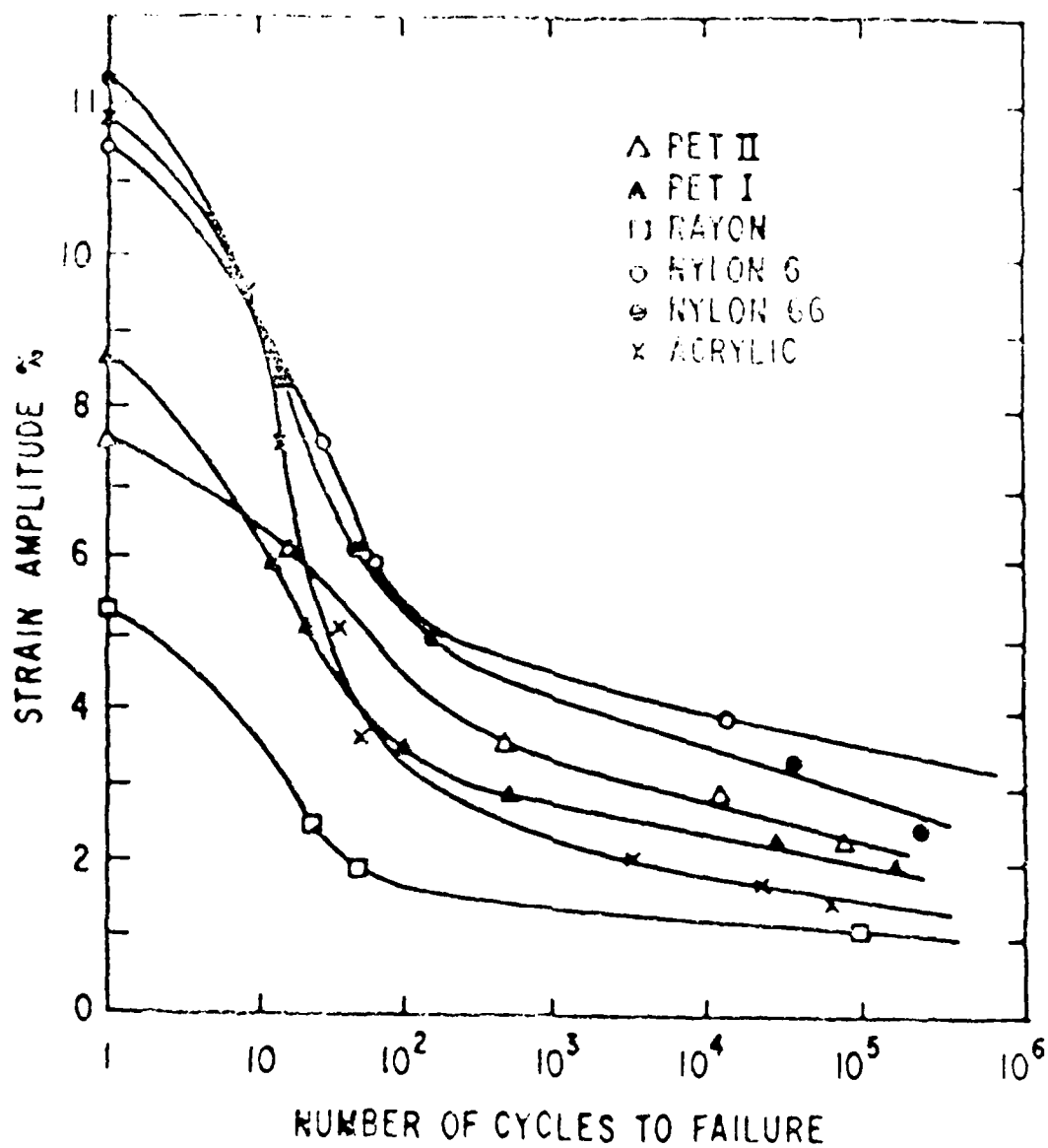
Figure 5
Number of cycles to failure as function of cyclic strain amplitude
for a variety of fibers. [Prevorsek and Kwon, Ref 4]

Chapter 2
Testing Apparatus and Materials

2.1 Testing Apparatus

2.1.1 General

Though there have been cyclic testing machines specifically designed for the use of testing fibers, yarns and ropes, such as the Lyon's [6] apparatus and the tensile testing machine at the USCG R &D Center, Avery Point in Groton, the selection of apparatus was limited by availability and economic concerns.

A configuration was desired which would allow for cycling of the designated ropes and provide feedback as to the load and elongation experienced by the rope at any particular instant, under both dry and wet conditions. The configuration depicted in Figure 6 outlines the set up.

2.1.2 Instron Model 1331 with Servohydraulic Actuator

The primary apparatus used for physically cycling the lines was the Instron model 1331 with servohydraulic actuator. It is equipped with a 10,000 lbs load cell and has a permissible stroke variation of + or - 5 inches from center. The Instron is capable of being operated in either stroke or load control with manual amplitude input. The actuator mean level, the zero position in any of the 6 different waveform functions possible, is also manually controlled. All the functions are aberrations of the basic triangular pulse function. The machine is capable of operation in a wide spectrum of frequencies.

Feedback and command load and stroke data can be monitored with the organic digital voltmeter (DVM). The DVM records, in volts, the load from the load cell and the stroke displacement from the linear variable displacement transducers (LVDT) located in the actuator.
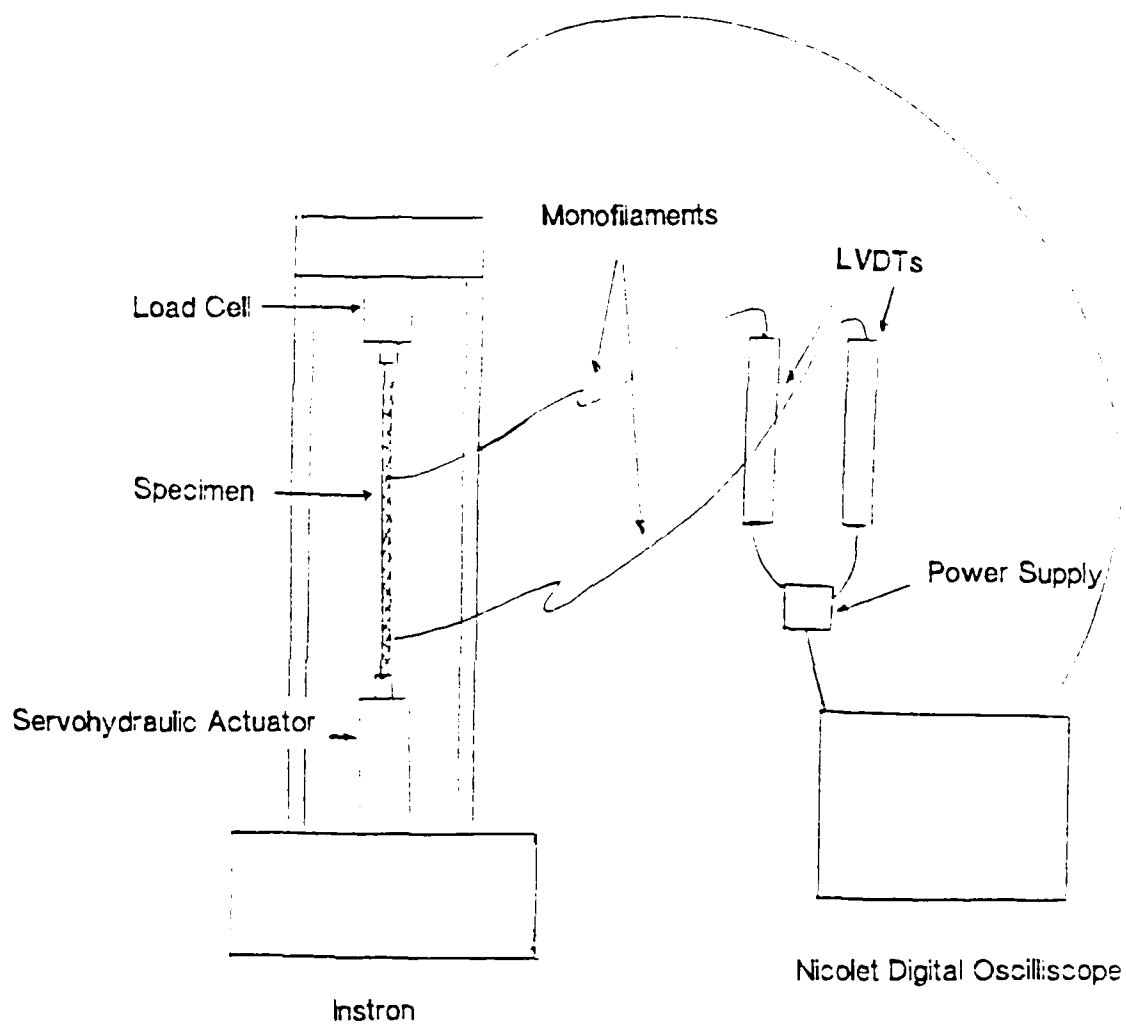
Figure 6
Experimental setup

2.1.3 Schaevitz LVDTs

In order to assure maximum accuracy as to the displacement the rope was undergoing, apart from any end effects, two Schaevitz LVDTs were mounted and connected to the rope using size 20 nylon 6.6 monofilament. The LVDTs were used in parallel and relative end displacement of the connecting points on the rope caused a voltage to be emitted. The LVDTs were capable of measuring a maximum 10 inch stroke.

In order to keep the monofilament taut, and increase the responsiveness of the LVDTs to displacement changes, 200 gram weights were suspended from the ends of the monofilament. In a series of tests, it was shown that the monofilament registered no measurable extension after being subjected to the 200 gram weight for over 72 hours. Thus, the 200 gram weight had no creep effect on the monofilament and did not degrade the accuracy of the results.

2.1.4 Nicolet Digital Oscilloscope

Both the load feedback from the Instron load cell and the LVDTs were routed to a Nicolet digital oscilloscope which was used to monitor the incoming load and displacement waveforms. The Nicolet was equipped with a disc recorder which was able to record data as displacement versus time or load versus time. However, direct indication of load versus displacement could not be recorded.

The Nicolet also possessed several software programs which were helpful in the analysis of the waveforms. The "Area XY" program was helpful in that the area inside any curve in the load-displacement viewing mode could be calculated. Since the hysteresis for any cycle is defined as such an area, this program was extensively used.

2.2 Ropes Used in the Study

2.2.1 General

There are many different synthetic fiber ropes commercially available of many different constructions. The large number of materials and constructions present

a myriad of mechanical and material properties which could be available for examination in this study.

Consideration for rope selection for the work at hand was based on the limitations of the available testing apparatus and on the requirements for upcoming towing programs. The ropes selected were 1/2 in diameter Samson Stable Braid Polyester Rope with Duron II finish and 1/2 in diameter Samson 2-in-1 Nylon Stable Braid. These double braided ropes were 1/2 in lines of the same materials and construction as the towing hawsers being considered for the upcoming Navy towing program. In a simulation of actual conditions, prototypes of the actual sized ropes to be used would have been desired since exact similitude conditions do not normally exist between various sized ropes. However, the limitation of the Instron load cell and the servohydraulic actuator restricted the size of the ropes to 1/2 in.

2.2.2 Double Braided Rope Construction

Double braided ropes are naturally held in form by their interlocking structure. According to the manufacturer, double braided ropes most nearly approach the configuration of straight parallel strand construction.

These ropes are constructed of a braided core which is inside a braided cover as shown in Figure 7. In looking at the geometry of the double braided ropes, there are several characteristics which are important. Double braided ropes are constructed of an equal number of strands with S direction helices and Z direction helices (as seen in Figure 8), hence they are torsionally stable under tension. The stability is enhanced by the twist direction of the strands, which correspond to their helix direction in the braid.

The angle that the strand helices make with the rope axis is designated as β, where $\tan \beta = 2\pi r/h$. The greater the helix angle, the greater the extension under a given load for ropes of the same material and construction. The lower the helix angle, the higher the relative strength, but the lower the stretch at any given load, including failure.

2.2.3 1/2 in Samson Polyester Double Braided Rope

The Samson Polyester rope used in the study is a high strength double braided rope when compared to double braid nylon ropes or 3 strand constructions of most fibers. It is constructed of a 8 strand core with each strand
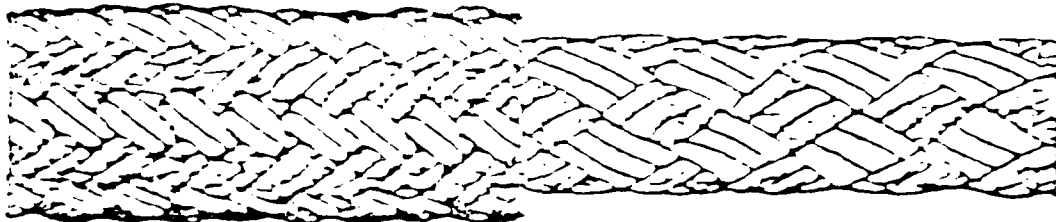
DOUBLE BRAIDED

Figure 7

The construction of a double braided rope . [Paul, Ref 12]
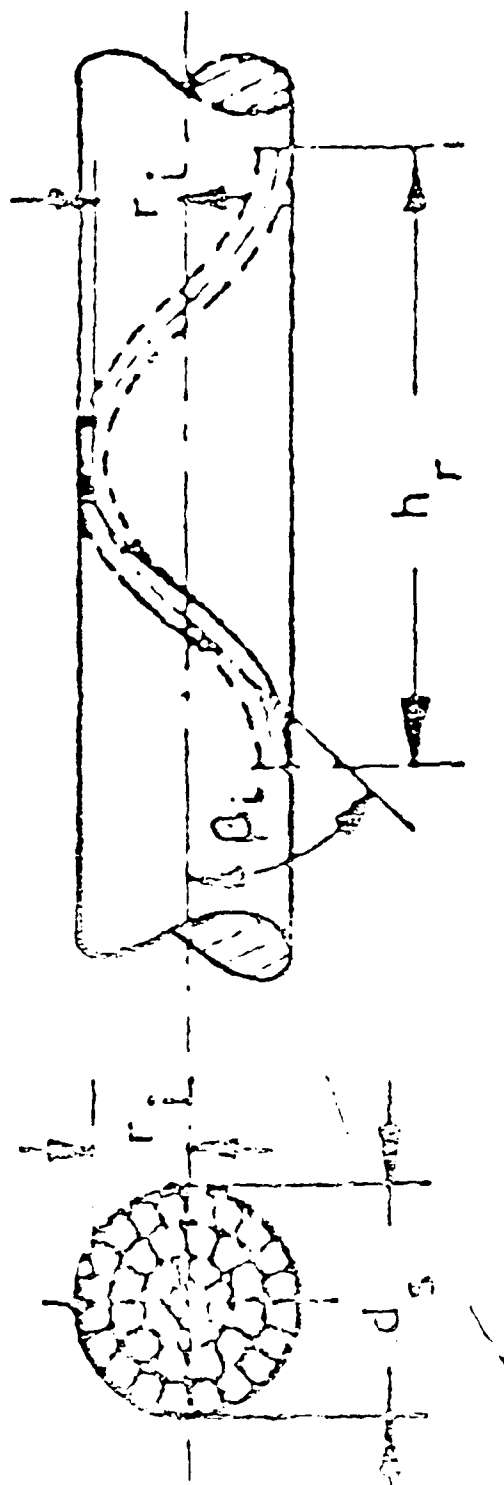
Figure 8

Geometrical representation of a rope strand as a helix

composed of 4 yarns of 14,000 denier. The core fibers are polyester 1W82 fibers made by Allied Signal Corporation. Load-elongation curves for new 1W82 fibers are shown in Figure 9. Figure 10 shows the load elongation curves for the new yarns. Over the core is a cover of 1W70 fibers also made by the Allied Signal Corporation, laid in 20 stands of 2 yarns each of 10,920 denier. The load elongation curves for these new fibers and yarns are seen in Figure 11 and Figure 12. Both these fibers are high strength fibers with the 1W70 fiber possessing the higher tenacity.

This polyester rope is rated by Samson Ocean Products as having a nominal rated breaking strength (NRBS) of 9400 lbs. Tests done at Avery Point USCG Research and Development Center for both wet and dry spliced ropes reveal the load-elongation curves seen in Figure 13. The tests were conducted with 9 ft spliced specimens. The ropes were first loaded to a tensile load of 200 $D^{**}2$ lbs where D is the diameter in inches and the appropriate gage length was measured. The rope was then subjected to 10 cycles of from 0-20% of the NRBS at a displacement rate of 11 inches per minute. Following the last cycle, the rope was ramp loaded to failure. Figure 14 shows the results for dry samples. The wet ropes were not kept continually wet, but were soaked for 24 hours prior to the test. All specimens failed in the splice.

The weight of the polyester rope, in the stretched configuration, is 8.39lbs/100 ft, or 1,123,517 denier when dry. The polyester fibers have a specific gravity of 1.38. The rope's weight increases by 65%, but experiences little geometrical change after soaking in fresh water for 24 hours. When dry, the rope has the characteristics listed in Table 2.1.

Table 2.1
Construction of 1/2 in Samson Stable Braid with Duron II

	Core	Cover
Diameter (in)	.375	.50
Circumference (in)	1.188	1.57
Period (in)	2.28	2.05
Helix Angle (deg)	27.33	37.72
Picks Per Inch	1.75	4.88
Strands	8.00	20.00
Yarns per Strand	4.00	2.00

The temperature for initial degradation of the fiber properties is 177 ° C while the melting temperature is 243 ° C according to the manufacturer.
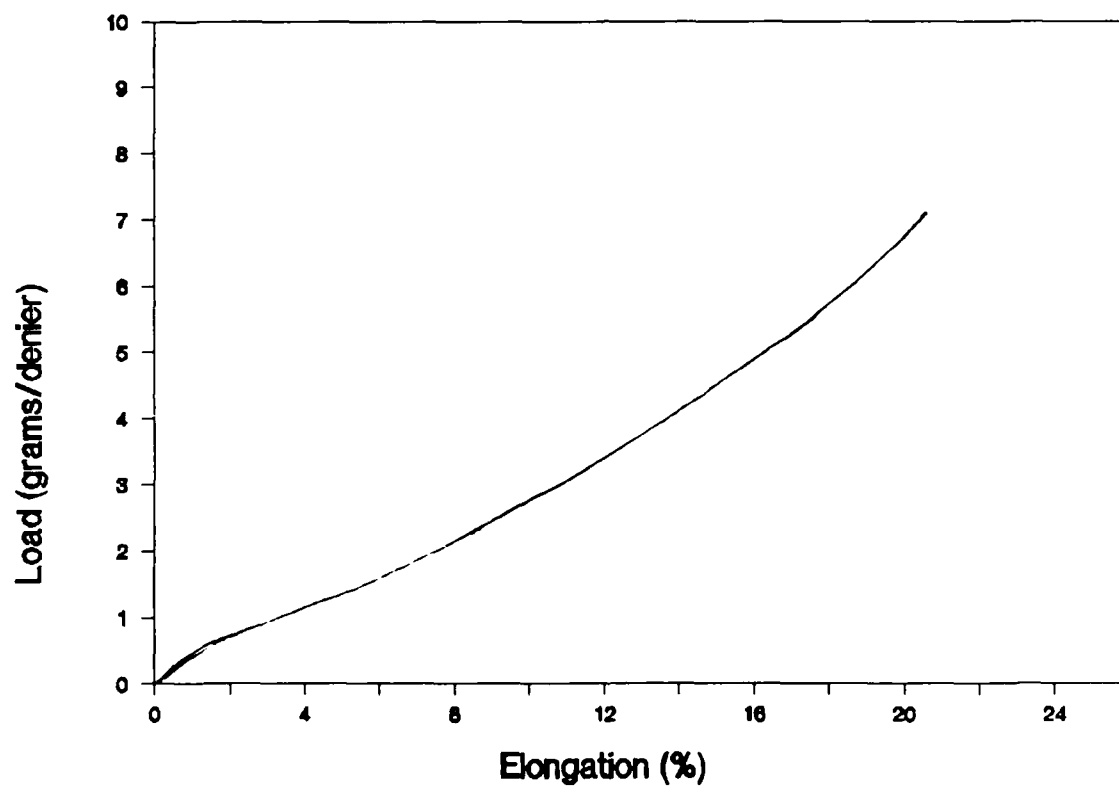
Figure 9

Load–elongation curve for new, 1W82 polyester fibers

(Based on tests of 10 fibers)
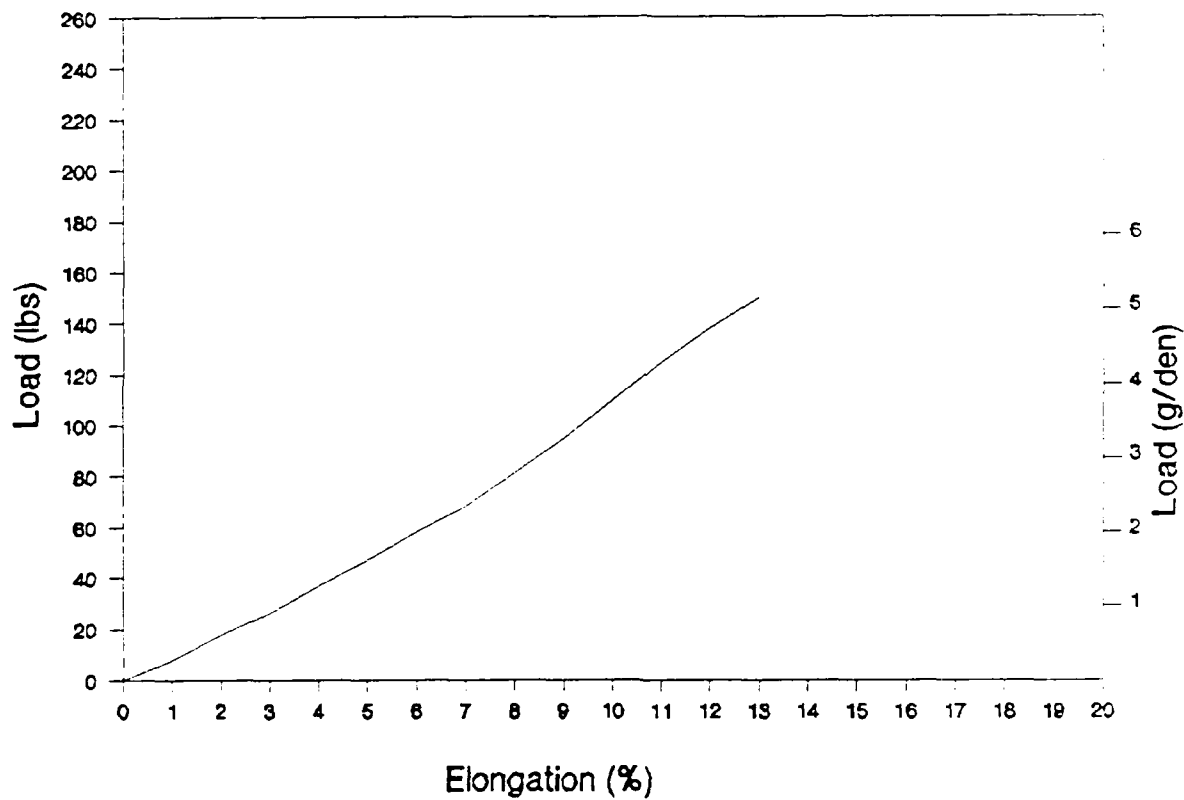
Figure 10
Load–elongation curve for 1W82 twisted polyester core yarns
(14,000 denier, based on the tests of 5 yarns)
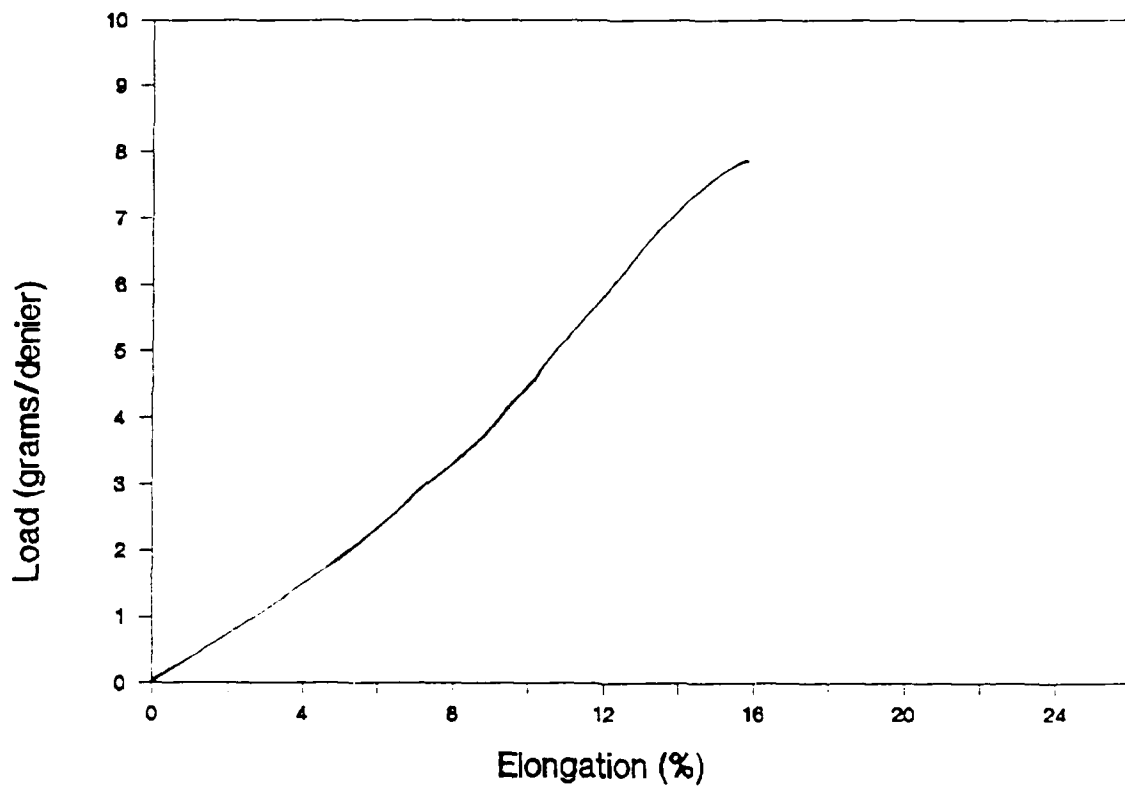
Figure 11

Load-elongation curve for new, 1W70 polyester fiber

(Based on tests of 10 fibers)
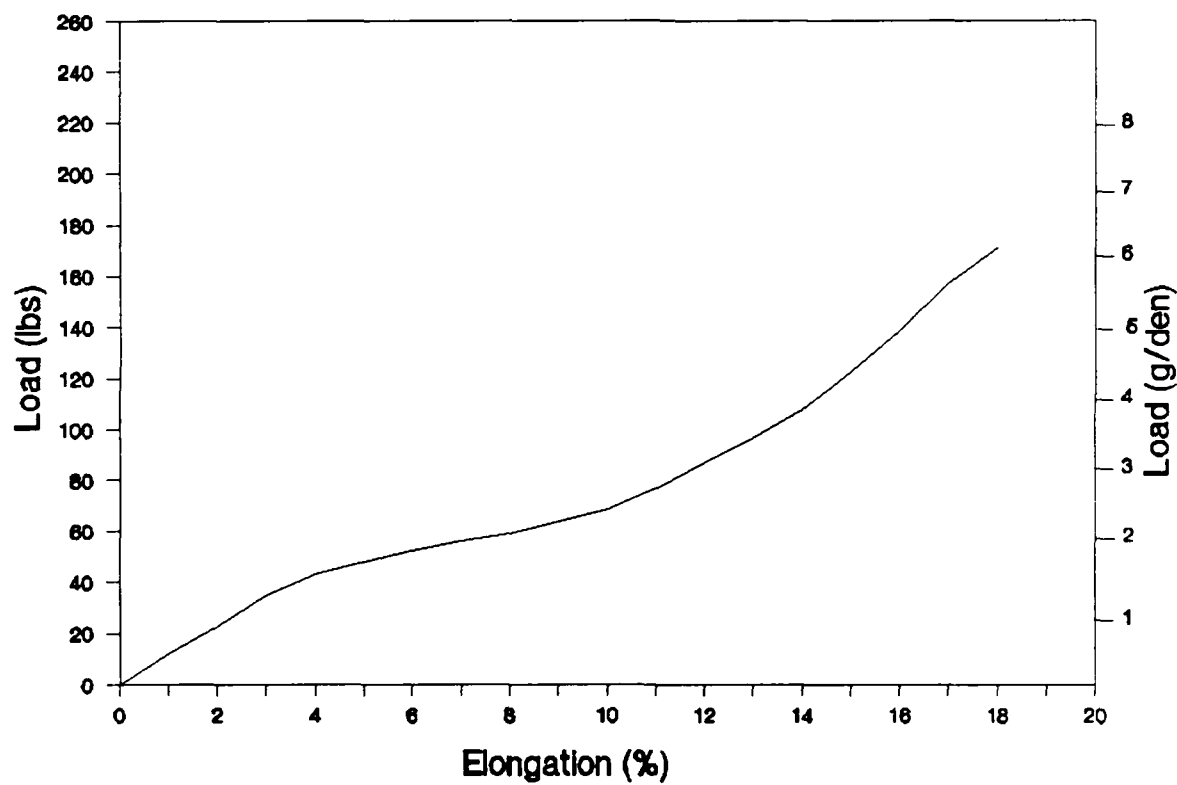
Figure 12

Load–elongation curve for 1W70 twisted polyester cover yarns.
(10,920 denier, based on tests of 5 yarns)
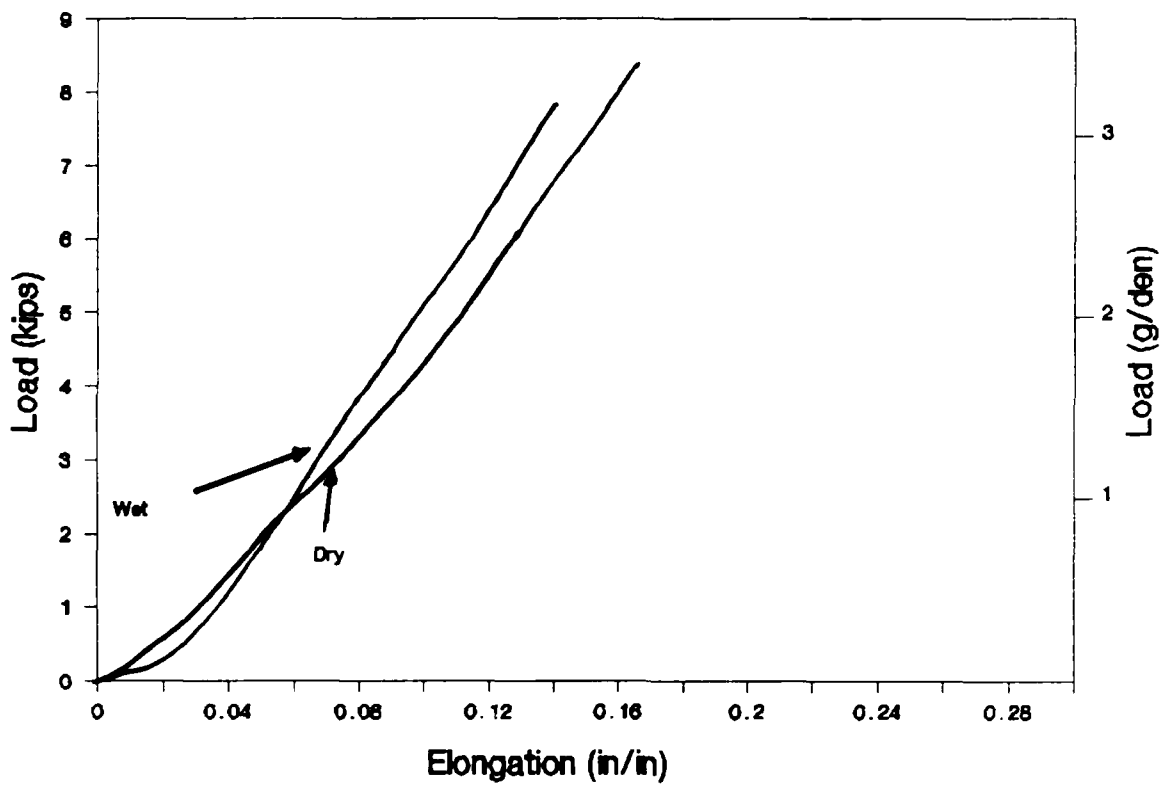
Figure 13

Load–elongation curve for new 1/2" Samson Stable Braid
Polyester Rope with Duron II
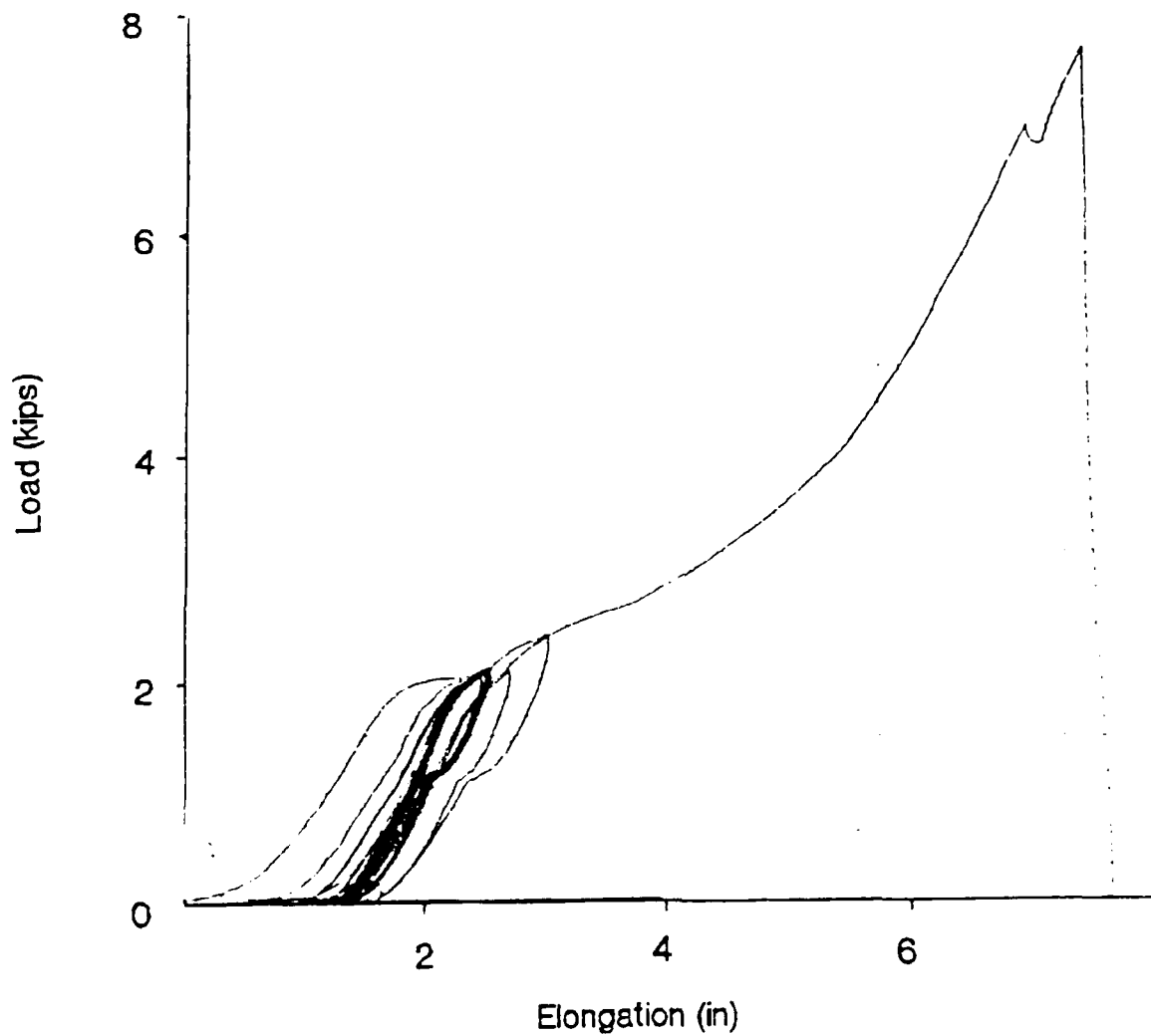
Figure 14
Load–elongation history for a polyester dry tensile
test conducted at the USCG R&D Center, Avery Point.

2.2.4   1/2 in Nylon Double Braided Rope

The nylon rope used in the study is 1/2 in Samson 2-in-1 double braided rope. The nylon double braided rope is a rope of higher extensibility but lower ultimate tensile strength than comparable polyester ropes.

The nylon rope is constructed of a cover of 20 strands of 2 yarns of 7,560 denier. The fiber used in the cover is Dupont 707 nylon 6.6 fiber whose load elongation curve is shown in Figure 15. The core is also composed of this fiber and is constructed of 8 strands of 4 yarns of 15,120 denier. Load-elongation curves for the cover and core yarns are shown in Figures 16 and 17.

A comparison of these fibers with those used in the polyester rope described in 2.2.3 reveal that the fibers used in the nylon rope are more extensible than both polyester fibers and have a higher strength than the polyester fibers.

This rope is listed by the manufacturer as having an NRBS of 8500 lbs. Tests similar to those described in 2.2.3 were done using 9 ft spliced specimens, both wet and dry. The results in terms of load-elongation curves are shown in Figures 18, 19 and 20. The relatively low ultimate strength shown is due to the stress concentration in the splice. All the nylon specimens failed in the splice.

The weight of the nylon rope is 6.34 lb/100 foot, or 789,800 denier. Nylon filament has a specific gravity of 1.14%. The rope's weight increased by 82% when soaked in fresh water for 24 hours. Geometrically the nylon rope was reduced 2.8% in length when soaked in the water and swelled 11.7% radially. These values were found by measuring the geometric properties of 5, 5 foot sections of dry line and then soaking them for 24 hours in fresh water at 20 C. According to the manufacturer, the melting temperature for the nylon fiber is 238 C with a degradation temperature of 170 C. Table 2.2 lists other properties of the rope.
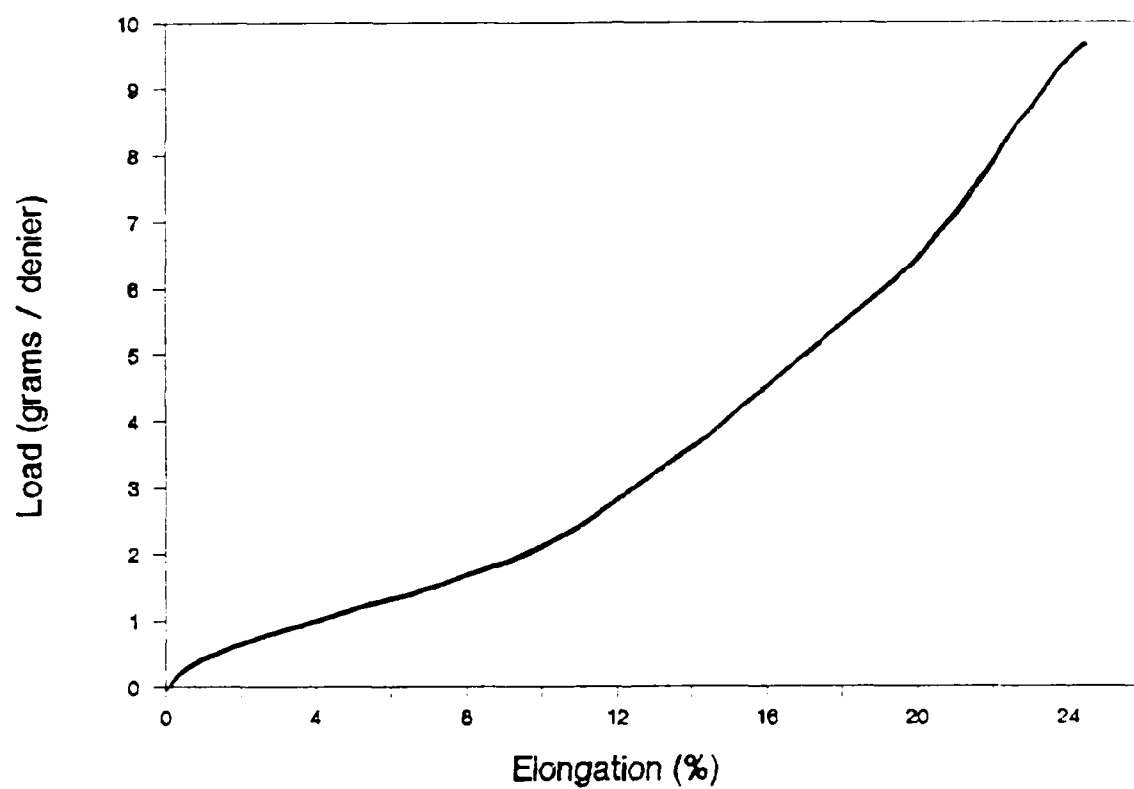
Figure 15
Load–elongation curve for new nylon 6.6 fiber
(Based on tests of 10 fibers)
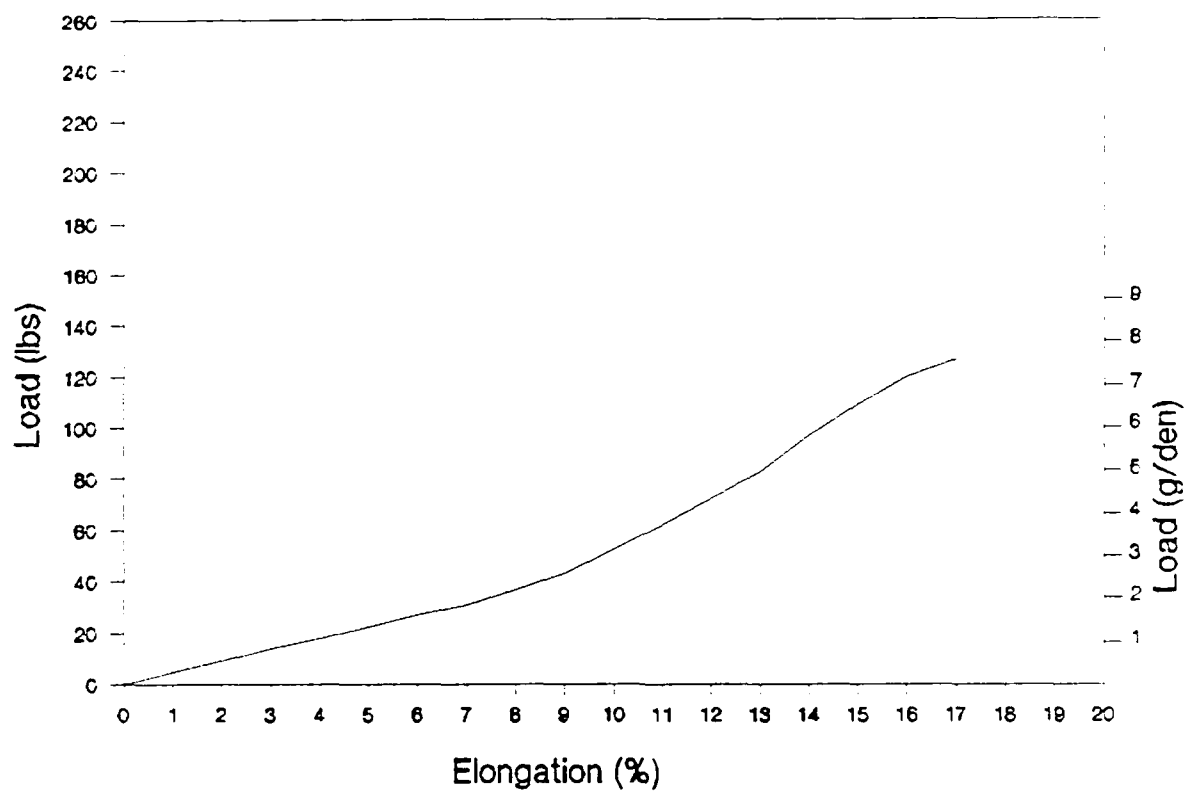
Figure 16

Load-elongation curve for twisted nylon cover yarns
(7,560 denier, based on tests of 5 yarns)
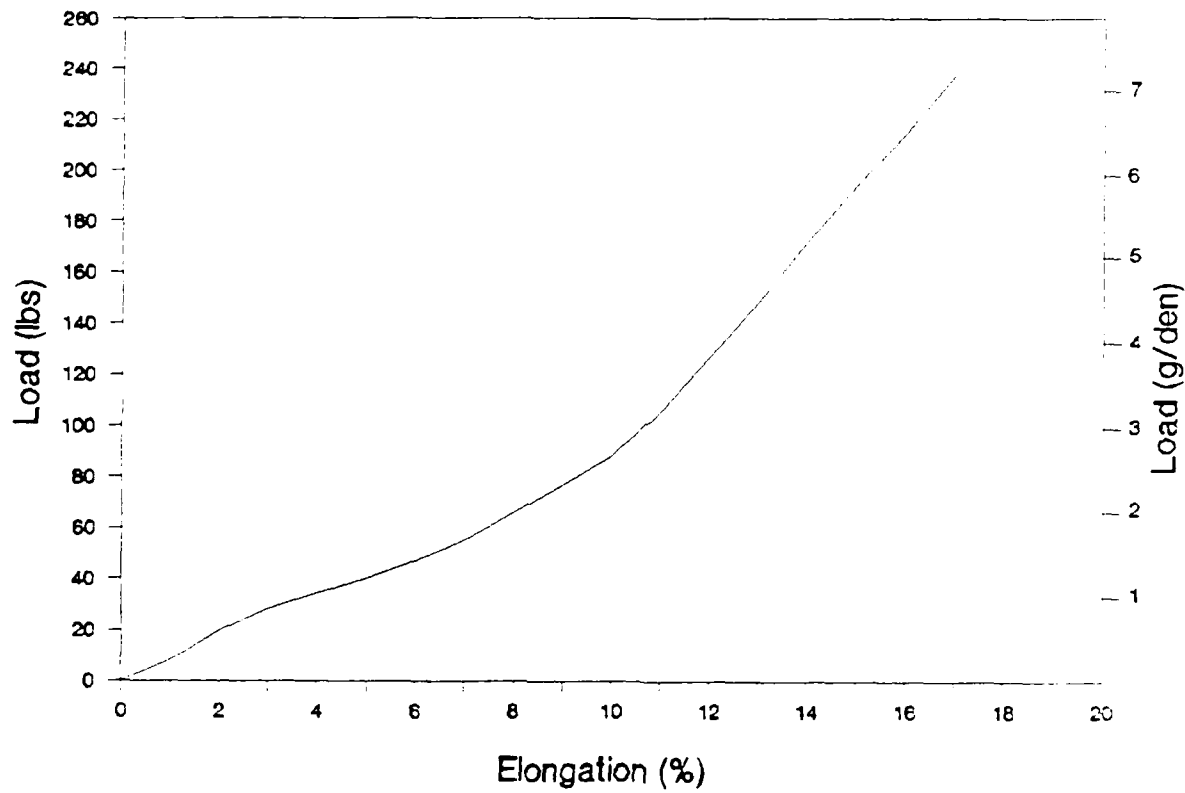
Figure 17
Load-elongation curve for twisted nylon core yarns
(15,120 denier, based on tests of 5 yarns)
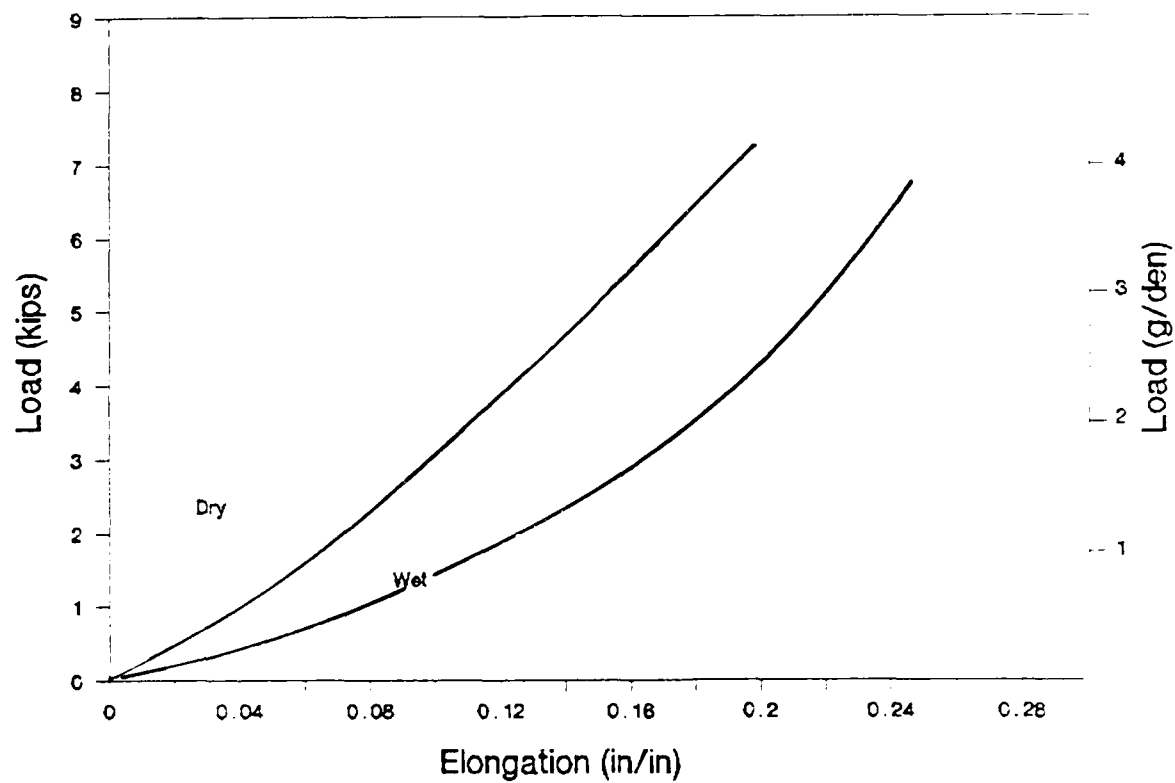
Figure 18

Load-elongation curve for new 1/2" Samson 2-in-1 Nylon
Double Braided Rope
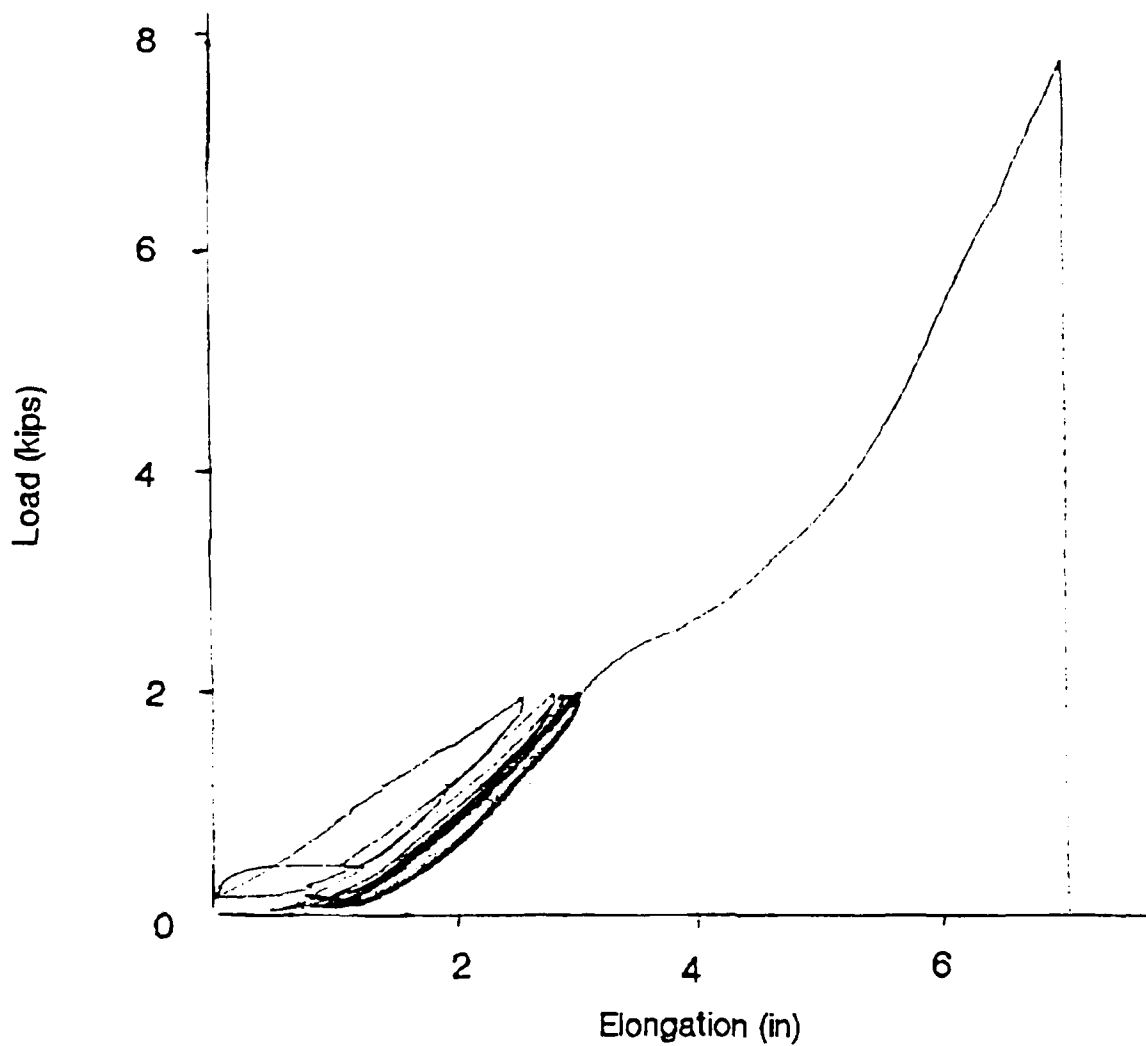
Figure 19
Load–elongation history for a nylon dry tensile
conducted at the USCG R&D Center, Avery Point.
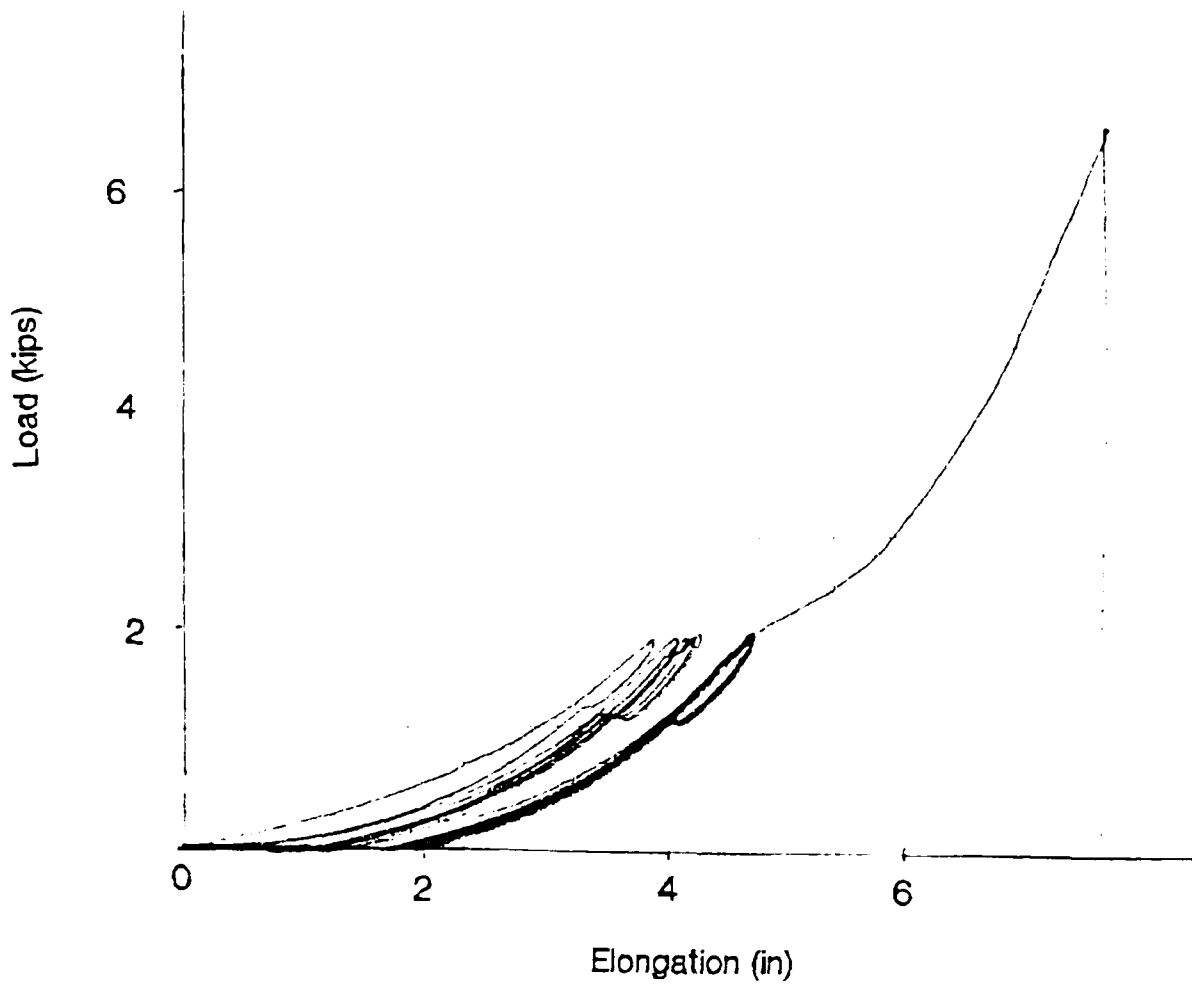
Figure 20
Load-elongation history for a nylon wet tensile
test conducted at the USCG R&D Center, Avery Point.

Table 2.2

Construction of 1/2 in Samson Nylon 2-in-1 Double Braided Rope

	Core	Cover
Diameter (in)	.375	.50
Circumference (in)	1.19	1.57
Period (in)	2.00	2.05
Helix Angle (deg)	30.50	37.72
Picks Per Inch	2.00	4.88
Strands	8.00	20.00
Yarns per Strand	4.00	2.00

2.3 Rope Mounting Techniques

2.3.1 General

One of the key problems to be addressed in conducting the cycle tests on the 1/2 in rope was the development of a technique to properly mount the ropes on the Instron. The mounting technique developed was to be reproducible and compatible for both wet and dry testing. Also. the method had to allow for a long enough free span in order to make displacement readings meaningful, but not so long that the rope loading was restricted by the stroke length of the servohydraulic actuator. Further, the method had to minimize, as much as possible, slipping at the mounting point. In order to meet these requirements, two methods we re developed , a specially designed short splice for dry testing and a potted grip for wet testing.

2.3.2 Short Eye Splice

In past studies pinning the rope with eye splices to the jaws of the Instron, has been the preferred method of mounting the rope. It has the advantage of being easily and consistently reproduced. A disadvantage is that it presents a nonuniform structure at the extremities. An additional disadvantage is that conventional splices for 1/2 in double braid rope, when restricted to 42 in eye to eye (gage length), the maximum Instron jaw distance which would permit full advantage of the actuator stroke length, allows for only 4-5 inches of unspliced

section. Since the majority of the specimen would be a nonuniform structure with a relatively small section of free length, it was felt that results would not accurately depict true conditions where the spliced section is a small percentage of total length. In order to rectify this a short splice with the dimensions shown in Figure 21 was developed. The new splice had the advantage of maintaining a strength comparable to conventional splice, but allowed for a generous free length.

2.3.3 Potted Grip and Wet Cell

In order to test the ropes under wet conditions, it was necessary to ensure that the rope remained wet during the entire cycling process. In past studies, this has been accomplished by continually spraying the rope or immersing the rope in a water filled testing cell. Because of the confines of the testing area and the vertical position of the ropes during testing, it was decided to construct a unique wet testing apparatus.

The apparatus developed consisted of two potted grips which securely held the ends of the rope. The lower grip was firmly attached to a clear lexan tube. Rubber O-rings formed a water tight seal. The upper rope end was attached to a 15 inch attachment which fit inside the tube. Thus, as the actuator moved in its cycling pattern, it moved the tube over the upper attachment. This set up allowed for free span lengths of up to 36 in and allowed for 100% immersion.

The ends of the rope were potted using a polyester thermoset resin. Silicon rubber was used on the rope at the point where the rope end entered the grip in order to prevent polymer wicking into the rope and to allow for effective stress transfer at the point where the rope entered the grip. Figure 22 depicts the potted grips.

There were several limitations associated with using the potted grip. The first limitation was that it took approximately 24 hours to prepare each sample. This restricted the number of specimens which could be tested. A second limitation was that a small amount of slippage occurred at the potted ends. Since the elongation was based on the original length, the slippage forced the use of an external LVDT rather than using the actuator displacement.
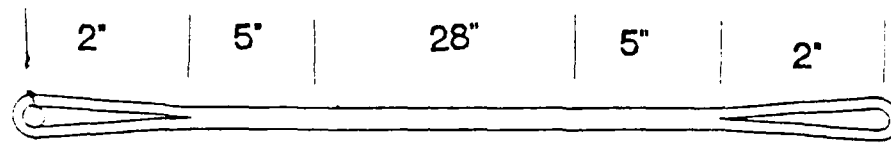
Figure 21

Dimensions of spliced specimens
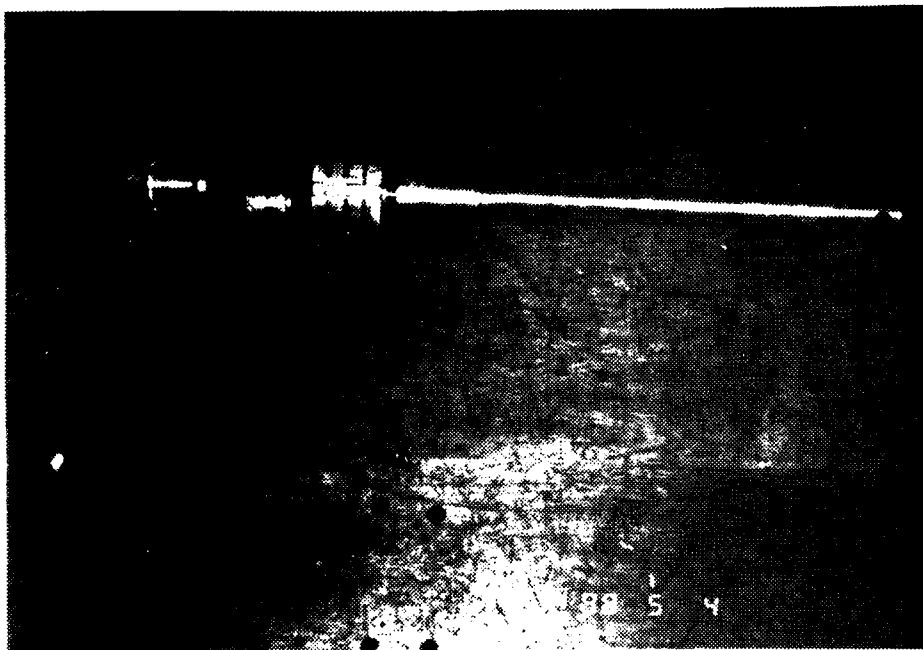
Figure 22
Potted grips used in the study .

Chapter 3
Towline Tension Simulation

3.1 General

Paramount to the objective of this study was the development of a method, at least to a first approximation, to simulate the tensions experienced by a tow during actual operations. A first task was to define what tensions actually act on the rope and of what field variables these tensions are functions. Secondly, using the apparatus available, it was necessary to develop a method of simulation which adequately represented the actual conditions but maintained the number of independent variables at a manageable level. Lastly, for the independent variables identified, it was necessary to discern a realistic range of values for testing. The simulation process would produce the independent variables to be manipulated, within the designated range of values, so as to discover their effect on the dynamic behavior of the rope.

3.2 Towline Tensions

3.2.1 General

In order to discover what factors contributed to the tension being experienced by the rope, it was necessary to investigate what actually happened to the rope and what forces acted on it. In defining the forces acting on the rope, three basic types are identified. There is a steady tensile force. A tension induced by the towed vessel yawing across the centerline of the tow as in Figure 23. A third tensile force is induced by relative vessel displacement caused by waves present in the marine environment.

3.2.2 Steady Tension

The steady tension is the tension or force which would exist if there were no waves and no yawing. It is a function of many field variables, most notably

YAW ANGLE
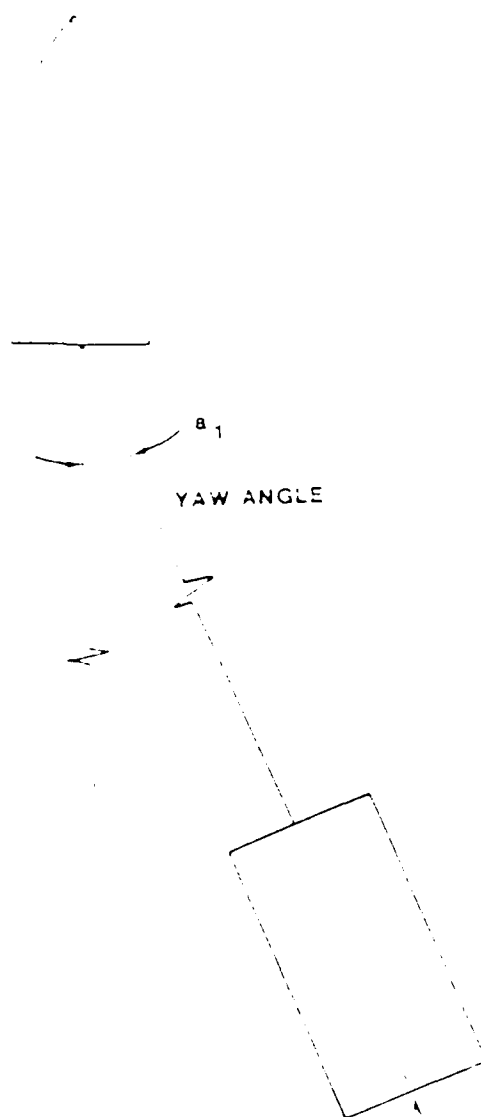
Figure 23
An representation of a vessel yawing . [Ref 7]

the tow speed, heading, wind speed and the aerodynamic and hydrodynamic resistances of the vessels involved, as well as resistances on the rope itself.

For many tows of sufficiently long duration, such that the variables defined above are essentially constant, the steady tension can be treated as the constant as marked with the dashed line in Figure 24. Since this load is essentially a static load which is always present, it can be easily simulated. For any dynamic loads or displacements superimposed over the steady tension, the steady tension is that load which is present when the dynamic forces are at their zero level position.

3.2.3 Yaw Tension

The tension caused by the slowly varying yaw and slideslip of the tow across the centerline of the tow, as seen in Figures 24, can be considered as a quasi-static tension. The slow swinging of the towed vessel from side to side of the course line normally takes several minutes. The load induced by this motion also takes several minutes to go from a maximum to a minimum. Because of this large period, and because the servohydraulic actuator can only generate one function at a time, the yaw tension is neglected in this first approximation.

3.2.4 Dynamic Tensions

The tension due to the wave induced seakeeping motions of the tug and tow is a dynamic tension component of the total tow-line tension. As shown in Figure 24, it is a very random process, replete with half-periods. The dynamic tension depends on the dynamic responses of the tug, tow and towline to time varying forces. In actual practice, the time taken for the tension to vary from a maximum to a minimum range from 1 to 15 seconds.

In most practical applications, the random process is dealt with on a statistical basis based on the largest acceptable rope tension and the probability of encountering a load in excess of this tension. For the purposes of this study, the dynamic tension will be simulated by applying a triangular wave of varying displacement amplitude and frequency. This triangular displacement wave will be superimposed over the steady tension such that, if the displacement waveform
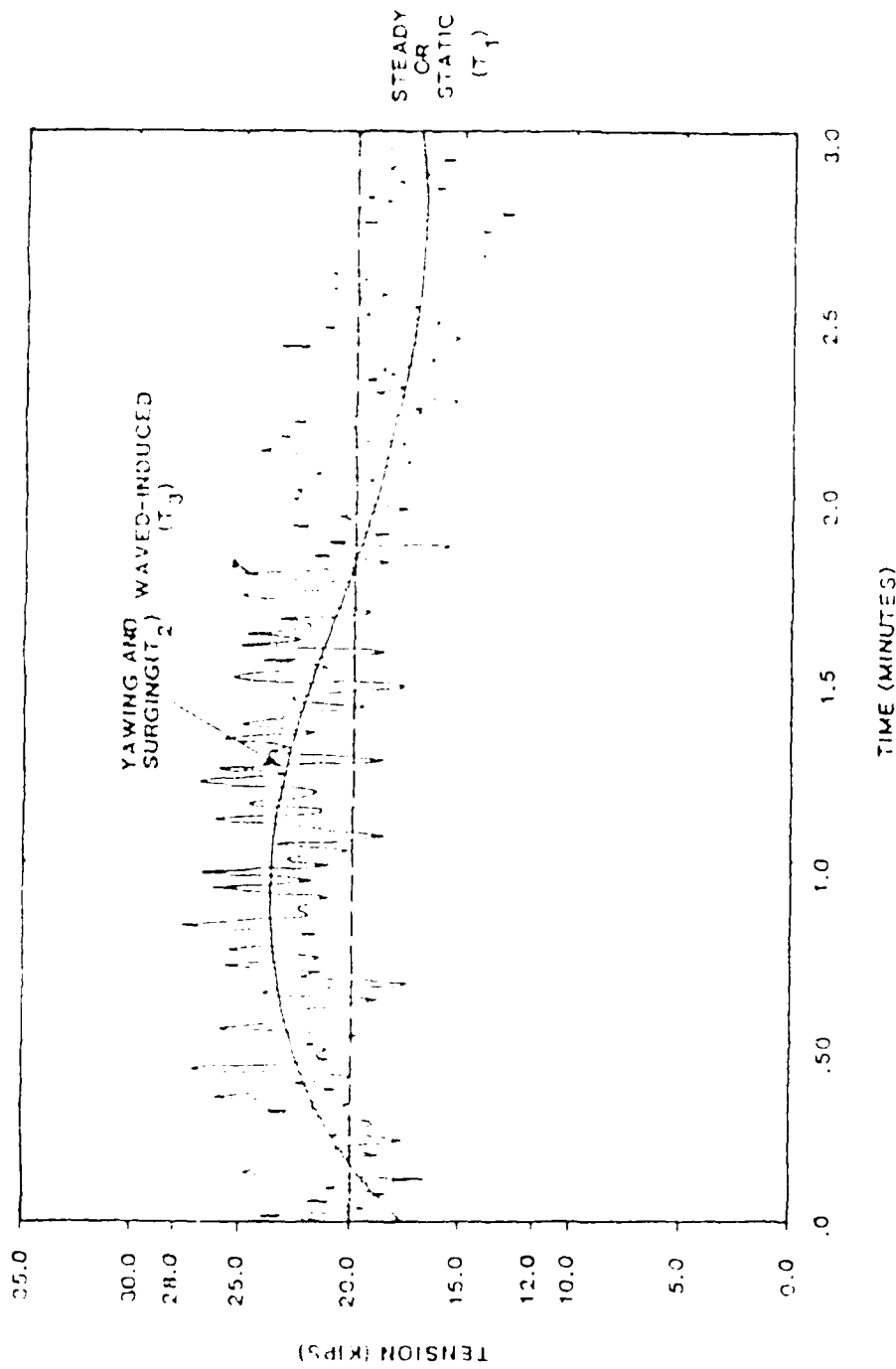
Figure 24

The components of the towline tension. [Ref 7]

were removed, the tension remaining in the rope would be the steady tension. Figure 24 illustrates this effect.

Applying the dynamic load induced by a constant displacement waveform is felt to more closely approximate the true motion of the vessels in the dynamic environment, in contrast to imposing a load waveform. In actual operations, it is the wave heights and period which primarily induce the dynamic tension in the rope.

3.3 Independent Variable Ranges

Based upon the discussion in section 3.2, the independent variables associated with the simulation are the steady load, the displacement waveform which is expressed as strain amplitude and the cyclic wave frequency. In order to determine an appropriate range of values for each independent variable, it was necessary to investigate existing rope data and data relevant to the normal motions of vessels in actual operations.

It was decided that the appropriate range of values for the steady tension should be from 0-25% of the NRBS of the rope based upon the Samson usage guidelines and other sources. This translated to up to 2.125 kips for the 1/2 in nylon and 2.35 kips for the 1/2 in polyester. Since these ropes are listed as being safe, for static loads, for extended use up to 20% of the NRBS, the steady tension range provides a responsible upper bound while still being in the low load range.

The cyclic frequency range is based on actual data for normal wave frequencies. Wave periods usually occur in the order of from 1 to 15 seconds which translates from 1 to .0667 Hz for acceptable frequencies.

Strain amplitude data was slightly more difficult to determine since most data available records the load history as a function of time. The option selected was to select a reasonable strain amplitude range and examine w hat peak loads were induced, then, based on load data, modify the strain ranges accordingly [9].

All the ranges include both wet and dry rope. Since normal operations include both wet and dry sections, both conditions must be examined.

Chapter 4
Experimental Procedure

4.1 General

Using the aforementioned apparatus and ropes, procedures were developed to determine the change in the dynamic modulus, K, and the hysteresis, H. Both these values were normalized with respect to the original length of the rope and are expressed in units of force x length/length. In the course of the testing, data was also taken of the temperature, total elongation, residual elongation, change in geometry, and the maximum and minimum loads experienced by the rope.

The following procedures for both dry and wet testing were developed to examine the change in the dependent variables of stiffness and hysteresis by manipulating the independent variables of steady tension, frequency and strain amplitude.

4.2 Dry Testing

The method of testing, with the exception of the applied raw values for loads, was the same for both polyester and nylon rope. The ropes were spliced with eye splices at both ends. Samples were from 37-42 inches measured crotch to crotch with a 2 inch eye. It was desired to have a standing portion of at least 20 inches.

In order to test the ropes, the spliced specimens were mounted on the Instron using pins through the splice. Since the internal LVDT which measures the displacement of the piston could not be used to record displacement in the standing section, due to the nonuniform nature of the spliced sections, 2 LVDTs were set up to record specimen displacement by connecting the LVDT monofilaments to the ends of a gage length restricted to the standing section of the line.

Load output, measured directly from the Instron load cell, and the LVDT output were fed directly to the input channels of the Nicolet. Also, a thermocouple was inserted into the center of the rope at the center of the free span to record the rope's core temperature.

The ropes were loaded to a load of 200D**2, where D is the diameter of the rope in inches, and the gage length A was measured in accordance with the Cordage Institute Standards.

The frequency control and the stroke in put were then set to their designated values. It was necessary to run one or two trial cycles at low loads in order to insure that the external LVDT feedback data actually represented the correct strain variation. The rope was then ramped to the steady tension, the function generator was started and cycling was initiated.

During cycling, particularly during early cycles when the rope's structure was continuously adjusting, it was necessary to diligently monitor the cycling process and manually control the stroke mean level to insure that the desired steady tension was being maintained. Waveform monitoring was done via the Nicolet. Periodically, cycling was halted in order to make adjustments to the mean level and remove slack resulting from creep or slippage.

During the course of the cycling, the core temperature was monitored and recorded at appropriate intervals.

As the rope cycled, changes in the elongation and changes in stiffness gradually decreased and the load-elongation curve became a repeatable closed curve. At this point, the rope was said to be stabilized with respect to its loading condition. For the purposes of the study, a rope was considered stabilized when its maximum load changed by less than 10 lbs over a 100 cycle period or 10,000 cycles were reached, which ever occurred later.

Following stabilization, the elongation at the steady tension was recorded and listed as length B. Cycling was then interrupted and the rope was returned to 200D**2 force and the length was measured. This measurement was defined as length C. The rope was then relaxed in a slack position for 30 minutes. Following the relaxation time, the rope was returned to 200D**2 and length D was measured.

In accordance with the standards prescribed by the Cordage Institute, the following elongations were calculated:

% Total Elongation = (B-A)/A X 100
% Non-Elastic Elongation = (C-A)/A X 100
% Residual Elongation = (D-A)/A X 100
% Recoverable Elongation = (C-D)/A X 100

The dynamic modulus, K, was based upon the load elongation curve, that is, K represents the secant modulus over a given load or strain increment. Specifically, K is equal to the ratio of the difference between the maximum and minimum load and twice the strain amplitude. A representation of K is shown in Figure 25.

The hysteresis, H, was calculated based upon the area inside the loading and unloading stabilized curve. This was done using the Area XY program discussed in Chapter 2. Figure 26 graphically defines the hysteresis.

4.3 Wet Test

The procedure for the wet test followed the same procedure as the dry test with the exception of the differences noted in the following paragraphs.

Rather than using splices, the rope was mounted using the grip and cell construction described in Chapter 2. Due to occasional slipping of the rope at the point of entry of the rope into the grip, the external LVDTs were used to measure the displacements.

A problem was posed as to the sufficiency of the water in the cell to serve as a reservoir. Careful monitoring of the water temperature indicated only minimal temperature rise in the water at the most potentially extreme rope temperatures, based on the dry results. Apparently, within the scope of the study, the water cell served as a effective reservoir.

4.4 Errors in the Hysteresis Loop

Figure 27a shows a typical hysteresis loop which represents actual load and elongation feedback from the load cell and the external LVDTs. As can be seen, there is considerable sinusoidal motion in the curve which was caused by unavoidable, irregular motions in the rope-monofilament-LVDT connection. Figure 27b shows the elongation versus time for this case. In an attempt to eliminate these irregularities, a smoothing program was employed on the data shown in Figure 27a. The program, "N-Point Smooth" which is part of the Nicolet Standard Waveform analysis software package, takes the average values of points from 1 to N points. In effect, it calculates a weighted running average
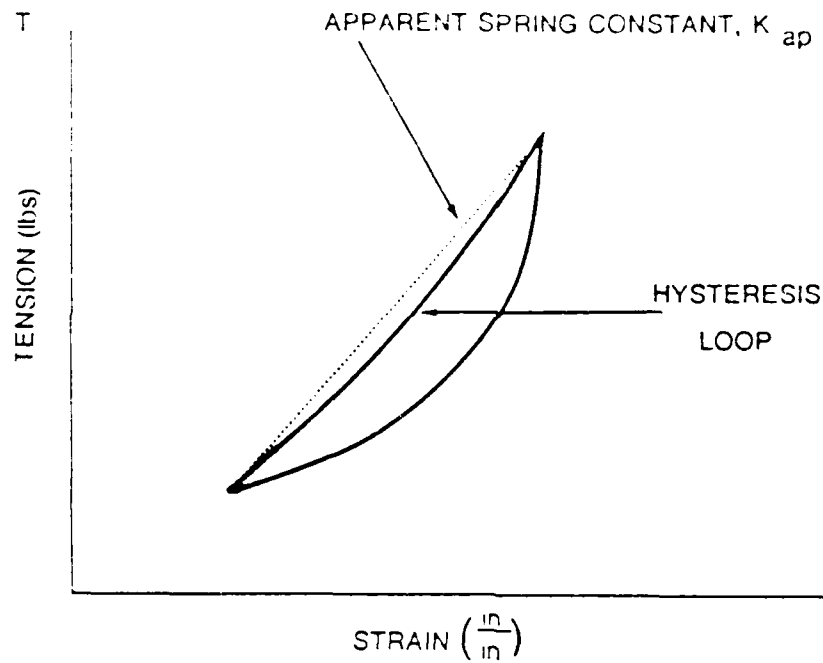
Figure 25
Representation of a stabilized loading-unloading curve
showing the dynamic modulus, K, and the hysteresis, H. [Ref 10]
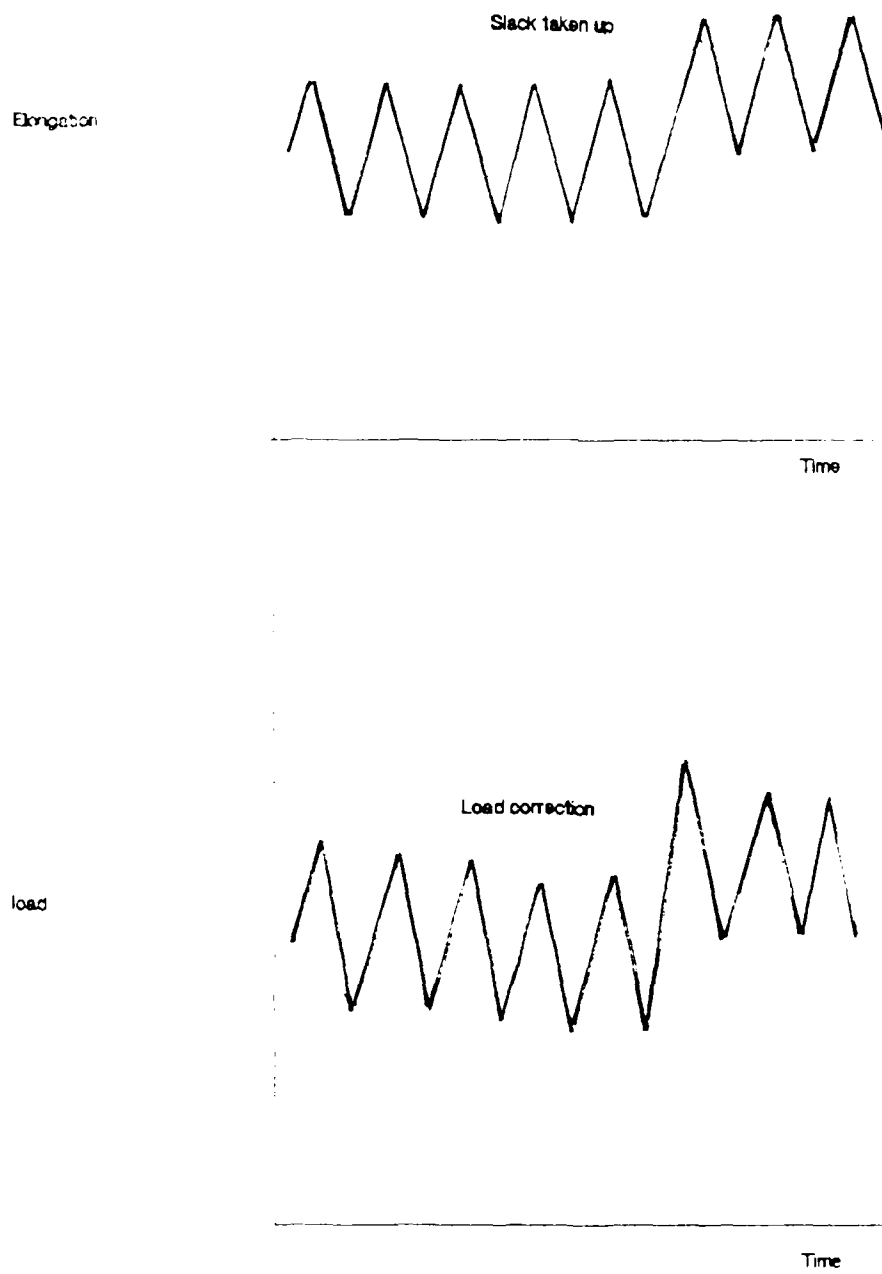
Figure 26
Removal of slack
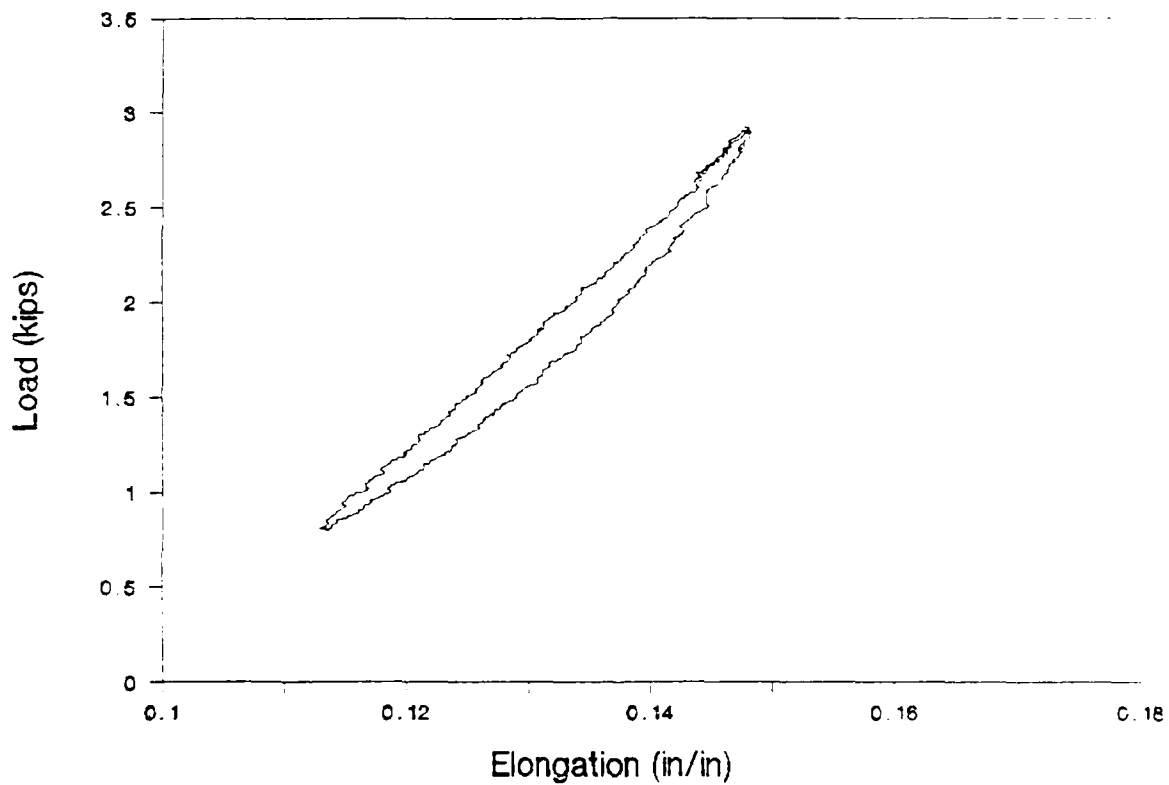
Figure 27a

Unsmoothed hysteresis curve for nylon rope, dry, cycled at a steady
tension of 1.8 kips, frequency of .2 Hz and a strain amplitude of
.017 in/in.
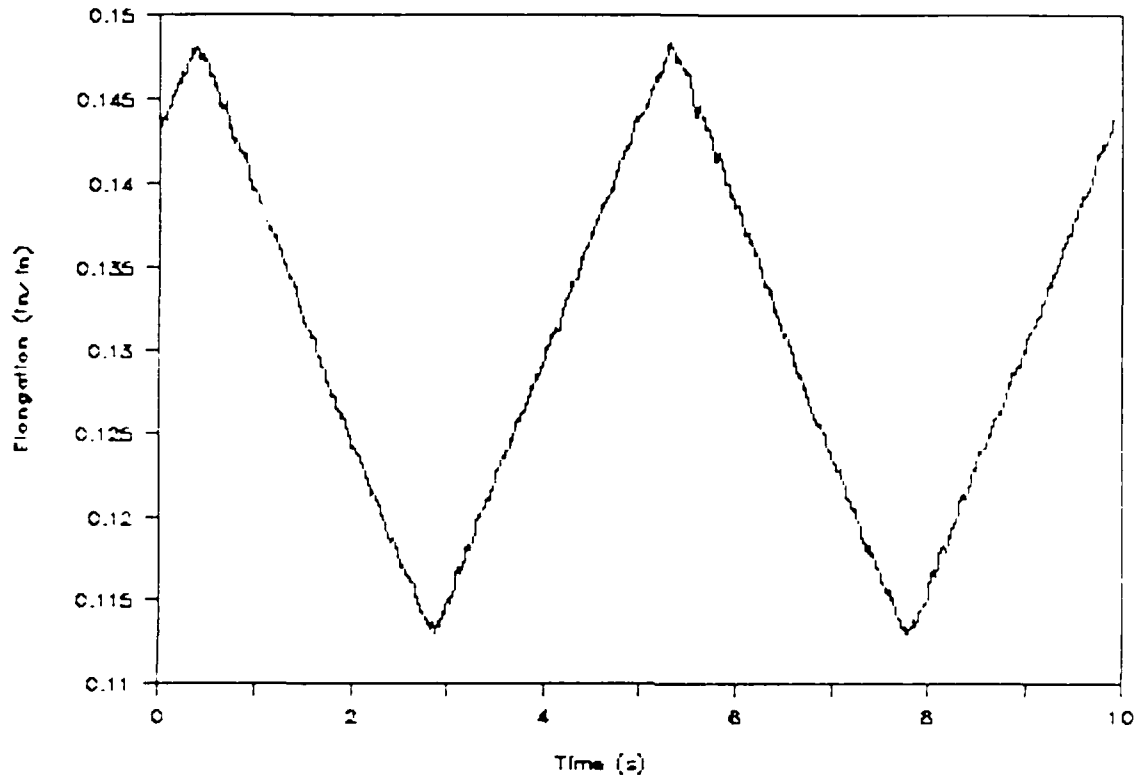
Figure 27b

Unsmoothed elongation versus time for nylon, dry, cycled at a
steady tension of 1 . 8 kips, frequency of . 2 Hz and a strain amplitude
of . 017 in/in .
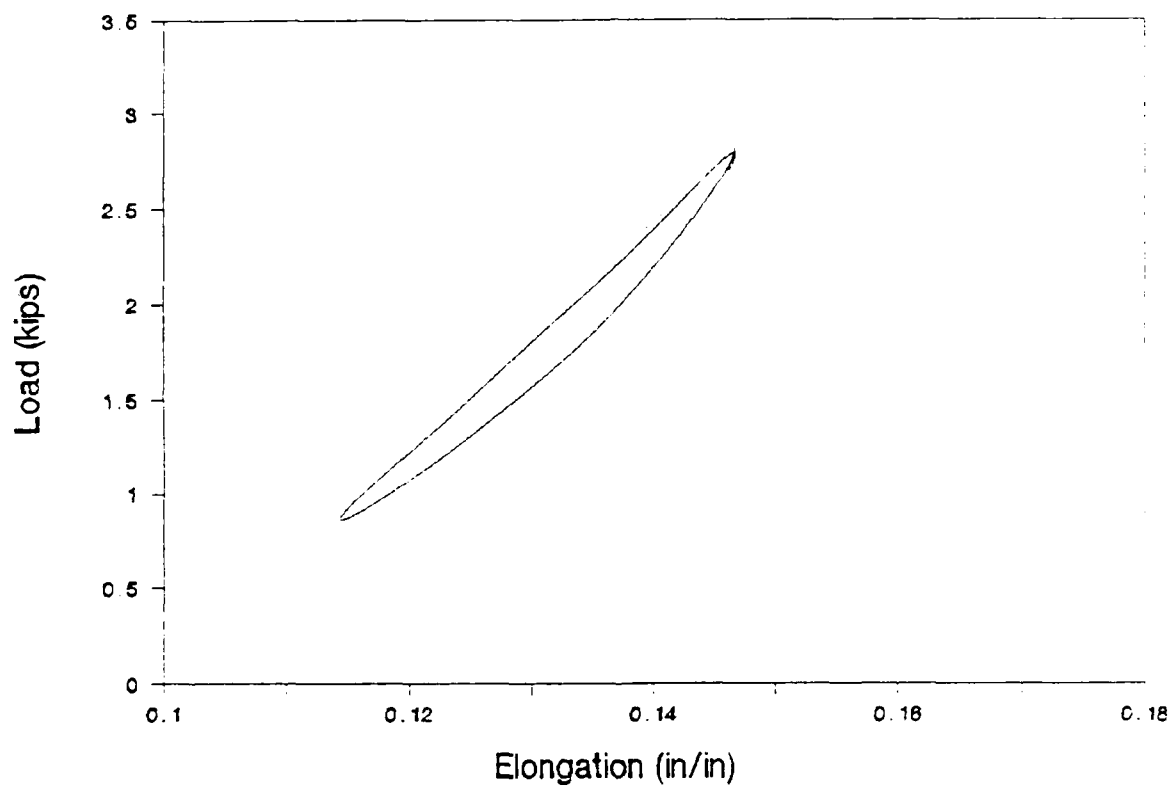
Figure 27c
Smoothed hysteresis loop for nylon, dry, cycled at a steady tension
of 1.8 kips, frequency of .2 Hz and a strain amplitude of
.017 in/in
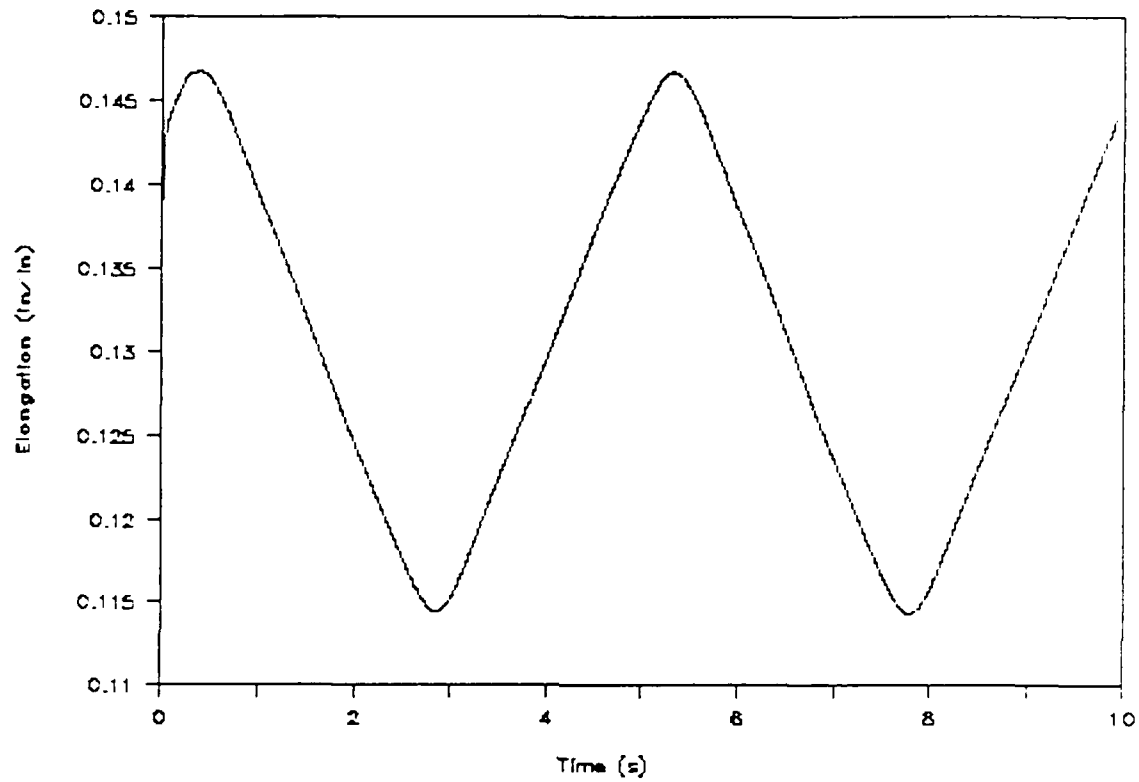
Figure 27d
Smoothed elongation versus time for nylon, dry, cycled at a steady
tension of 1.8 kips, frequency of .2 Hz and a strain amplitude of
.017 in/in.

of the data points. In most operations, N was selected to be 33. This had several effects on the data. First, it removed the irregularities. As seen in Figure 27c, which is the curve in Figure 27a after smoothing, the curve is smoother, but there is no change in the dynamic modulus.

However, as seen in Figure 27d, the smoothing caused the peaks of the elongation waveforms to be blunted. This caused the curves to take on the more rounded ends as shown in Figure 27c. This affected the resulting hysteresis values .

An investigation was made into the quantitative effect that the smoothing had on the hysteresis. Generally, the smoothed curves showed hysteresis values of from 10-15% lower than the hysteresis from the unsmoothed curves. Though the smoothing removed area within the hysteresis loop which was caused by the irregularities of the LVDT, the most significant loss of area within the loop was due to the blunting of the peaks.

Based on the above, it is important to note that the hysteresis data presented in this thesis, which is from smoothed curves only, may be as much as 15% below the actual hysteresis. This error tended to be greater at lower strain amplitudes. However, because the program was consistently run on the raw data and because of inaccuracies which would normally be associated with the hysteresis data (i.e. the presence of noise which cannot be representative of actual rope displacements), the hysteresis data presented is considered qualitatively correct and, within the margin of error, quantitatively meaningful.

Chapter 5 Results

5.1 General Results

5.1.1 Introduction

As expressed in Chapters 3 and 4, the polyester and nylon ropes were subjected to a constant strain amplitude in the form of a triangular wave of set amplitude and frequency, superimposed over a steady tension which was the tension in the rope at the zero strain amplitude point. This was accomplished for both the wet and the dry condition. In general, all the ropes displayed the same qualitative behavior while obtaining a stabilized configuration.

5.1.2 Dynamic Tensile Behavior Common to All the Ropes Tested

In order to appreciate the differences in the response of the nylon and polyester ropes under the various conditions, it is necessary to examine the general response of the ropes during the stabilization period.

When the new rope, either wet or dry, was subjected to a constant elongation, the load immediately began to relax. If the load were then reapplied by increasing the extension of the rope, the load would again begin to relax. However, the relaxation would not be as severe as in the first instance because the rope was becoming mechanically conditioned to the load. If a constant displacement amplitude were applied, the rope would experience a maximum dynamic load which, with time, would decrease. Consequently, if the cyclic displacement were halted, the steady tension would be lower than the desired steady tension. This is caused initially by the rope structurally realigning itself due to the induced dynamic load. However, once the structural alignment was accomplished, for the particular loading condition, the rope continued to experience a decrease in load as the fibers themselves continued to stress relax. In order to maintain the proper steady tension, the slack must be removed in the rope in order to restore the appropriate steady tension. Under actual towing conditions, this slack removal is accomplished through a change in the relative position of the vessels. The removal of slack is shown in Figure 26 and was repeated until the rope became

mechanically conditioned to the steady tension and cyclic displacement. The stabilized closed cyclic loop discussed in Chapter 4 was thus obtained.

The majority of the mean level adjustment necessary to remove slack occurred during the first 100 cycles. The removal of the slack represented a change in the elongation of the rope. This corresponded to a gradual decrease in the elongation gradient as a function of cycles.

Once structural rearrangement has stabilized, the ropes experience deformation primarily from fiber stretching. Because the fibers, and hence the ropes, behave as viscoelastic materials which experience secondary and primary creep, the ropes experience permanent deformation in terms of the residual elongation defined in Chapter 4.

Figure 28 shows actual load-elongation curves for an individual dry, nylon rope cycled at a frequency of .2 Hz, strain amplitude of .017 in/in and steady tension of 1.8 kips. The curves depict the 10th, 100th, 500th and 10,000th cycles. As can be seen, most of the elongation reflected in the shifting of the curves along the elongation axis, due to slack removal, occurs early and the change in elongation per cycle is reduced during the later cycles. In fact, by the time the rope stabilizes, there is no need to remove any measurable slack for over 100 cycles.

In observing the curves in Figure 28, which are qualitatively characteristic of all the rope tested, it is seen that the rope stiffens and the dynamic modulus increases as it becomes mechanically conditioned. This is due in part to the structural realignment and in part to the fibers deforming and stiffening as the rope elongates. The increasing elongation was due to slack removal necessary to maintain the steady tension.

Since the fibers and the ropes are stiffer and the strain amplitude remains constant, the maximum load experienced by t he rope will also increase. This increase in loading, however, tapers off with the increase in elongation. Prevorsek and Kwon [4], as shown in Figure 29, reported that, for fibers, the amount of increase in maximum load and total increase in creep extension rise sharply at the beginning of the test, but soon plateau.

An interesting aspect of Figure 28, and a result common to all the ropes, is that the hysteresis initially increases from the 10th to the 100th cycle, but then begins to decrease as the rope is stabilized. Much of this early hysteresis is a result of interyarn abrasion and fiber hysteresis [1]. As the rope becomes mechanically conditioned and approaches a more stable configuration, the observed hysteresis will also become stabilized.
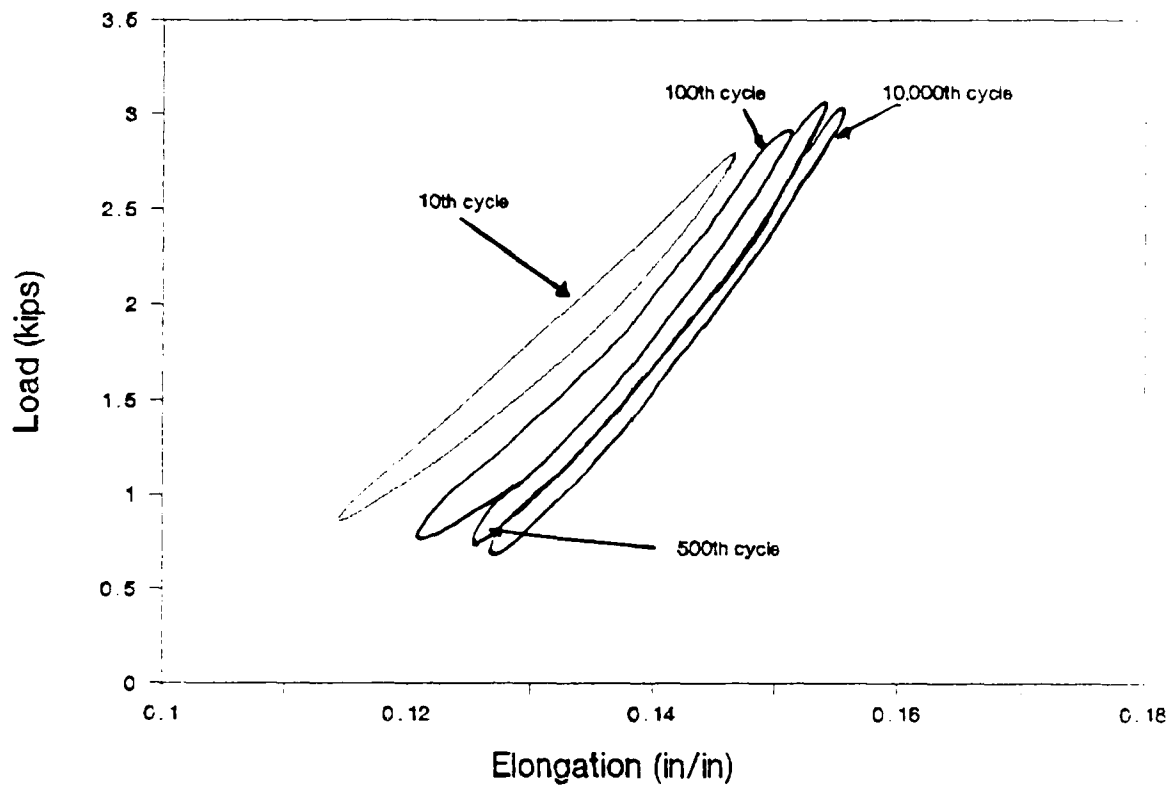
Figure 28
Hysteresis loops for nylon, dry, cycled at a steady tension of
1.8 kips, frequency of .2 Hz and a strain amplitude of .017 in/in
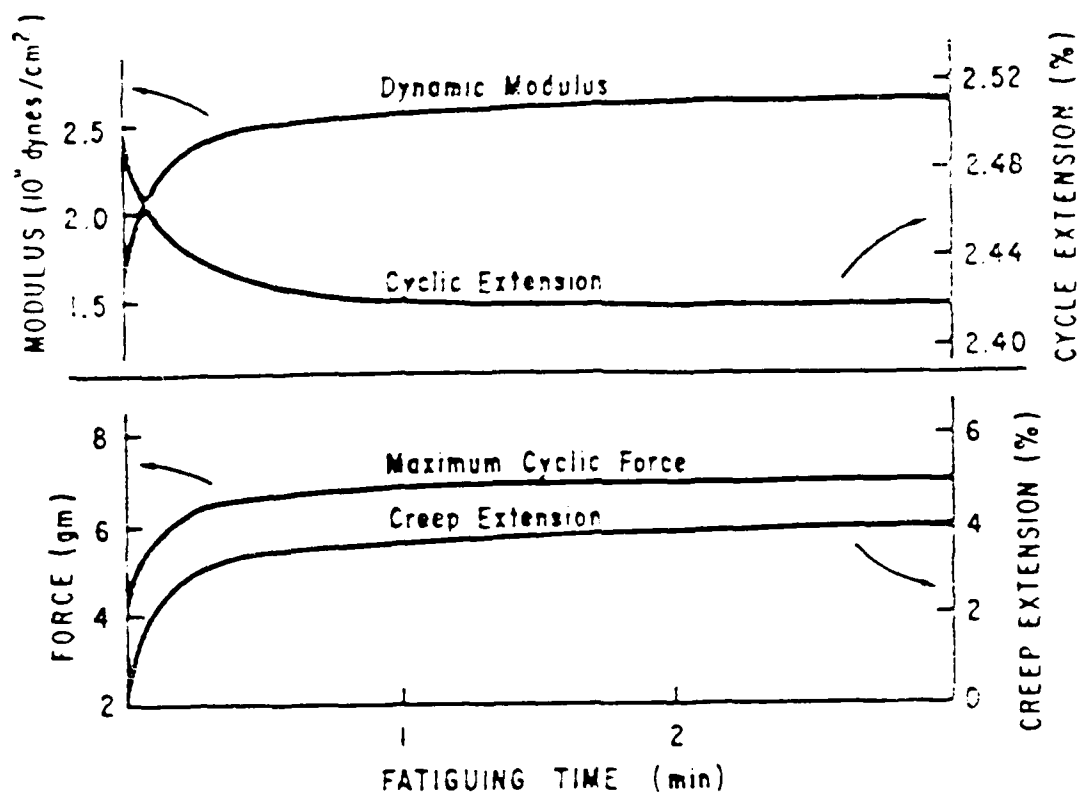at the 10th, 100th, 500th and 10,000th cycle.

Figure 29
Reduction in the change in elongation, change in maximum load,
change in creep extension and dynamic modulus, with time, for
synthetic fibers . [Prevorsek and Kwon, Ref 4]

An aspect which is of integral importance to all the aforementioned effects is the temperature that the rope experiences during the stabilization process. All the rope tested experienced some temperature rise which normally occurred during the first 100-200 cycles and then stabilized, as seen in Figure 30. The temperature rise is a direct result of the heat generated by the conversion of mechanical hysteresis to thermal energy.

5.2 Changes in the Dynamic Behavior of Polyester and Nylon Rope

5.2.1 General

In testing polyester and nylon 1/2 in lines, specimens were cycled to stabilization at 10,000 cycles under various steady tensions, cyclic frequencies and strain amplitudes within the range of values described in Chapter 3. In accordance with Chapter 2, information was recorded as to the total elongation, residual elongation, stabilized temperature, maximum and minimum load, stiffness, K, and the hysteresis, H.

The results of the quasi-static, monotonic loading conducted at Avery Point revealed that polyester had a nearly constant stiffness of 40 kips-in/in in both the wet and dry condition. Nylon, on the other hand, had relatively nonlinear load elongation curves for the wet and dry samples. Figures 13 and 18 show these load-elongation curves. All the ropes broke at the splice. These curves have the same shape as those determined by Bitting [2] and Flory.

The polyester and nylon ropes were cycled at a variety of strain amplitudes from .003 in/in to .030 in/in. The steady tensions used were, for nylon, 1.8 kips and .9 kips. These represented, respectively, 21.5ropes were cycled at a steady tension of 1.88 kips and 1.3 kips which are 201 Hz and .2 Hz. Though the 1 Hz represents a very small wave period which is not normally encountered, it was used in order to reduce the total test time. However, because of subsequent high rope temperatures observed at 1 Hz, it affected certain dependent variables. In order to investigate the differences between wet and dry ropes, nylon was tested at a variety of strain amplitudes, a steady tension of 1.8 kips and a cyclic frequency of .2 Hz under both wet and dry conditions. The polyester was similarly tested, but a steady tension of 1.88 kips was used.
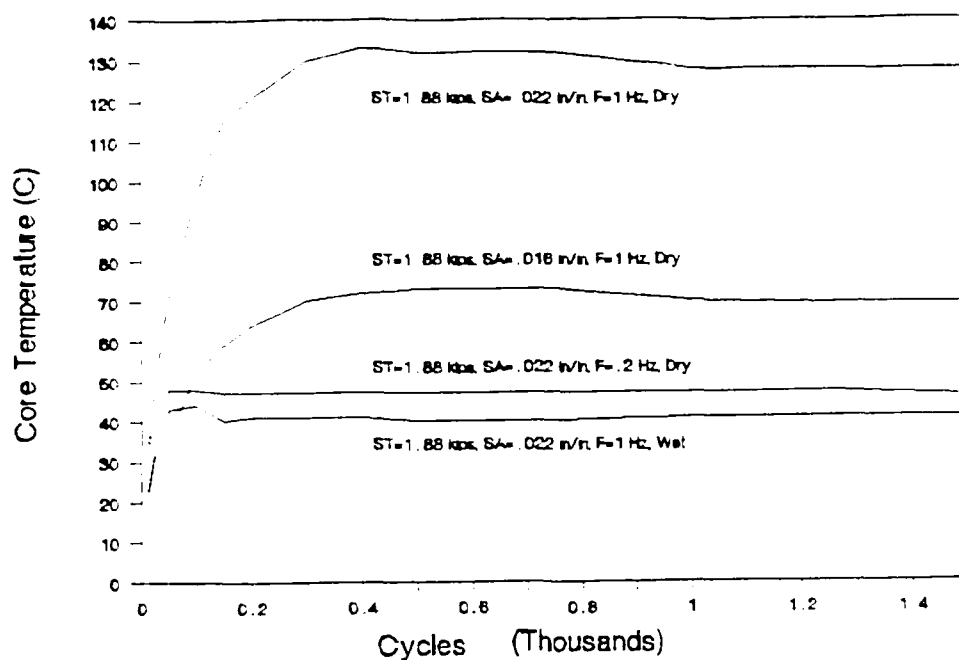
(a) Polyester
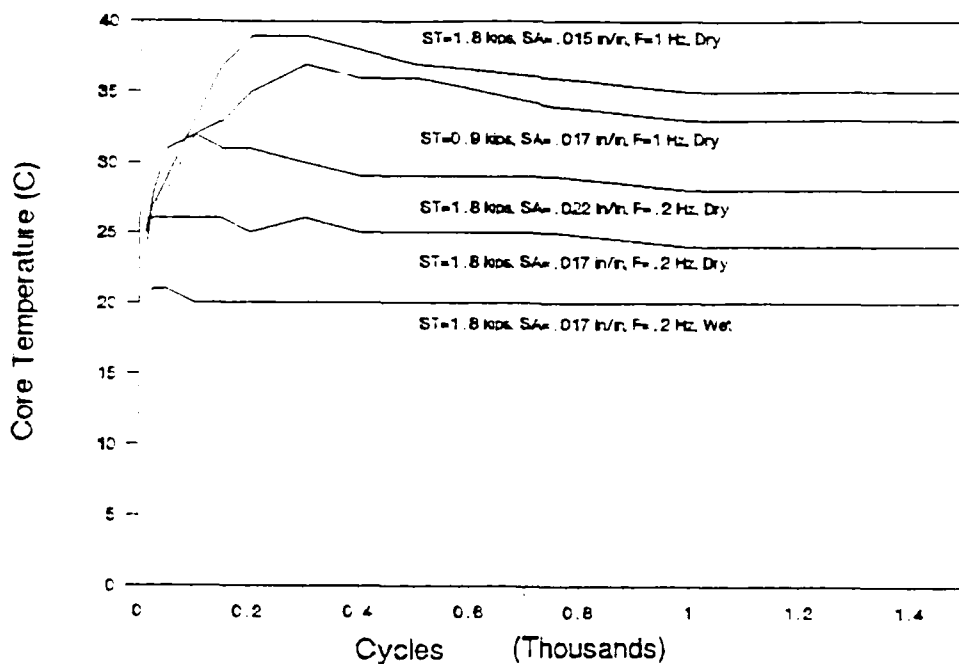
(b) Nylon

Figure 30

Change in core temperature with cycles.
ST=Steady Tension, SA=Strain Amplitude, F=Cyclic Frequency
Control Temperature 20 C

5.2.2 Dynamic Behavior with Changing Strain Amplitude

As the ropes were brought to stabilization under various strain amplitudes, several effects were observed independent of the material, testing condition, frequency or steady tension.

A very noticeable effect, shown in Figures 31 and 32, and most pronounced in the dry ropes, was the temperature rise in the core of the rope. As the figure indicates, the temperature at stabilization became quite severe for the polyester rope and, at high frequencies and strain amplitudes an extrapolation to higher strain amplitudes may begin to approach the polyester heat stiffening temperature of 170° C. In nylon, the temperature rise was not as severe, but an increase was noted. In all the curves shown in Figure 31 and 32, an increase in strain amplitude brought an increase in core temperature.

A second effect which was seen was a decrease in the stiffness, K, of all the ropes with an increase in strain amplitude. As seen in Figures 33 and 34, the severity of the decrease varies, but, qualitatively, the reduction in dynamic modulus is consistent throughout.

Elongation, both total and residual, increase with increasing strain amplitude regardless of the values of the other parameters as shown in Figures 35, 36, 37 and 38.

The maximum load and total load amplitude experienced by the rope increased with increasing strain amplitudes for all the ropes and under all conditions investigated. Figures 39, 40, 41 and 42 show this result.

Lastly, the hysteresis, the measure of the internal damping and the mechanical energy absorbed in the rope increased with increasing strain amplitude. As seen in Figures 43 and 44, this was found to be true in all cases.

5.2.3 Dynamic Behavior with Changing Frequency

In all the figures initially p resented in section 5.2.2, attention should be given to the differences between the polyester and nylon ropes cycled at .2 Hz and those cycled at 1 Hz and at steady tensions of 1.8 kips and 1.88 kips for the nylon and polyester, respectively.

As can be seen from Figures 31 to 44, the effect of changing frequency was consistent across the range of strain amplitudes. An increase in frequency served
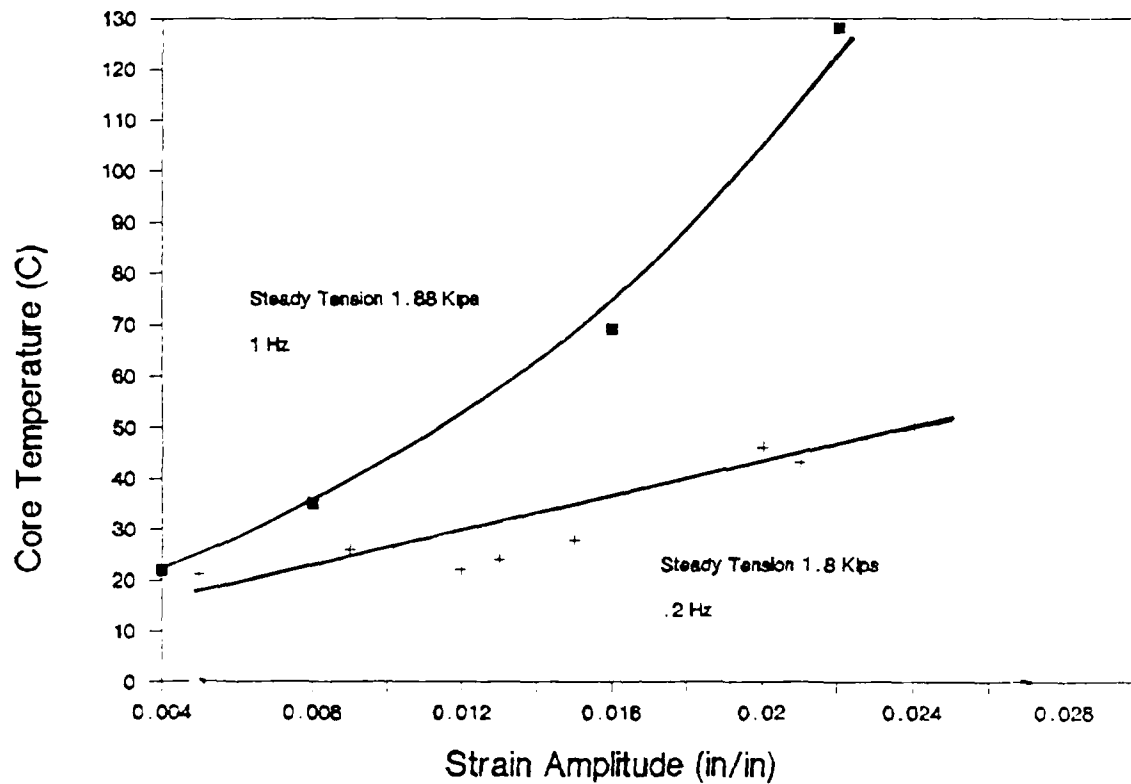
Figure 31

Stabilized core temperature of polyester rope, dry, after 10,000 cycles.
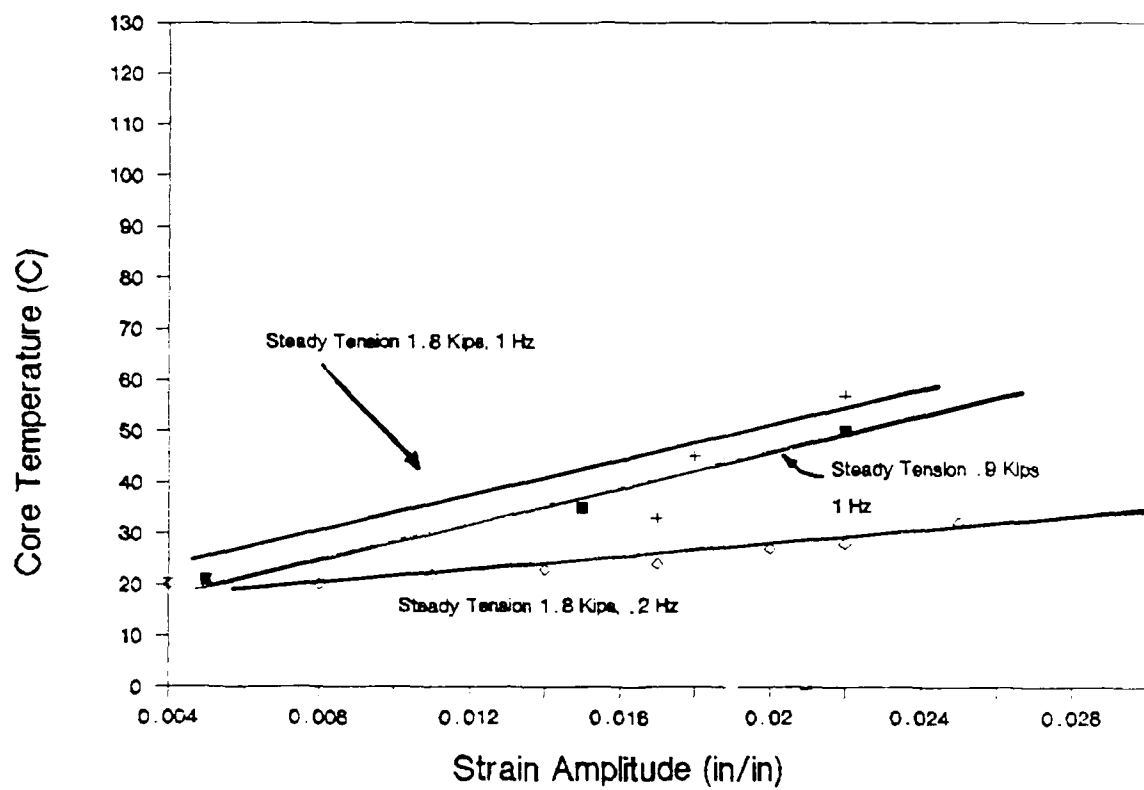
Figure 32

Stabilized core temperature for nylon rope,dry
after 10,000 cycles.
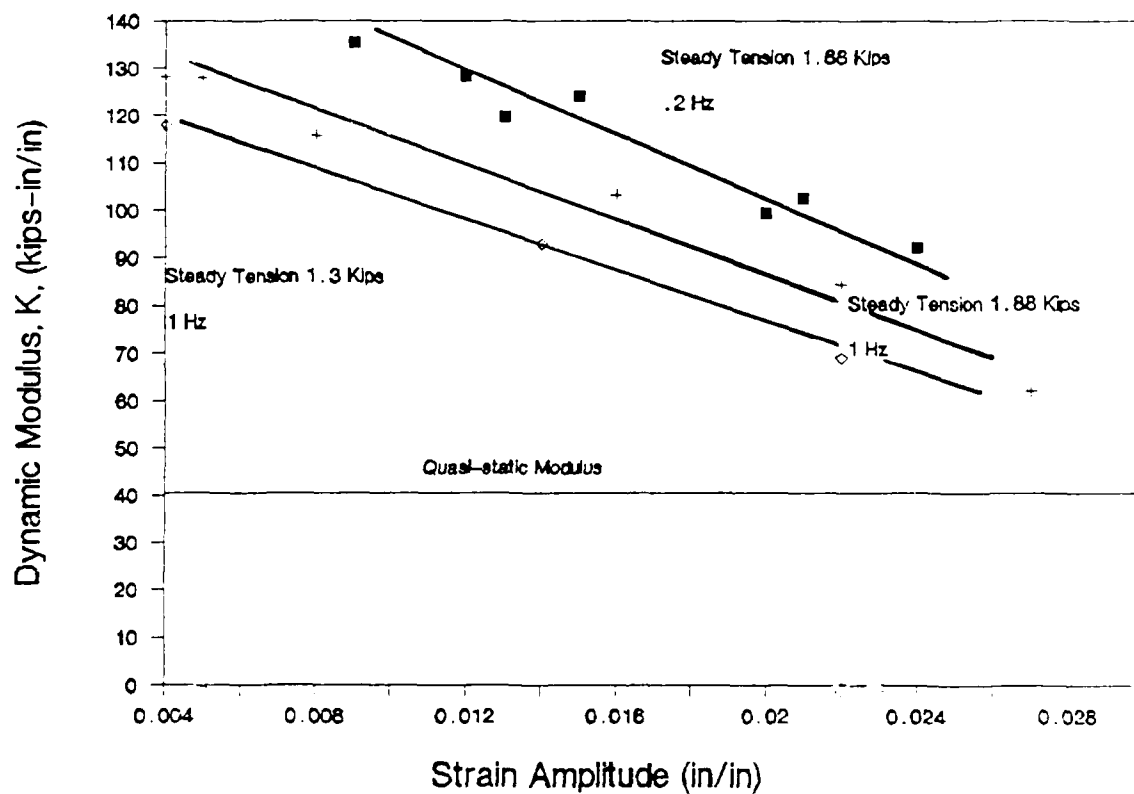
Figure 33
Stabilized dynamic modulus for polyester rope, dry,
after 10,000 cycles.
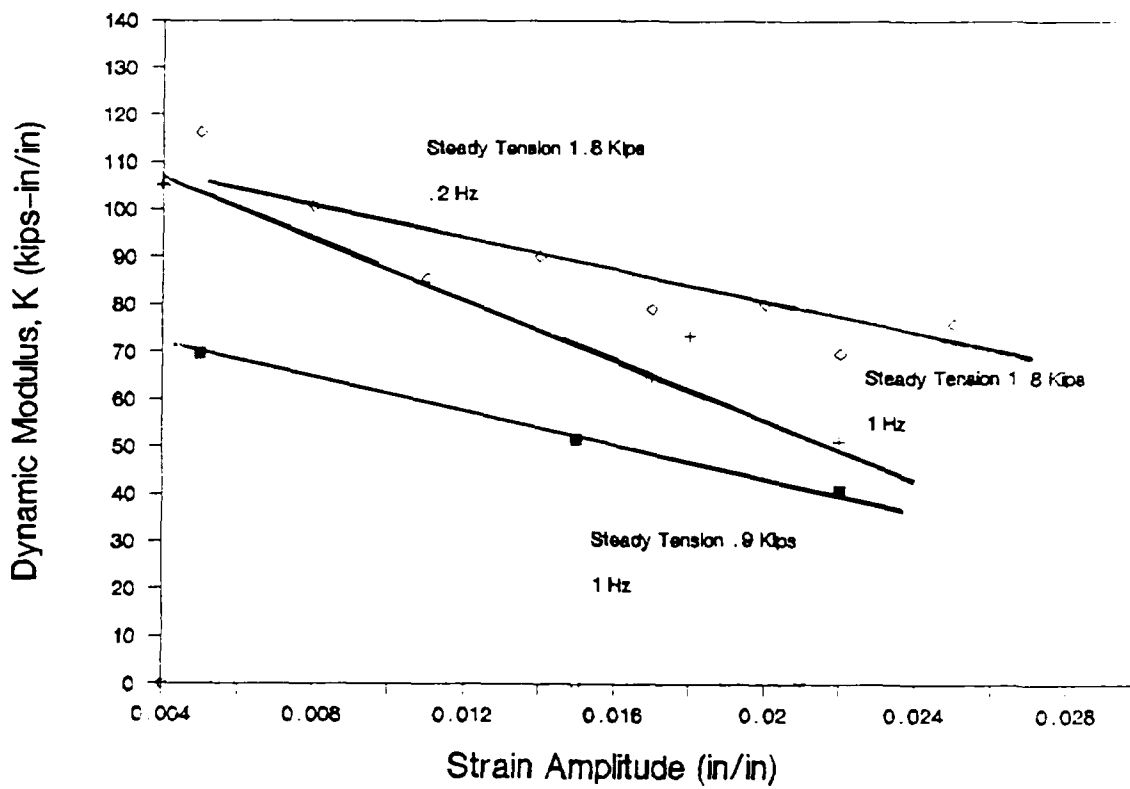
Figure 34
Stabilized dynamic modulus of nylon rope, dry
after 10,000 cycles.
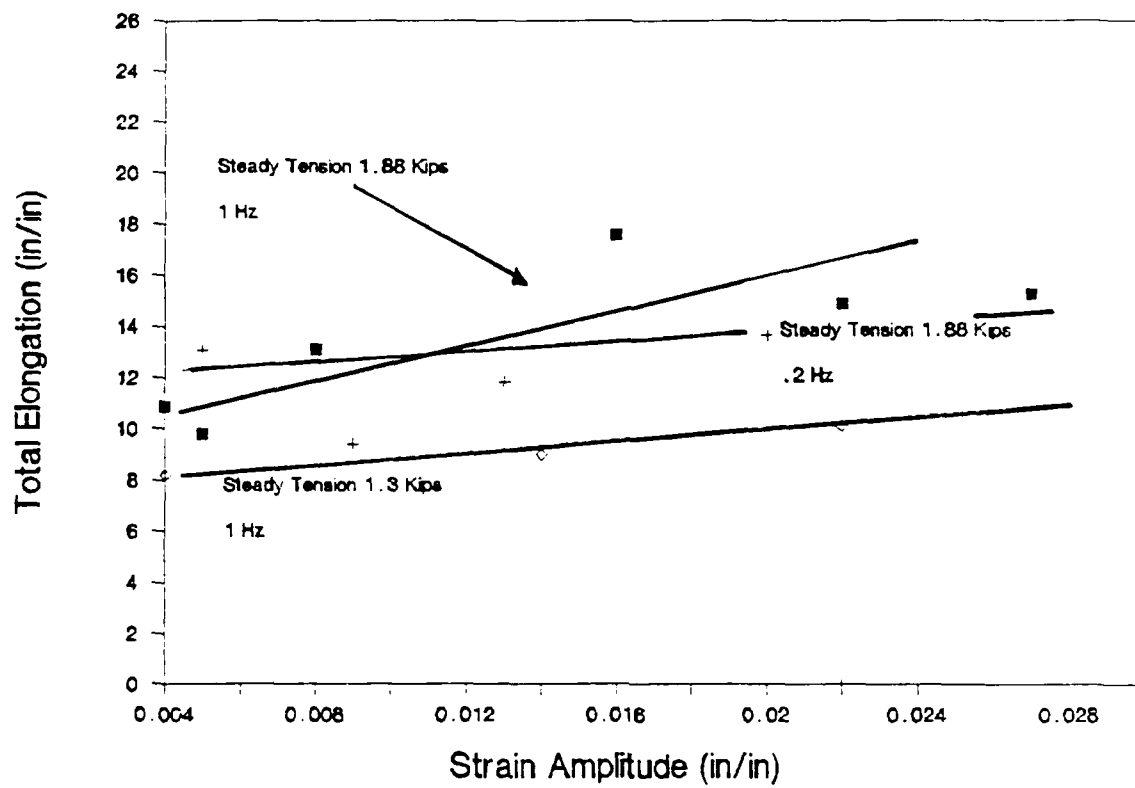
Figure 35
Stabilized total elongation for polyester rope, dry
after 10,000 cycles.
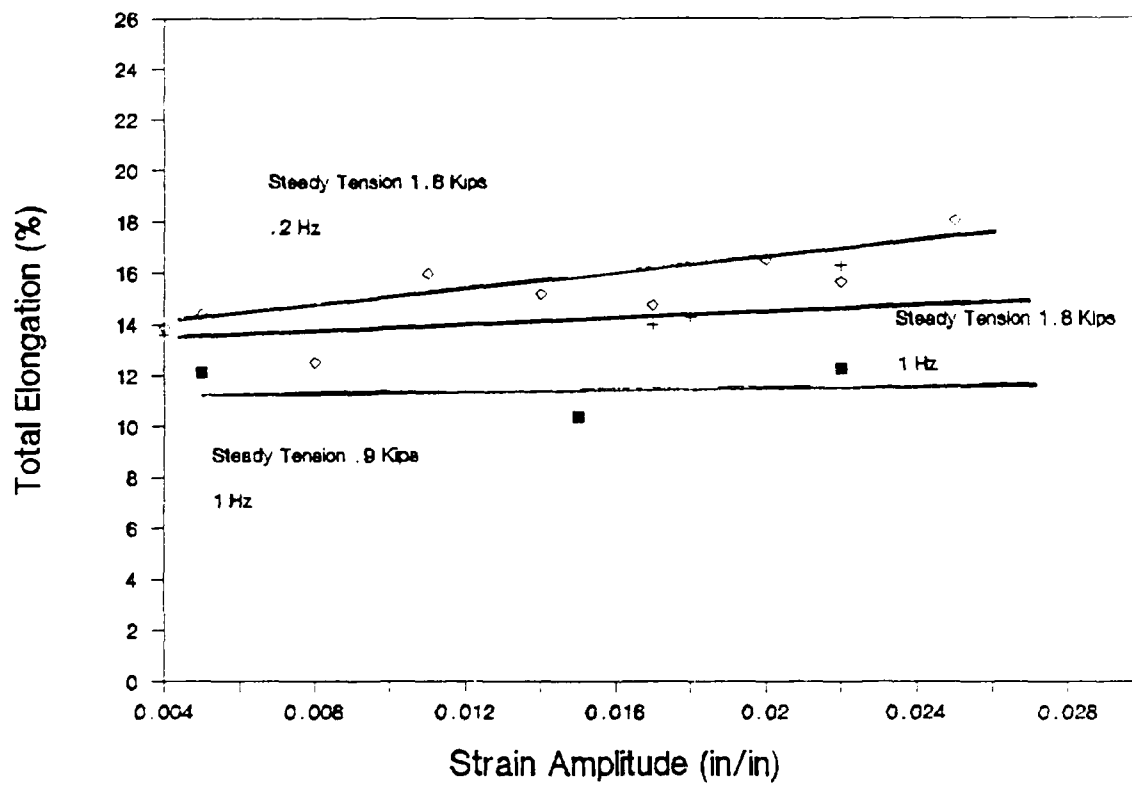
Figure 36

Stabilized total elongation for nylon rope, dry,
after 10,000 cycles.
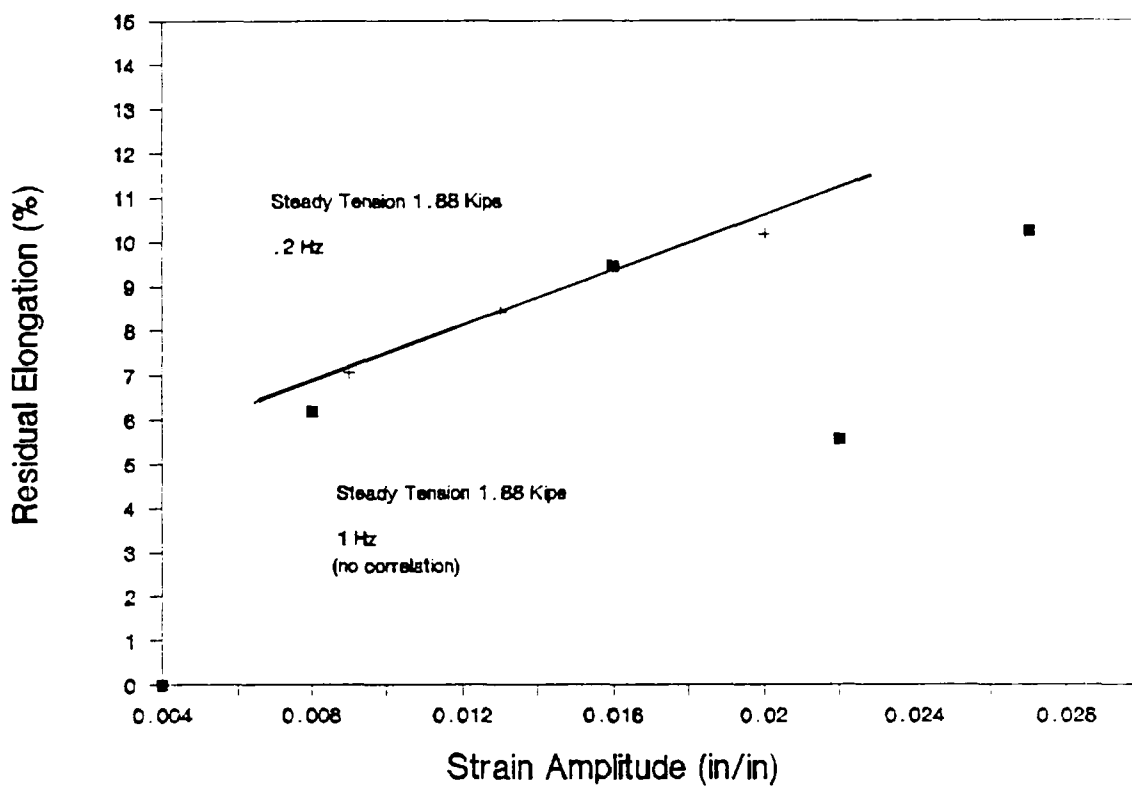
Figure 37

Residual elongation of polyester rope, dry,
after 10,000 cycles.
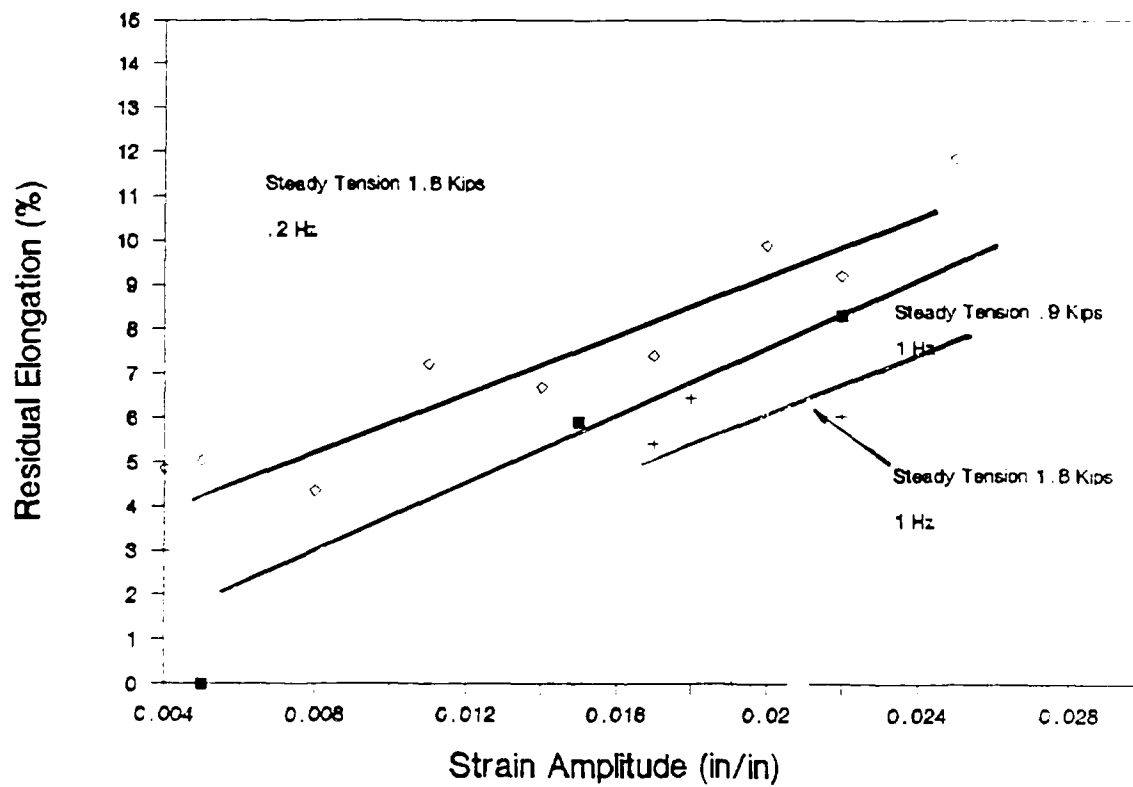
Figure 38
Residual elongation of nylon rope, dry,
after 10,000 cycles.
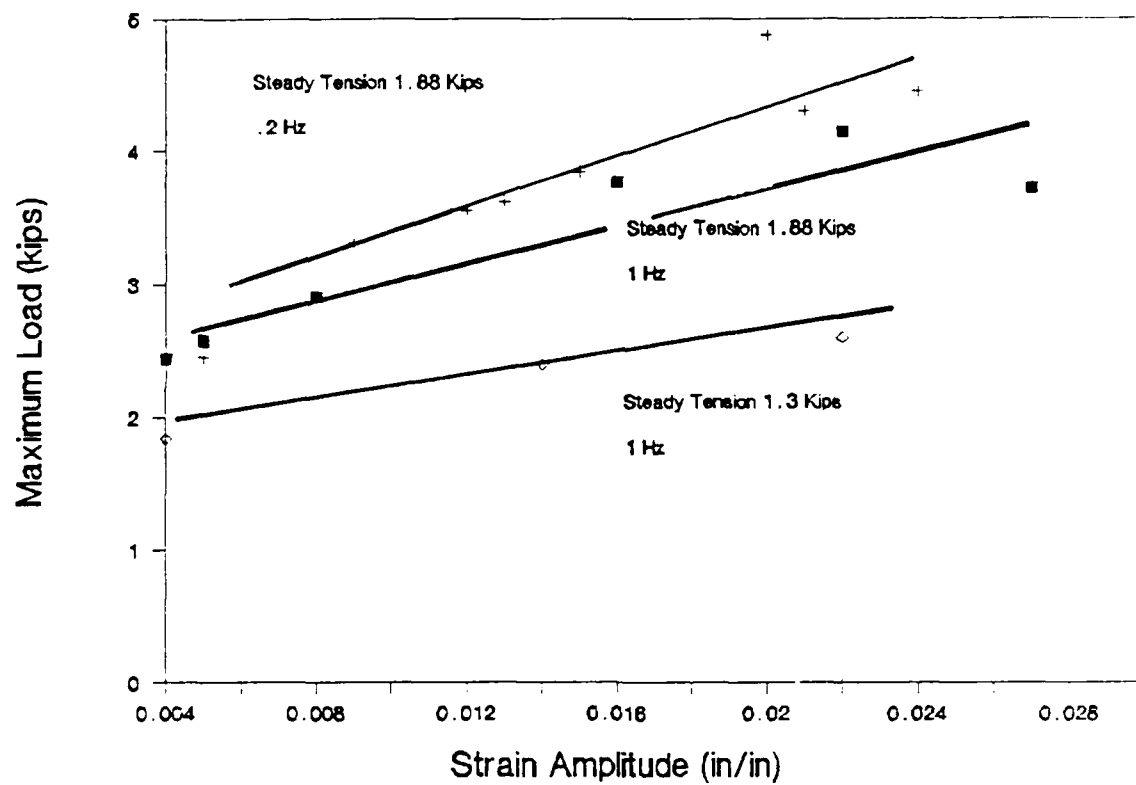
Figure 39

Maximum dynamic load for polyester rope, dry

after 10,000 cycles.

Figure 40
Maximum dynamic load for nylon rope, dry
after 10,000 cycles.

Figure 41
Stabilized load amplitude for polyester, dry,
after 10,000 cycles.

Figure 42

Stabilized load amplitude of nylon rope, dry, after
10,000 cycles.

Figure 43

Stabilized hysteresis for polyester rope, dry
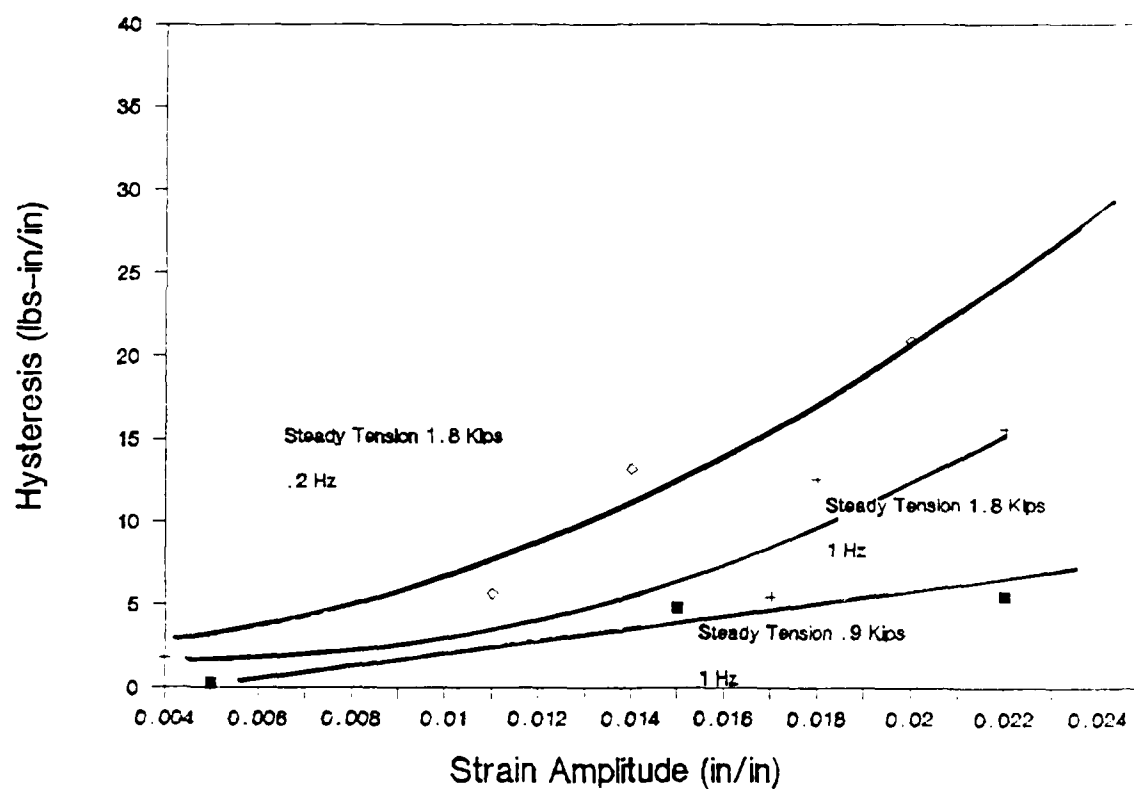
after 10,000 cycles.

Figure 44

Stabilized hysteresis for nylon rope, dry,
after 10,000 cycles.

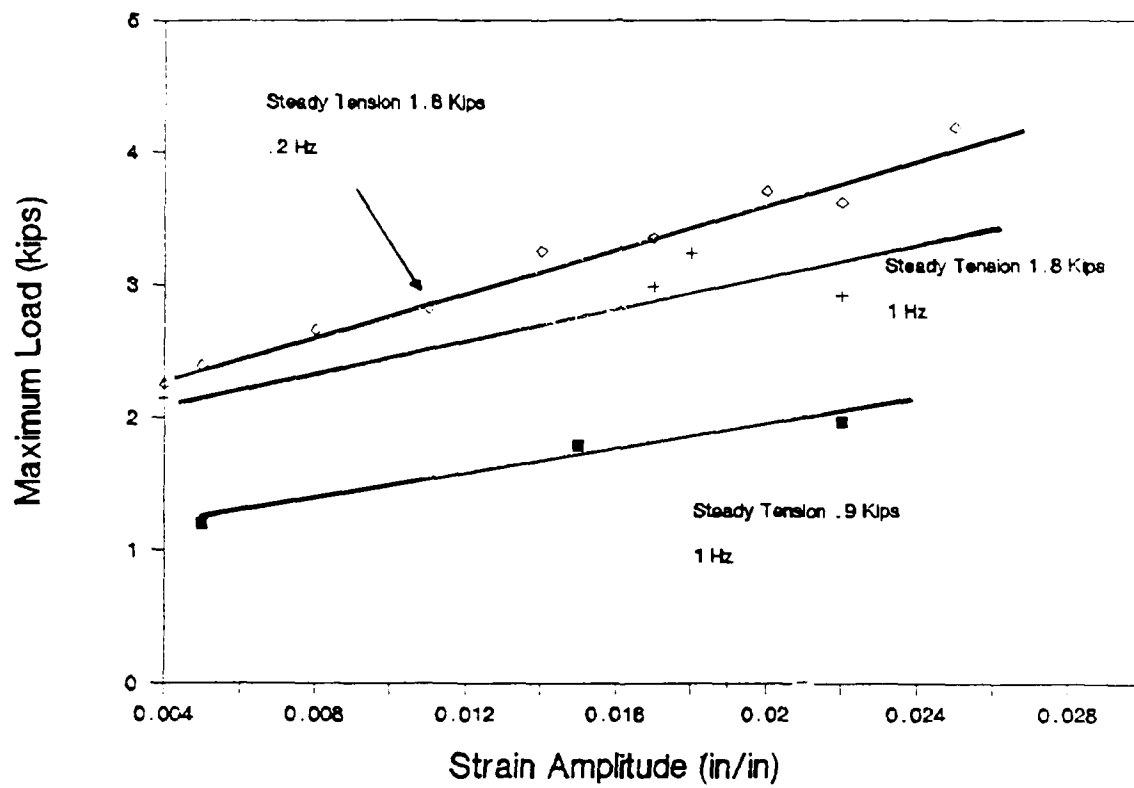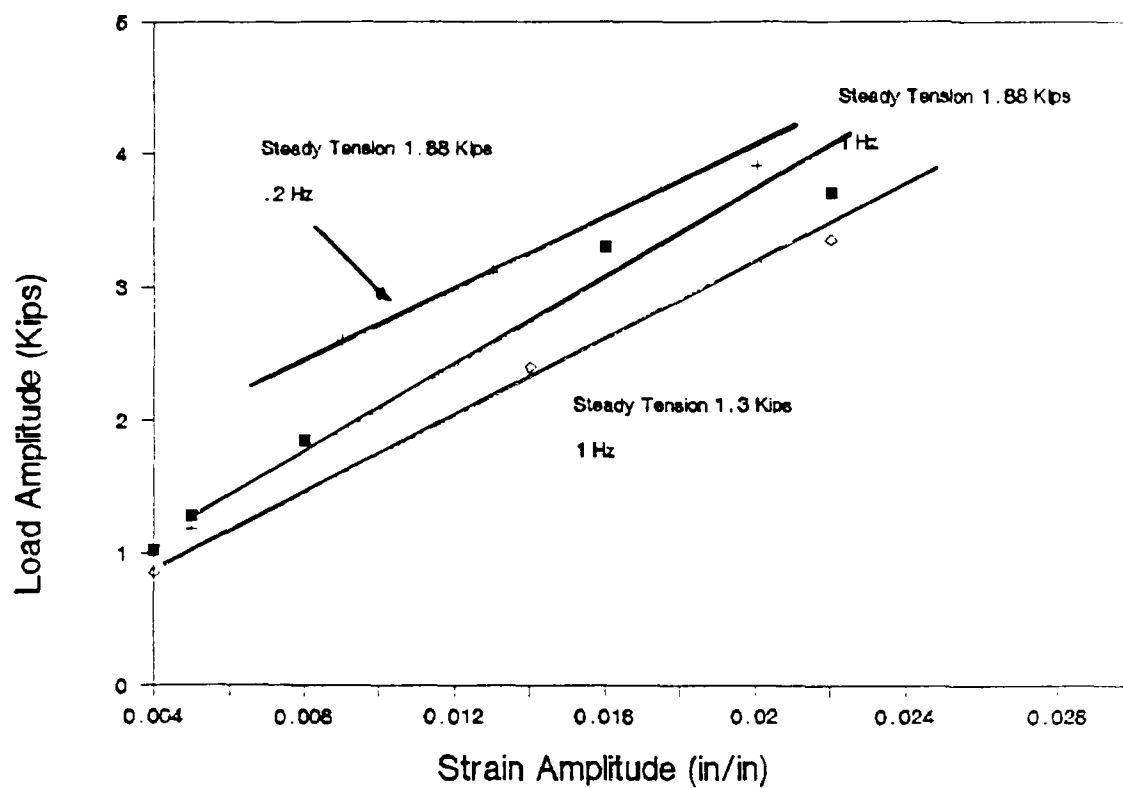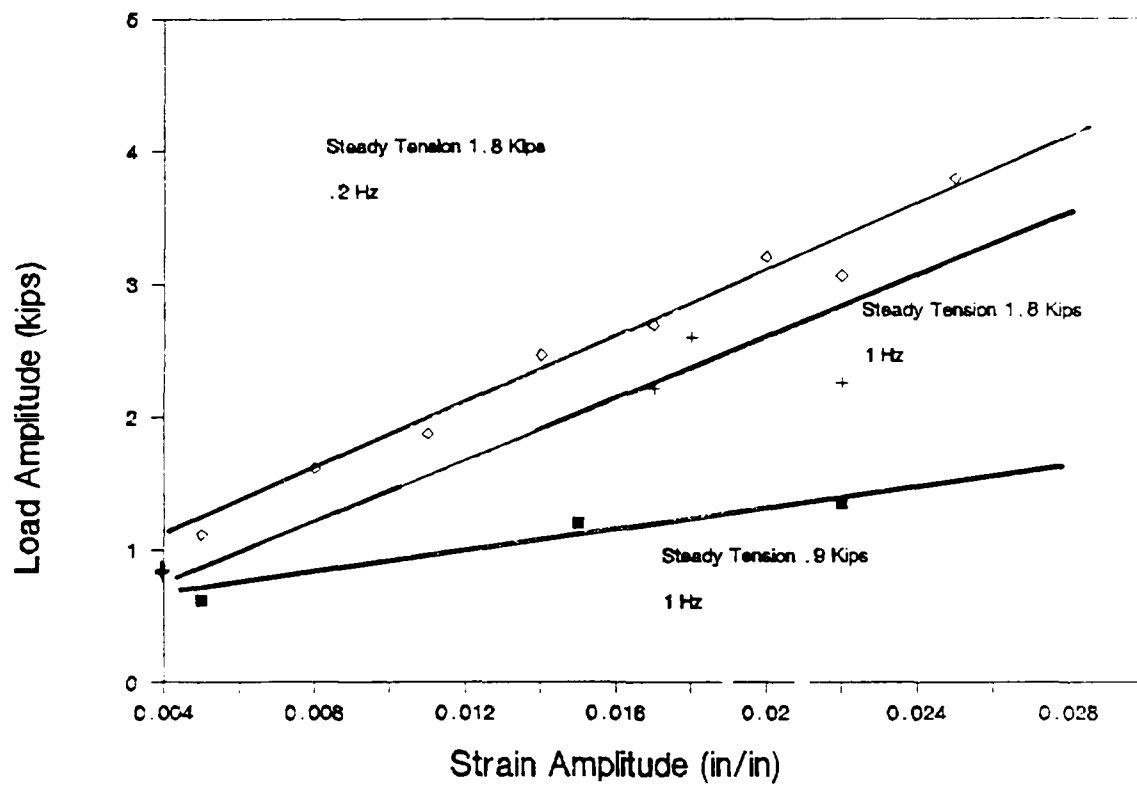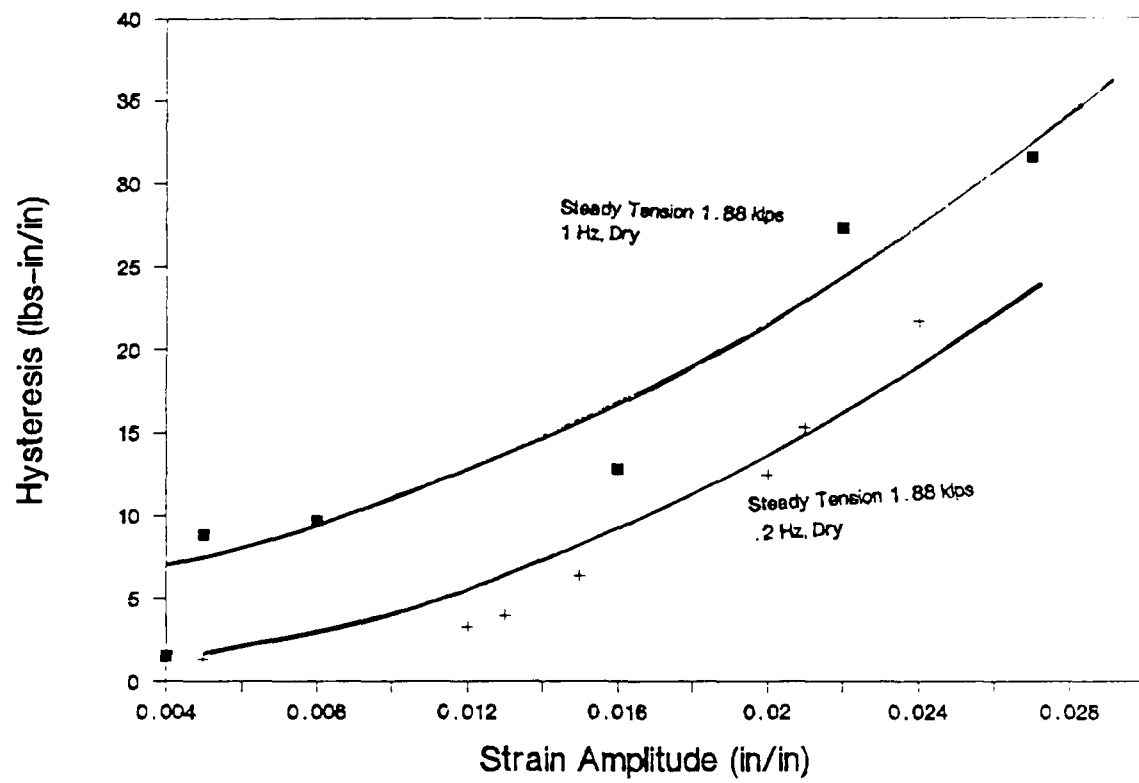to increase the core temperature in both nylon and polyester. However, ropes tested at the lower frequency, .2 Hz, manifested greater dynamic stiffness, K, for both polyester and nylon. They also were subjected to a greater maximum load and load variation. Hysteresis was also greater for the ropes cycled at the lower frequency.

5.2.4 Dynamic Behavior with Changing Steady Tension

The nylon and polyester ropes were cycled throughout the range of strain amplitudes, at 1 Hz and at steady tensions of 1.8 kips and .9 kips for nylon and 1.88 kips and 1.3 kips for polyester.

As Figures 31 to 44 indicate, increasing the steady tension serves to increase the severity of all the effects investigated for both nylon and polyester.

5.2.5 Results of Dry versus Wet testing

Wet tests were conducted in order to examine the differences between wet and dry rope. In the case of nylon, specimens were tested under both wet and dry conditions by cycling at a steady tension of 1.8 kips, a cyclic frequency of .2 Hz and several strain amplitudes. Figures 45 to 51 show the results. As the figures show, the primary effect of cycling the rope while continually wet was to drastically reduce the core temperature. The nylon rope showed greater elongation when wet. Maximum load and load amplitude was greater for the dry (versus wet) nylon rope, as was the dynamic modulus. The hysteresis was also greater for the dry rope.

The polyester, which was cycled across the range of strain variations at a steady tension of 1.88 kips and .2 Hz, under both the wet and dry condition, also experienced a substantial reduction in core temperature when cycled wet. As shown in Figures 45 to 51, the dry polyester rope was not as stiff as the wet rope, but, unlike the nylon, experienced a lower maximum load and smaller load variation than the wet rope. The continuously wetted polyester rope also experienced a greater hysteresis at the higher strain amplitudes than the dry rope.

Figure 45

Stabilized core temperature for nylon and polyester rope
cycled at .2 Hz and a steady tension of 20% NRBS
after 10,000 cycles.

Figure 46

Maximum dynamic load for nylon and polyester rope
cycled at .2 Hz and a steady tension of 20% NRBS
after 10,000 cycles.

Figure 47

Load amplitude of nylon and polyester rope cycled
at .2 Hz and a steady tension of 20% NRBS
after 10,000 cycles.

Figure 48

Stabilized dynamic modulus of nylon and polyester rope
cycled at .2 Hz and a steady tension of 20% NRBS
after 10,000 cycles.

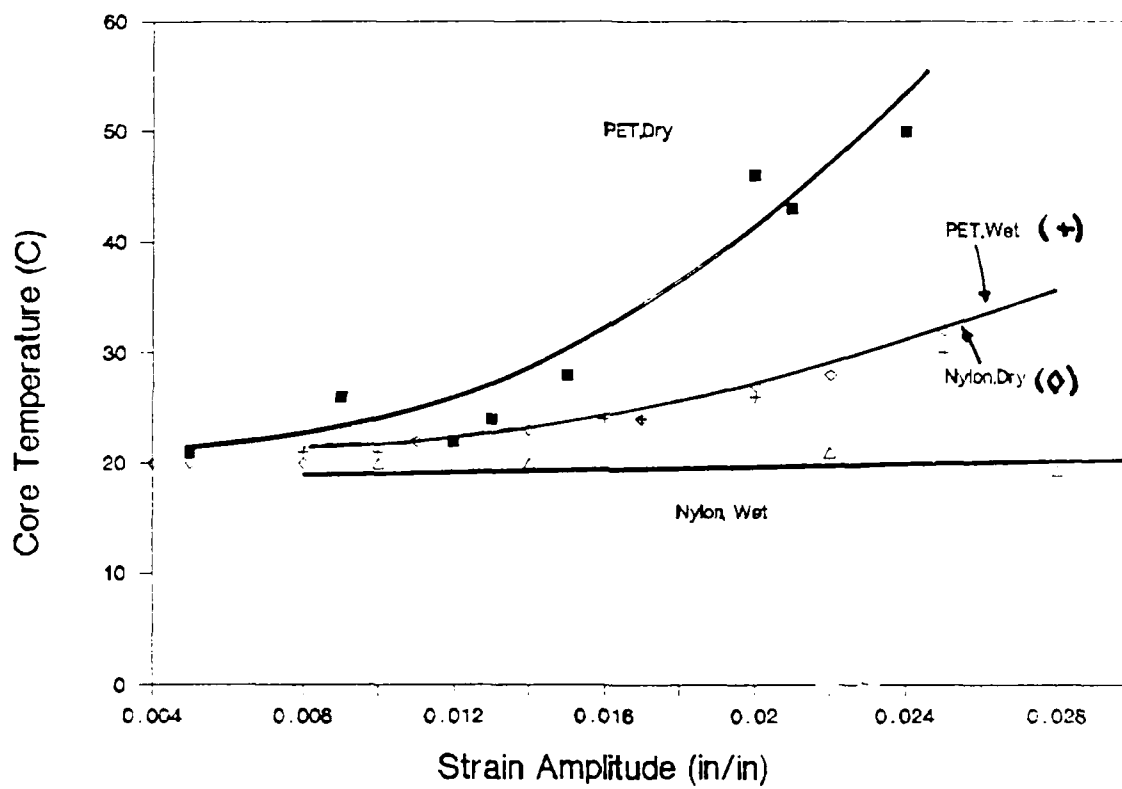Figure 49

Stabilized total elongation for nylon and polyester
rope cycled at .2 Hz and a steady tension of 20% NRBS
after 10,000 cycles.

Figure 50
Residual elongation of nylon and polyester rope
cycled at .2 Hz and a steady tension of 20% NRBS
after 10,000 cycles.

Figure 51

Stabilized hysteresis for nylon and polyester line cycled
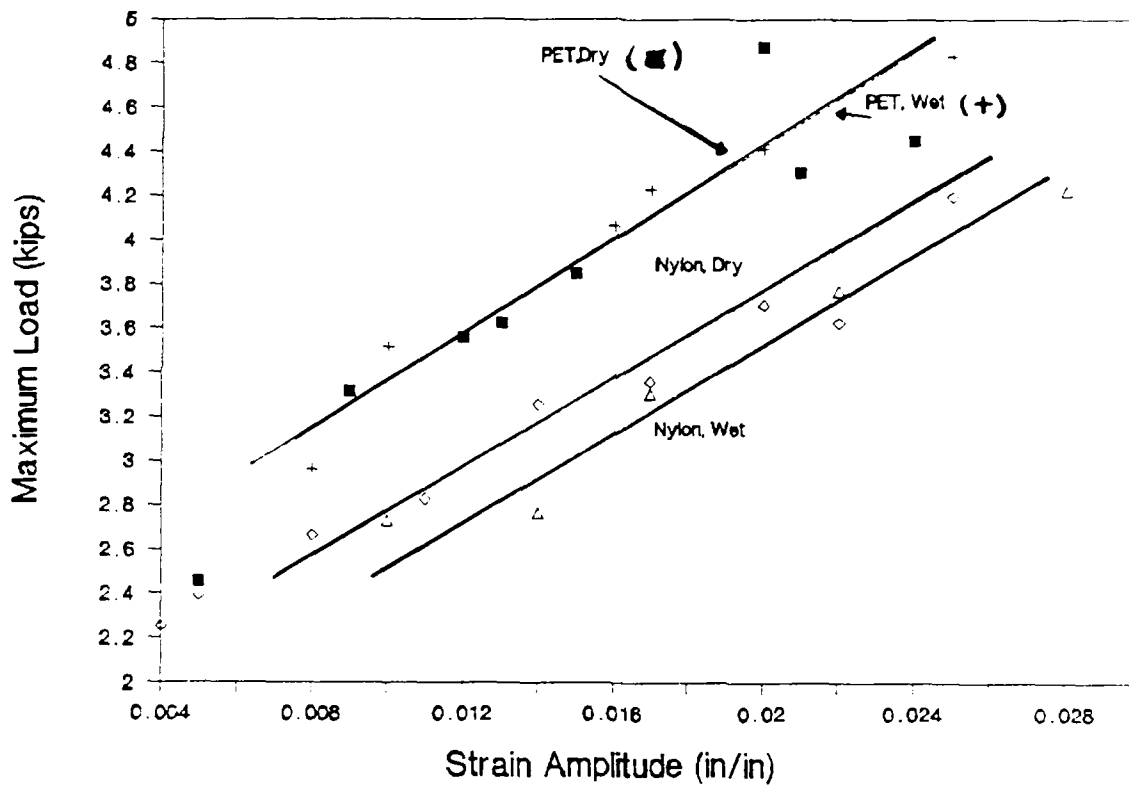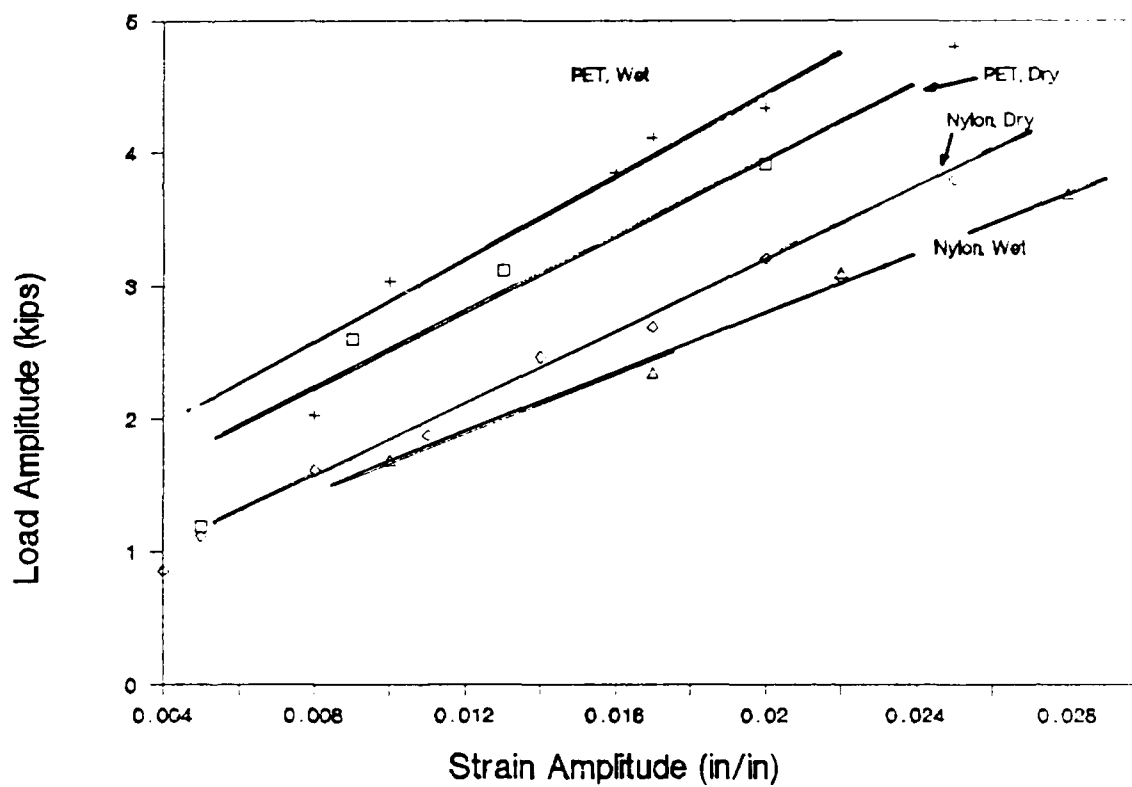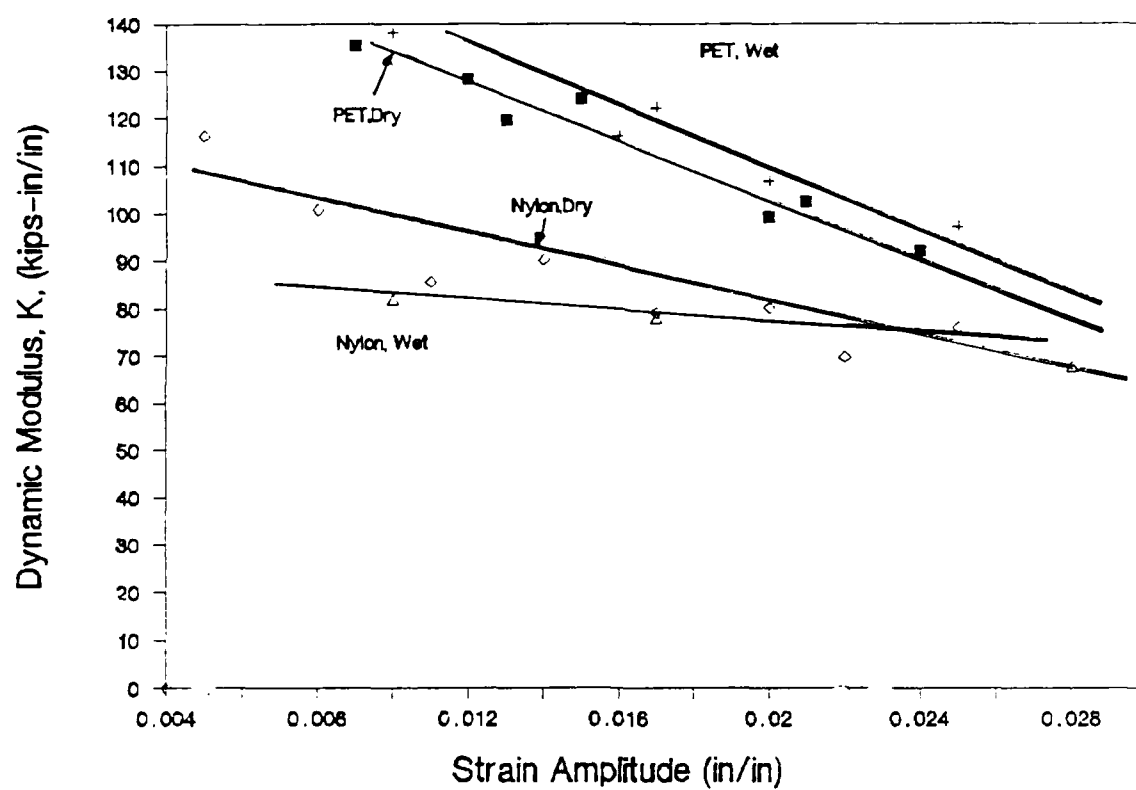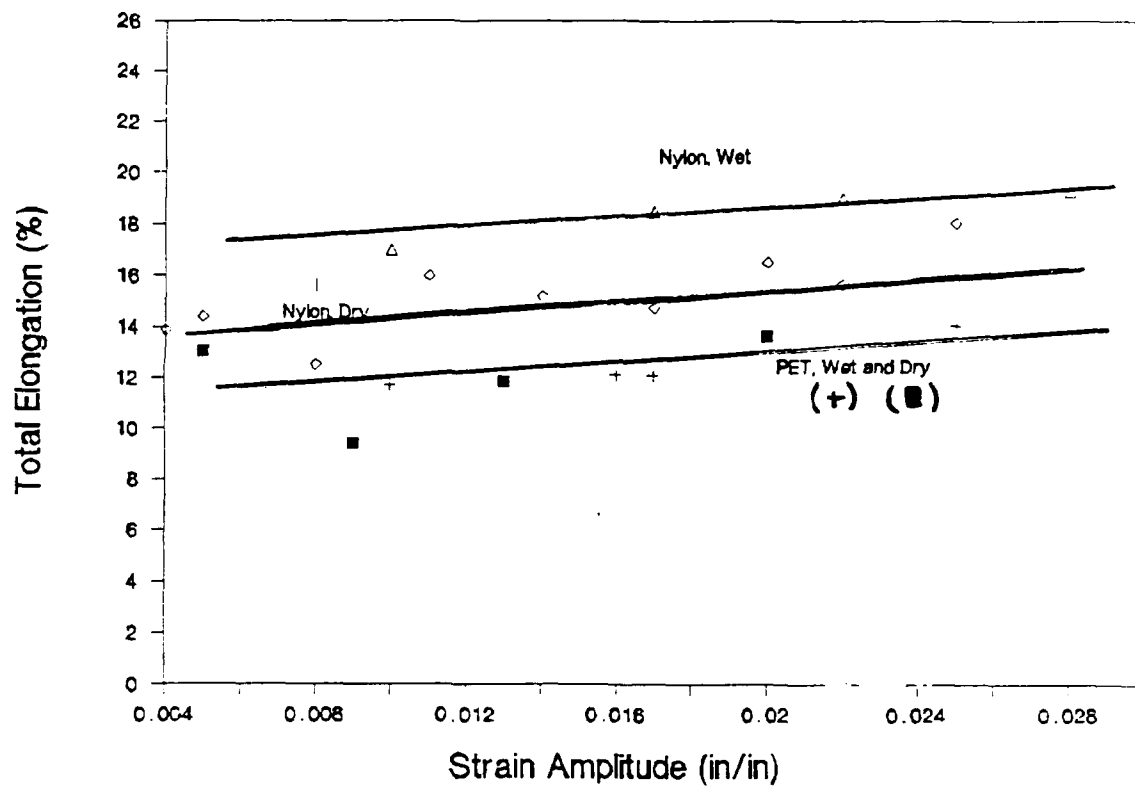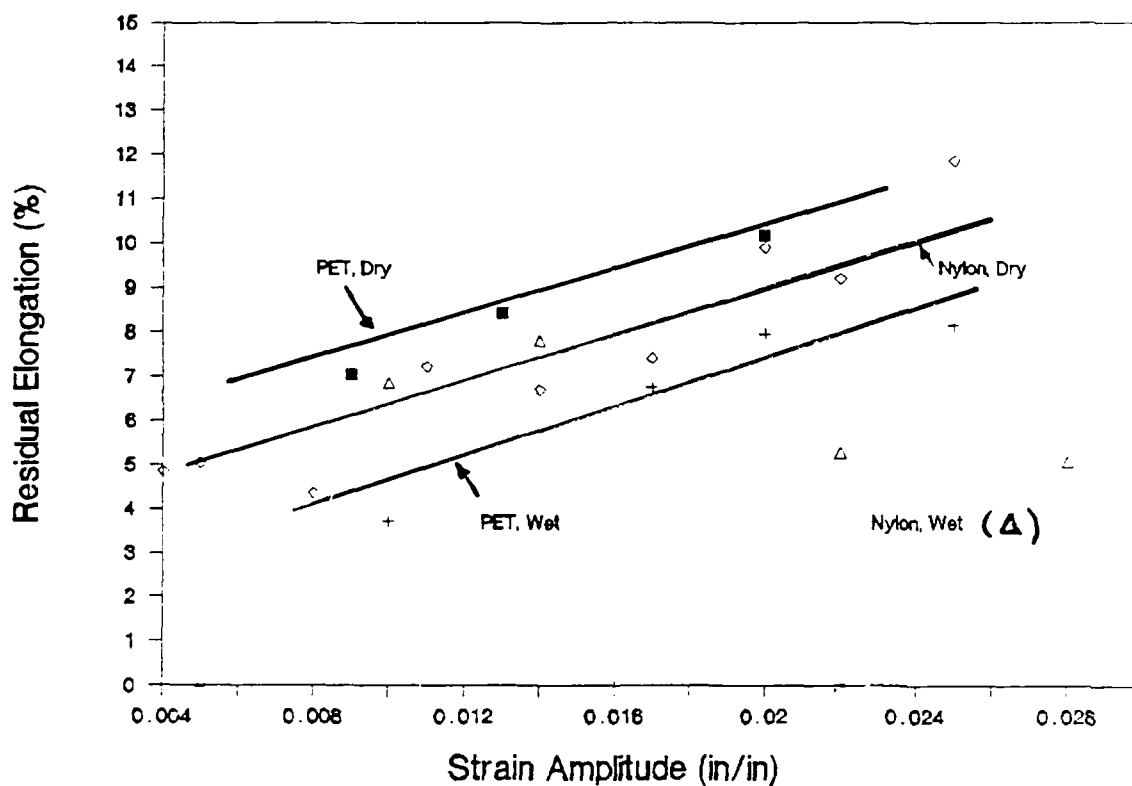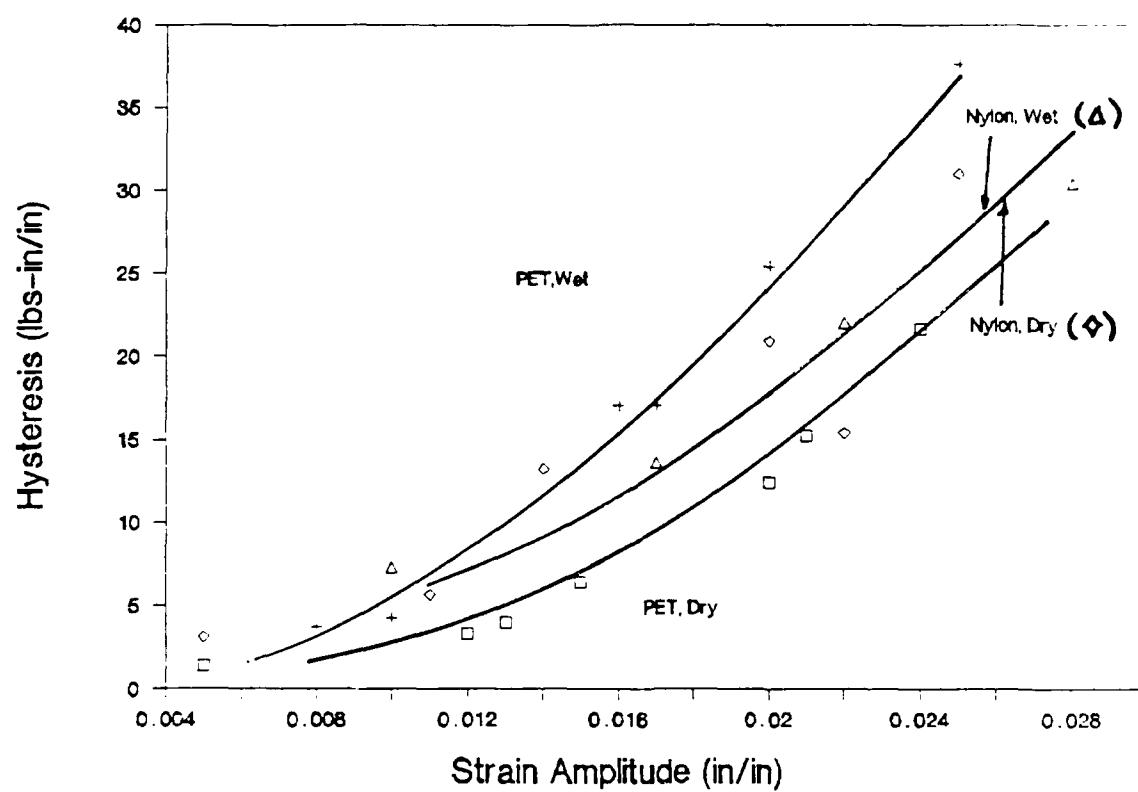at .2 Hz and a steady tension of 20 % NRBS
after 10,000 cycles.

Chapter 6 Discussion of Results

6.1 General

The results outlined in Chapter 5 will be discussed in this chapter in light of the qualitative and quantitative effects of manipulating one of the independent variables. Also, the differences between the results for nylon and polyester will be discussed.

6.2 Changes in the Dynamic Stiffness

Both polyester and nylon experienced changes in the dynamic modulus due to changing steady tensions, frequency and strain amplitude. An important result, well documented by Bitting [32] and Parsey [522], as well as others, is that the dynamic modulus is found to be considerably higher than the quasi-static modulus. This result was supported in this work. As seen in Figures 33 and 34, within the range of values examined, the dynamic modulus for polyester is at least 2 to 3 times greater than the quasi-static modulus of 40 kips-in/in (or 4.25% NRBS-in/in) and the nylon is at least 3 times greater. This is characteristic of viscoelastic structures. However, the reasons for the stiffness change may not be primarily due to strain rate differences, but due to differences between the early cycles which always have a lower stiffness, and the cyclic stabilized condition.

Increasing the steady tension in the presence of constant strain amplitude and frequency served to increase the dynamic modulus of the rope. A   steady tension increased, the rope was forced to become more structur   d along its axis. This was reflected in a reduction of the helix angle as   teady tension increased. Thus, the rope behaved more like an axially aniso   str cture and is stiffer. In the case of nylon, which possesses a fairly nonlinear quasi-static stress strain curve, the rope, when loaded to a higher steady tension, shifted to a stiffer portion of the load elongation curve. This induces a corresponding increase in the dynamic stiffness. The same feature is observe in the polyester rope, but to a much less degree because of the relative linearity of the polyester quasi-static load-elongation curve. These results are in agreement with Bitting [10] who found that the dynamic modulus increased with increasing mean loads (load limits).

Increasing the cyclic frequency or the cyclic strain amplitude served to increase the cyclic strain rate, defined as the product of the strain amplitude and

the frequency. Associated with the increase in the strain rate, was an increase in the measured stabilized core temperature, as seen in Figure 52.

The increasing core temperature, which became quite high at the larger strain rates, was a direct result of the increasing rate of the conversion of mechanical energy, in the form of hysteresis, to thermal energy, manifested as a temperature rise. As seen in Figures 43, 44 and 51, the net hysteresis per cycle corresponded to an increase in strain amplitude. If hysteretic energy is considered in terms of the power absorbed by the rope (hysteresis, H, multiplied by the cyclic frequency), it can be seen that there is a direct relation between the power absorbed and the measured stabilized core temperature (Figure 53). In short, as both the strain amplitude and strain rate increase, the power absorbed by the rope increases, making more mechanical energy per cycle available for conversion to thermal energy per cycle, effectively raising the core temperature, all other heat transfer factors being held constant.

As seen in Figures 54 and 55, increasing temperature lowers the stiffness of the constituent fibers for both the nylon and polyester ropes. The softening is translated to the rope serving to account for a lower dynamic modulus of both the polyester and nylon ropes. This effect is clearly seen in Figure 56 which shows a decreasing K (expressed as % NRBS-in/in) with increasing stabilized core temperature. The temperature rise was due to an increase in strain rate, as seen in Figure 52.

In comparing the results for wet and dry nylon and polyester ropes, it is evident that, since water allows for more effective heat transfer than air, the stabilized core temperature is not nearly as great for the wet ropes. This accounts for the less drastic change in dynamic modulus observed with increasing strain amplitudes for the wet line in comparison to the dry lines.

The core temperature rise as a function of strain rates, as seen in Figure 52, is much more pronounced for polyester than nylon rope. This is due in part to the inverse relationship between temperature rise and the thermal conductivity of the rope. The temperature of a rope with lower thermal conductivity will rise more because the heat generated is less able to conduct to the rope surface. The thermal conductivity of the bulk polymers is about .18 Watts/ meter-° C for polyester and is about .24 Watts/meter-° C for nylon. These values will be reduced drastically for heat flow across close packed filaments. On this basis, a higher temperature rise would be expected for polyester resulting in a greater reduction in dynamic modulus with increasing strain rate for polyester.

In terms of the stiffness under a specific loading condition, the polyester rope,
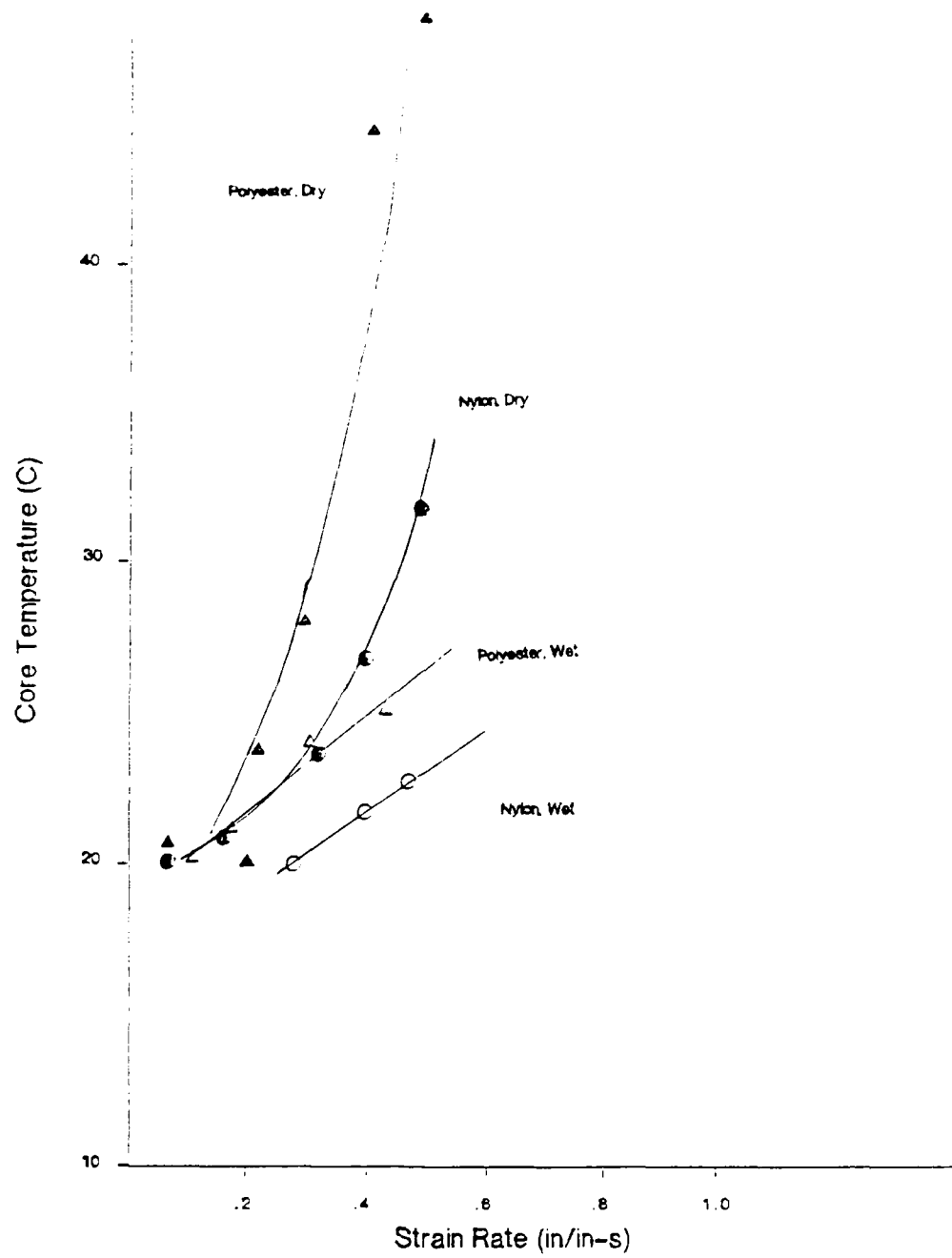
Figure 52

Strain rate versus core temperature
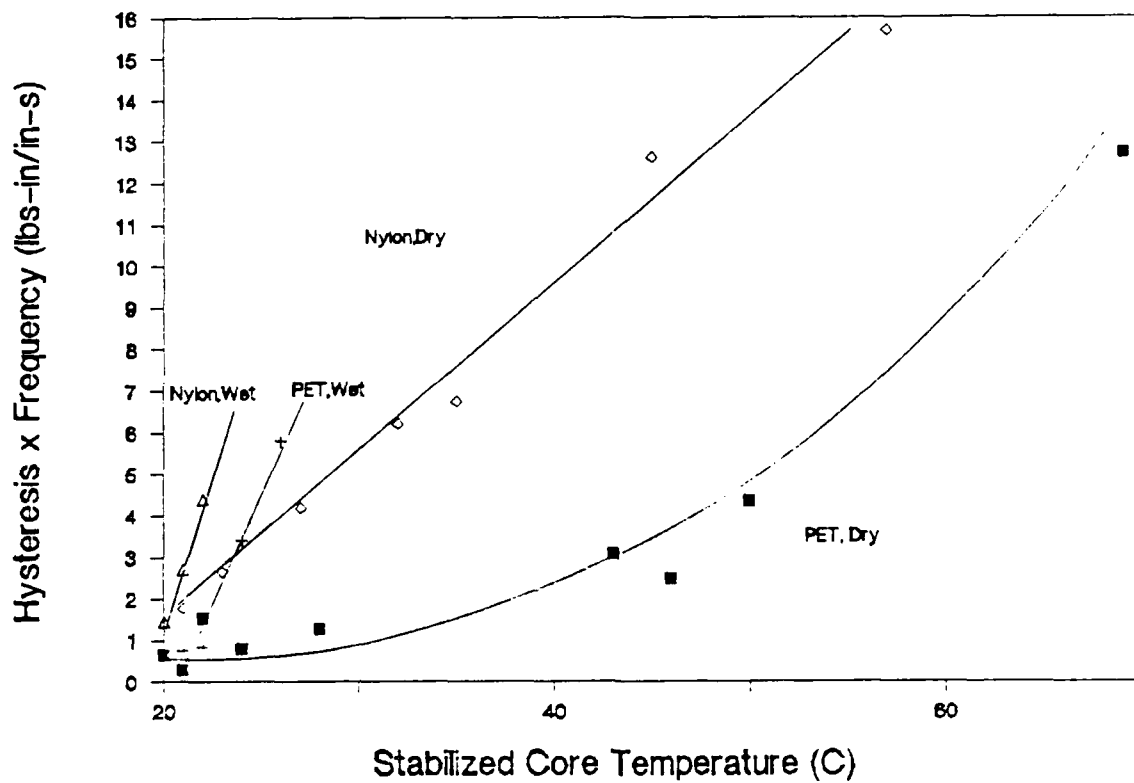
Figure 53

Power Absorbed per Cycle versus Stabilized Core Temperature for
Nylon and Polyester Rope Cycled with a Steady Tension of
20% NRBS

Figure 54

Load-elongation curves for dry nylon fibers tested at a variety
of temperatures. [Ref 13]

Figure 55
Load-elongation curves for dry polyester fibers tested at a variety
of temperatures. [Ref 13]
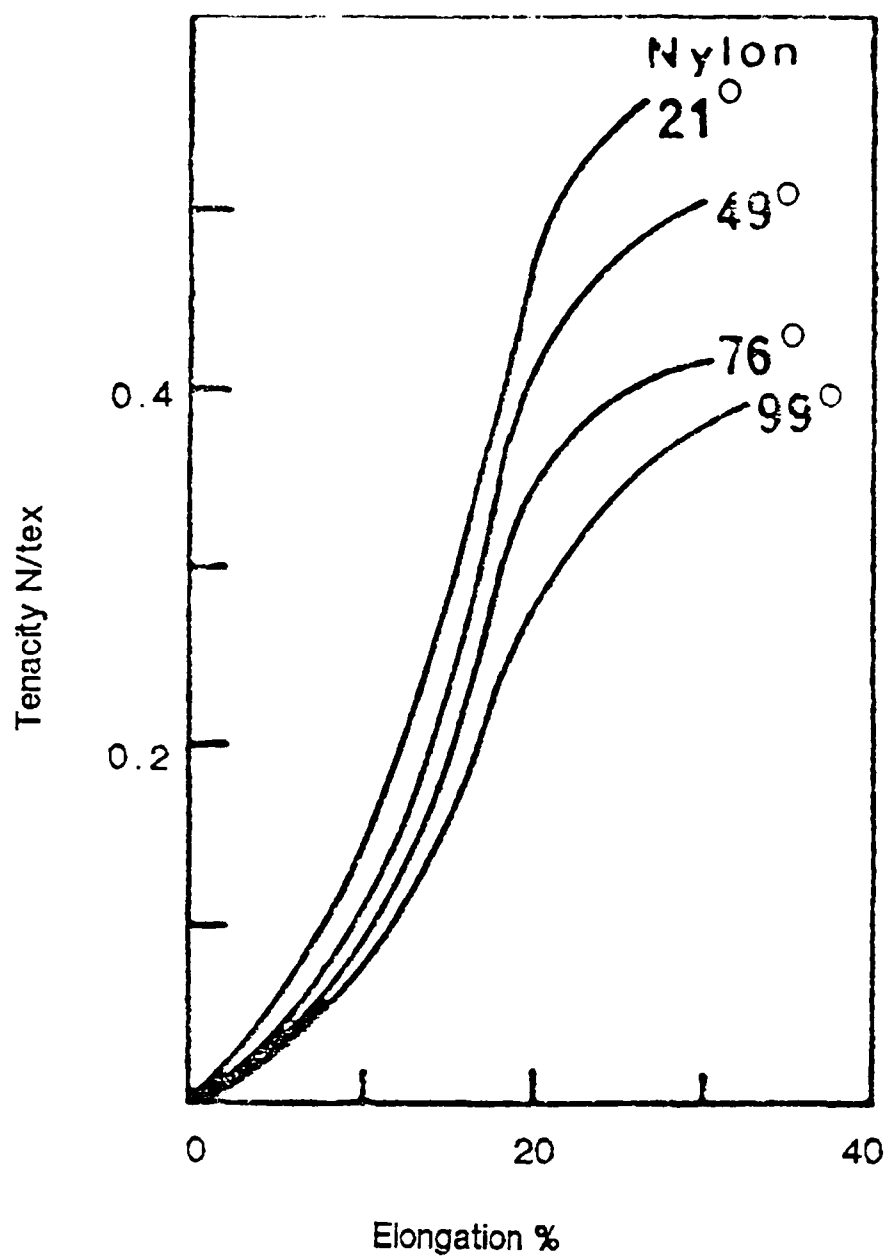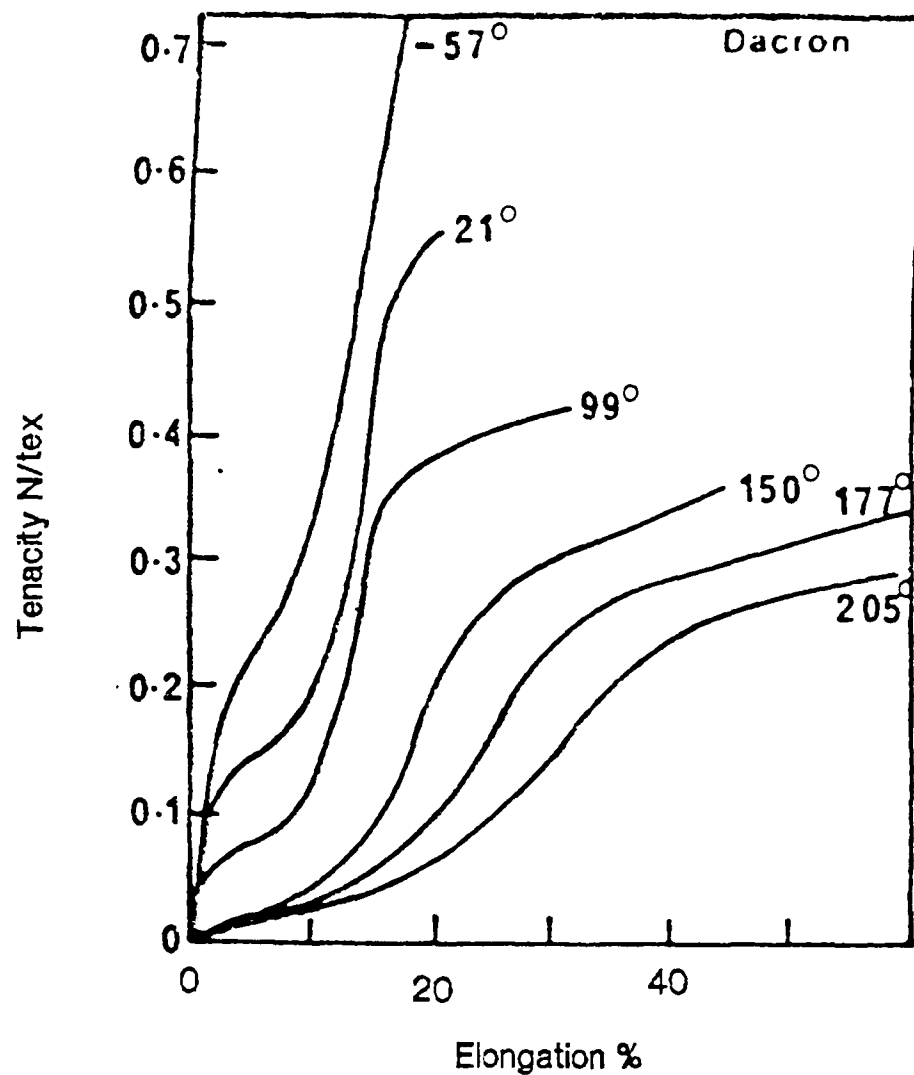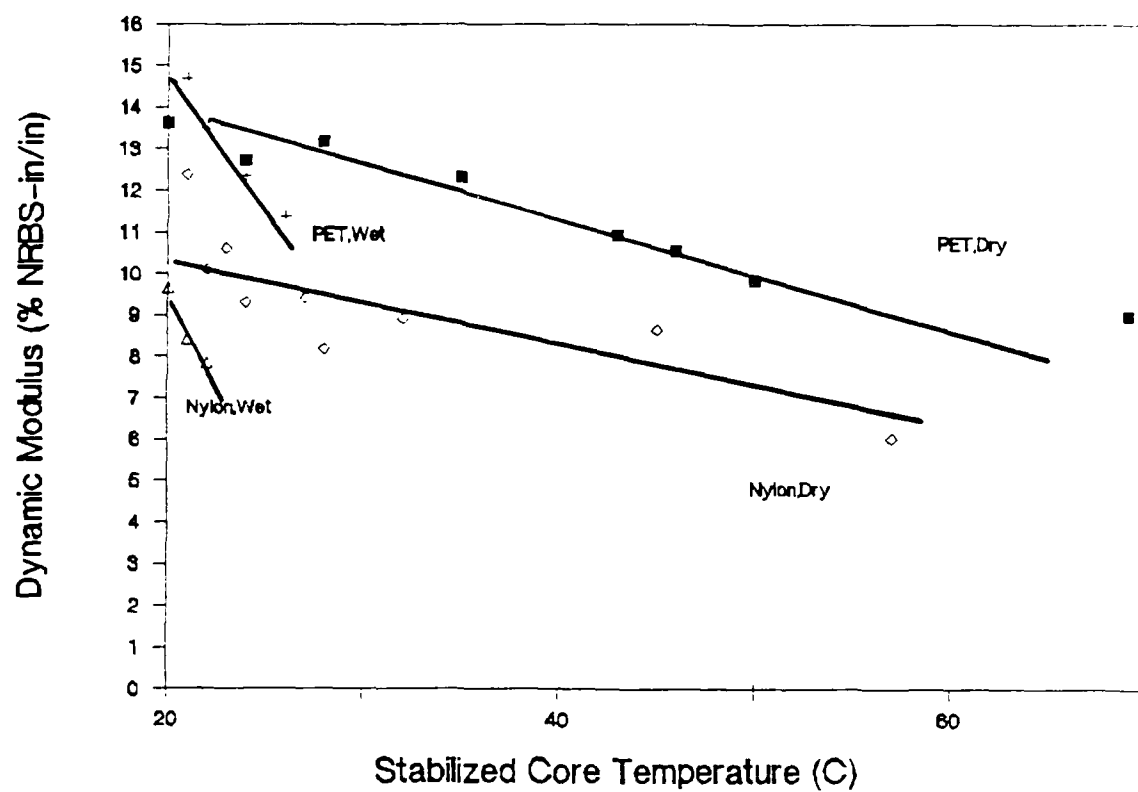
Figure 56

Dynamic modulus versus stabilized core temperature for nylon and
polyester rope cycled with a steady tension of 20% NRBS.

which is composed of the stiffer fibers and yarns, exhibits the greater dynamic modulus.

The major implications of an increase in stiffness at any particular strain amplitude concern the maximum load that the rope experiences and its total elongation. As seen in the results presented in Chapter 5, an increase in stiffness is normally associated with an increase in maximum load.

In the case of nylon, the ropes which experienced the greatest maximum load (at low frequency and high strain amplitude) also manifested the greater total and residual elongation. The only exception to this is in the case of the wet nylon which experienced a higher elongation than its dry counterpart, despite similar stiffness and maximum load. The explanation for this concerns the fact that nylon shrinks in water under low loads. As seen by the level of water absorption experienced by the nylon rope in Table 2.2, the nylon rope swells radially but shrinks longitudinally due to the hydrophilic groups in its molecular chains, which allow for penetration of water into the amorphous regions. This swells the fiber radially but shrinks it longitudinally. Under cycling, the wet rope starts from a shorter absolute length, but elongates more [14].

No apparent difference was seen in elongation or maximum load for the wet versus dry condition for polyester, as expected, due to the fact that it is not hydrophilic. Except for cooling, water appears to have little direct effect on polyester properties. However, its indirect effect due to cooling is significant in the context of tensile cycling between displacement limits.

6.3 Changing Hysteresis with Changing Conditions

6.3.1 General

As indicated in Chapter 5, all the ropes displayed the same qualitative behavior in respect to hysteresis while cycling to stabilization. It was shown in Figure 28 that the hysteresis increased from the 10th to the 100th cycle, but then stabilized at a slightly lower level between the 500th and 10,000th cycle. The stabilization represents the rope becoming mechanically conditioned to the imposed loading.

During the initial cycles, the loading condition was changing very rapidly due to the extensive creep elongation of the rope. This necessitated the removal
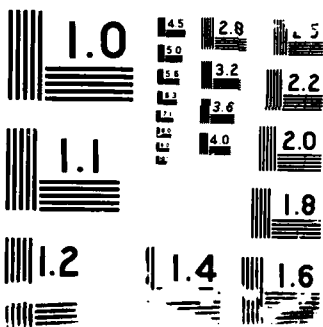
of slack, in order to maintain the specified steady tension, and this in turn imposed increasingly higher maximum loads on the rope as it stiffened and its dynamic modulus increased. The higher maximum cyclic tensile loads in turn, increased the lateral rope contraction which served to increase the normal (pressure) forces on the constituent yarns and fibers. This increase in pressure increased the interyarn and interfiber frictional forces which, in turn, manifested itself in terms of increasing frictional hysteresis.

The frictional hysteresis and its rapid increase during the initial cycles directly corresponds to the rapid rise in core temperature, as seen in Figure 30. In fact, the stabilization of the measured core temperature corresponds to the stabilization of the hysteresis. When stabilization occurs, the rate of conversion of mechanical energy to thermal energy is constant and is equal to the rate of heat loss to the ambient surroundings.

Viscoelastic deformation of the fibers themselves also contributes to the net hysteresis. Prevorsek and Kwon reported on the extent to which nylon and polyester fibers experienced viscoelastic deformation w hen subjected to cyclic displacements [4]. This deformation, as shown by total creep extension and extension per cycle in Figure 29, occurred primarily in the initial cycles. This parallels the behavior of the ropes, which is to be expected.

6.3.2 Nylon

In examining the results for nylon, it can be seen, as expected, that the hysteresis increased with increasing strain amplitude in all situations. It should be kept in mind that the hysteresis at lower strain amplitudes may be as much as 10-15% low due to the data reduction procedure discussed earlier. Not only is the absolute amount of energy increased with changing strain amplitude, at constant frequency, but the rate at which it was applied to the system also is also increased. This strain manifested itself in the general increase in temperature with the larger strain amplitudes.

An increase in temperature rise cannot be considered the sole criterion for judging the hysteresis of the system. Those ropes cycled at 1 Hz exhibited a higher temperature rise than those cycled at .2 Hz. However, the temperature rise accompanying the 1 Hz test tended to soften the rope and reduce its dynamic stiffness. Thus, in a constant strain amplitude test, a more severe loading

condition is incurred for ropes cycled at a lower frequency in terms of load variation and maximum load achieved. Here, the lower frequency rope test required greater energy input and proportionately more energy was absorbed.

The wet nylon ropes, which had a lower dynamic modulus than the dry rope, experienced lower loads than the dry ropes and experienced a corresponding lower hysteresis when tested at fixed displacement amplitudes.

6.3.3 Polyester

As seen in Figures 43 and 44, the polyester behaved, with respect to hysteresis, in the same manner as the nylon for changing strain amplitude and for essentially the same reasons as discussed in 6.3.2.

However, when addressing the effect of a change in frequency, the polyester behaves in a manner contrary to the nylon. A reason for this effect can be found in the tremendous temperature rise in the high frequency polyester tests which can be attributed to intense interstrand interaction due to the higher nominal loads incurred. Pathological studies done on various ropes after cycling indicated that the polyester ropes were possibly subjected to greater energy input than the nylon because they showed much greater deformation. In fact, the polyester ropes cycled at high frequencies and strain amplitude, resulting in high core temperatures, became rigid and displayed a much higher bending rigidity than new ropes. Tensile tests of cover yarns, as seen in Figure 57, indicate that the ultimate tensile strength and elongation to rupture of the yarns was substantially reduced when cycled at high frequency and high strain rates. This loss of strength is indicative of considerable more abrasion and energy absorption than found at the lower frequency. Nylon did not suffer these severe effects.

An apparent anomaly to this situation is the high hysteresis found for wet polyester as compared to the dry polyester. A comparison of the amount of energy input to each of these systems is similar. As seen in Figure 58, which shows actual load elongation curves for dry and wet rope cycled at .2 Hz, a steady tension of 1.88 kips and a strain amplitude of .02 in/in the wet rope appears to unload to a lower level, thus accounting for the hysteresis increase. Whether this unloading difference is related to pumping action of the recovering rope is a question for further study.
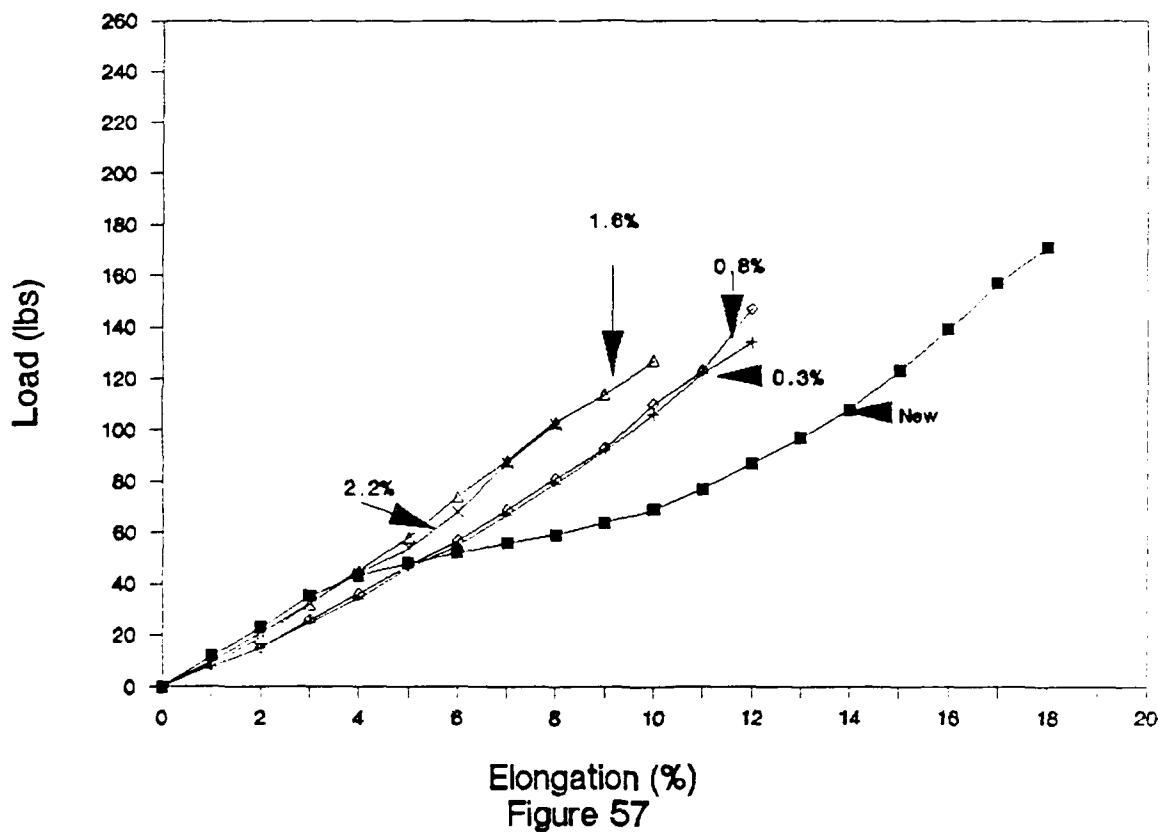
Elongation (%)

Figure 57

Load–elongation curves of polyester cover yarns from ropes cycled at 1 Hz and a steady tension of 1.88 kips and various strain amplitudes.
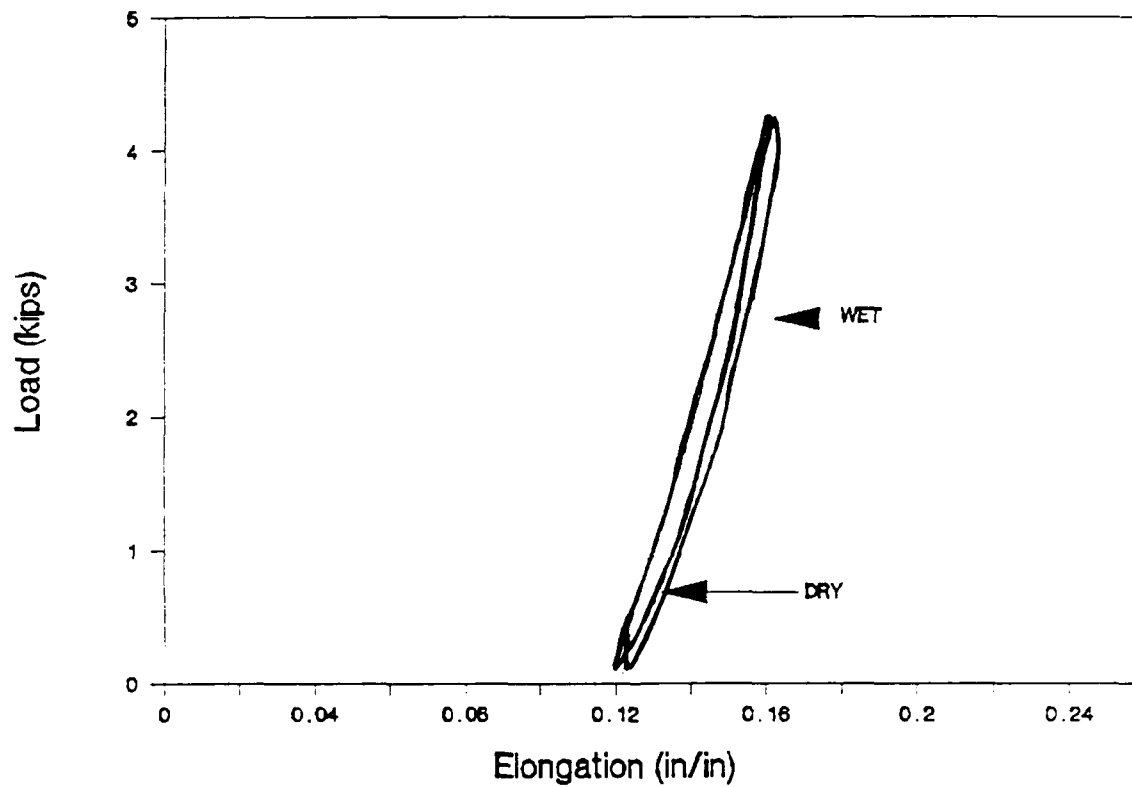After 10,000 cycles.

Figure 58
Hysteresis loops for polyester ropes cycled at a steady tension of
1.88 kips, strain amplitude of .02 in/in and a frequency of .2 Hz
both wet and dry, after 10,000 cycles.

Chapter 7

Conclusions

Based on the data presented in Chapter 5 and the discussion in Chapter 6, several conclusions can be made about the dynamic behavior of the ropes tested within the range of independent parameter values considered.

a. The cyclic stabilized stiffness, K, is found to be considerably higher than the quasi-static stiffness of uncycled ropes. This is in agreement with other studies in the literature. Polyester is found to be much stiffer than the nylon.

b. Internal rope temperature, which is higher in polyester than in nylon, can become significant in dry ropes subjected to high strain amplitudes and high frequencies. A reduction in dynamic modulus is sometimes observed to accompany such temperature in creases.

c. Under increasing steady tension, the rope will experience greater dynamic stiffness due to greater alignment of the yarns about the rope's central axis, as well as the higher modulus at higher elongation on the quasi-static load elongation curve of the component fibers.

d. Both polyester and nylon exhibit increasing hysteresis per cycle with increasing strain amplitude and frequency, reflected in increased mechanical energy input and a corresponding increase in rope temperature.

e. Under wet conditions, nylon experiences less hysteresis than polyester when similarly loaded. This is in contrast to past load control studies which consistently show polyester as having less hysteresis per cycle than nylon. Such results are shown in Figure 59, which is from the load control study done by Bitting [10]. The disagreement is due to the difference between strain control and load control testing presented in Chapter 1. Since hysteresis can be considered to influence internal degradation of rope, the testing method and effective characterization of actual deployment conditions, such as studied in this thesis, become quite important in considering the applicability of test results.
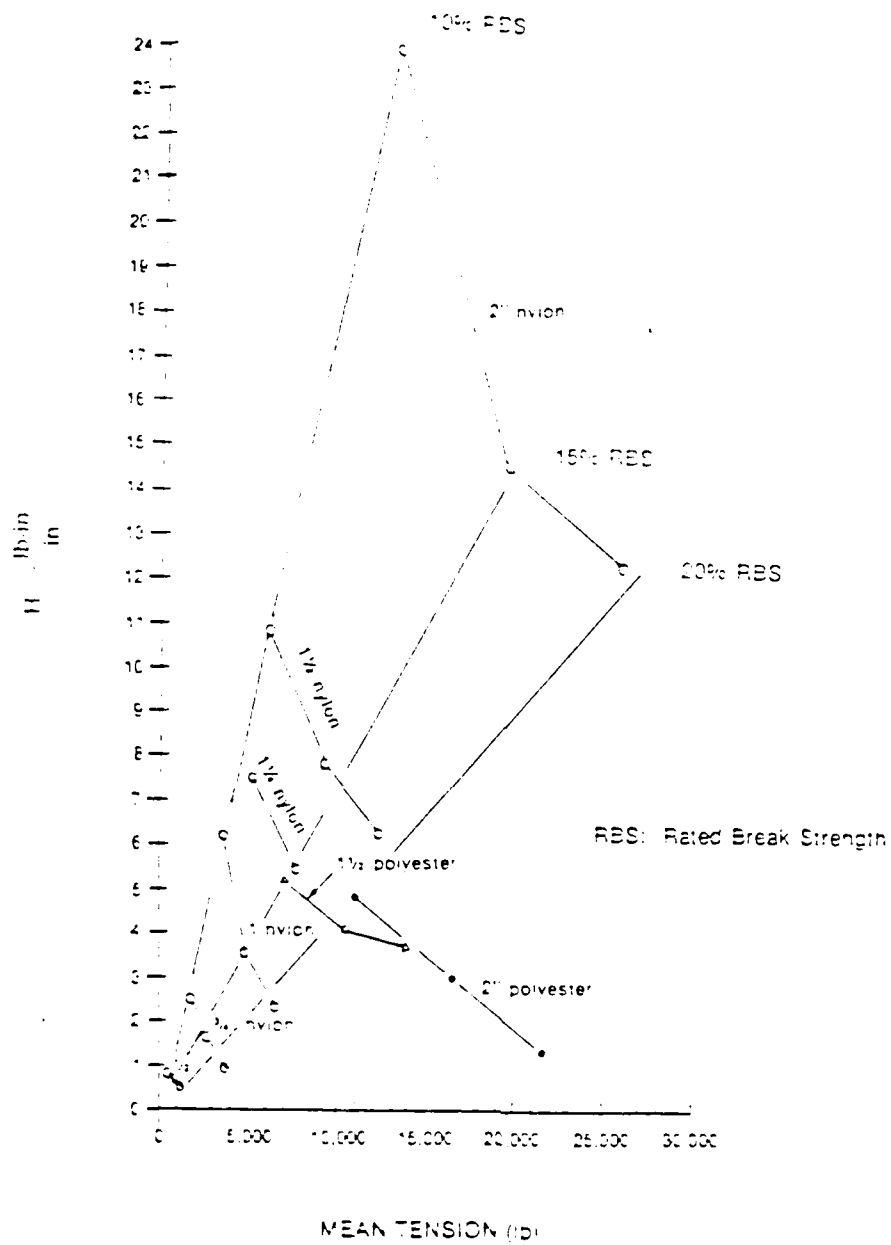
Figure 59
Hysteresis of nylon and polyester double braided line . [Bitting, Ref 10]

REFERENCES

1. Parsey, M.R. "The Fatigue Resistance and Hysteresis of Man-Made Fibre Ropes," Private Notes, Professor Stanley Backer.

2. Parsey, M.R. et. al., "The Dynamic Behaviour of Marine Hawsers," OTC 5009, 1985.

3. Bitting, Kenneth R. "The Dynamic Behavior of Nylon and Polyester Line, Final Report," USCG Report No CG-D-39-80, 1980.

4. Prevorsek, D.C. and Kwon, Y.D., "Structural Interpretation of the Endurance of Polymeric Fibers," *J. Macromol., Sci-Phys., B12940*, p. 447-485, 1976.

5. Bridon Fibres and Plastics, Ltd., "The Selection of Rope for Use on Single Point Moorings," British Ropes Report, 1985.

6. Lyons, W. James, "Fatigue in Textile Fibers. Part I. General Considerations; Fatiguing by cyclic Tension: Instrumentation and Fatigue Lifetimes," Textile Research Journal, p 448-459, 1962.

7. US Navy Towing Manual, SL 740-AA-MAN-010, Preliminary, 1 December 1986.

8. Sarsmore, N ., et. al., "Barge Motions and Towline Tensions Measured During a North Sea Tow," International Symposium on Ocean Engineering Ship Handling, p 13:1-13:15, 1980.

9. "Cordage Institute Standard Test Methods for Fiber Ropes," The Cordage Institute, June, 1980.

10. Bitting, Kenneth R. "Dynamic Modeling of Nylon and Polyester Double Braid Line," USCG Report No. CGR-DC-23-84, 1985.

11. Flory, Private notes, Professor Stanley Backer.

12. Paul, W. "Review of Synthetic Fiber Ropes," Research and Development Project, USCGA, August, 1970.

13. Morton, W.E., and Hearle, J.W.S., **Physical Properties of Textile Fibers,** The Textile Institute, Hienemann, London, 1962.

14. Hearle, J.W.S. and Wong, B.S. "A Comparative Study of the Fatigue Failure of Nylon 6.6, PET Polyester and Polypropylene Fibres," *Journal of the Textile Institute,* Vol.68, No. 3, 1977, pp 89-94.

END

DATE

FILMED

8-88

DTIC